

Design and Synthesis of Near-Infrared Absorbing Diketopyrrolopyrroles

Ph.D. Thesis

By
PATIL YUVRAJ ANANDA



**DISCIPLINE OF CHEMISTRY
INDIAN INSTITUTE OF TECHNOLOGY INDORE
APRIL, 2018**

Design and Synthesis of Near-Infrared Absorbing Diketopyrrolopyrroles

A THESIS

*Submitted in partial fulfillment of the
requirements for the award of the degree
of*
DOCTOR OF PHILOSOPHY

by
PATIL YUVRAJ ANANDA



**DISCIPLINE OF CHEMISTRY
INDIAN INSTITUTE OF TECHNOLOGY INDORE
APRIL, 2018**



INDIAN INSTITUTE OF TECHNOLOGY INDORE

CANDIDATE'S DECLARATION

I hereby certify that the work which is being presented in the thesis entitled **Design and Synthesis of Near-Infrared Absorbing Diketopyrrolopyrroles** in the partial fulfillment of the requirements for the award of the degree of **DOCTOR OF PHILOSOPHY** and submitted in the **DISCIPLINE OF CHEMISTRY, INDIAN INSTITUTE OF TECHNOLOGY INDORE**, is an authentic record of my own work carried out during the time period from **July 2014** to **March 2018** under the supervision of **Dr. RAJNEESH MISRA, PROFESSOR, INDIAN INSTITUTE OF TECHNOLOGY INDORE**.

The matter presented in this thesis has not been submitted by me for the award of any other degree of this or any other institute.

**Signature of the student with date
(PATIL YUVRAJ ANANDA)**

This is to certify that the above statement made by the candidate is correct to the best of my/our knowledge.

**Signature of Thesis Supervisor with date
(PROF. RAJNEESH MISRA)**

PATIL YUVRAJ ANANDA has successfully given his Ph.D. Oral Examination held on

Signature of Chairperson (OEB)
Date:

Signature of External Examiner
Date:

Signature(s) of Thesis Supervisor(s)
Date:

Signature of PSPC Member #1
Date:

Signature of PSPC Member #2
Date:

Signature of Convener, DPGC
Date:

Signature of Head of Discipline
Date:

ACKNOWLEDGEMENTS

It is my great pleasure to express my deep sense of gratitude to my supervisor Prof. Rajneesh Misra, for the wonderful opportunity to pursue research with colourful world of chemistry and believing my research abilities. His constant guidance, support and motivation has been immensely helpful to complete this journey. His assurance at the time of crisis, especially for standing by me when chemistry did not work, is humbly appreciated. I am really honoured to be his Ph.D. student. His enthusiasm and dedication has always inspired me. Further I would like to thank my PSPC members Dr. Shaikh M. Mobin and Dr. Santosh Kumar Vishwakarma for their valuable suggestions. I wish to express my gratitude to Prof. Pradeep Mathur, Director, IIT Indore for his continuous encouragement, help and support in every aspect.

I am grateful to Dr. Amrendra K. Singh (Head, Discipline of Chemistry, Indian Institute of Technology Indore) for his suggestions and guidance in various aspects. I am also grateful to Dr. Anjan Chakraborty, Dr. Tridib Kumar Sarma, Dr. Suman Mukhopadhyay, Dr. Apurba Kumar Das, Dr. Sampak Samantha, Dr. Biswarup Pathak, Dr. Sanjay Singh, Dr. Tushar Kanti Mukherjee, Dr. Satya S. Bulusu and Dr. Chelvam Venkatesh for their guidance and help during various activities.

I would like to extend my sincere thanks to Dr. Thaksen Jadhav, Dr. Bhausahab Dhokale, Dr. Shivendra Singh and Dr. Nidhi Singh for their kind and friendly nature and help in dealing with difficulties.

I would like to extend my special thanks to Jivan Shinde, Anupama Ekbote and Charu Popli for their kind and friendly nature and help.

I would like to extend my special thanks to my flatmates Dr. Rohit Rai and Mr. Sourabh Kumar for their friendly nature and help.

I extend my deep thanks to my group members Dr. Prabhat Gautam, Dr. Ramesh Maragani, Dr. Rekha Sharma, Madhurima Poddar, Yogajivan Rout, S. Bijesh, Manju, Faizal Khan, Indresh Singh Yadav, Nitin Gumber, Dr. Pramod Solanke, Dr. Sheshenshena Reddy, Dr. R. V. Ramana Reddy, Dr. Shubhra Bikash Maity, Dr. Gangala Shivakumar, Dr. Rami Reddy Eda, and Dr. Rakesh Kumar Gupta for their selfless co-operation and help to make my work successful.

I would also like to thank technical staff from Sophisticated Instrumentation Center (SIC), IIT Indore, Ms. Sarita Batra, Mr. Kinny Pandey, Mr. Ghanshyam Bhavsar, Mr. Rameshwar Dohare, Mrs. Vinita Kothari and Mr. Manish Kushwaha for their patience and timely technical support without which it was impossible to continue with my work.

I would also like to thank Ms. Anjali Bandiwadekar, Mr. Gati Krishna Nayak, Mr. Rajesh Kumar, Mr. Lala Ram Ahirwar and other library staff and Ms. Jaya Vakade, Mr. Prahalad Singh Panwar, Mr. Manoj Pal, Mr. Nithin Bhate, and other technical and non-technical staff for their constant help, whenever required.

Here, it is to be specially mentioned that, it has been wonderful to work with many friends together during my Ph.D. On this occasion I want to extend my thanks to my batch mates and friends Novina,

Chinky, Priyanka, Anubha, Siddarth and Amit who were always there and never let me down during these Ph.D. days.

I would like to record my thanks to seniors Dr. Bhagwati, Dr. Rajendar, Dr. Tamalika, Dr. Dnyanesh, Dr. Indrajit, Dr. Mahesh, Dr. Anvita, Dr. Sonam, Dr. Debashis, Dr. Anupam, Dr. Maruthi, Anuradha, Dr. Biju, Dr. Surajit, Roopali, Dr. Deepika, Sagar and Deepali for their generous co-operation and help.

I would like to take an opportunity to express my respect; love and gratitude to all the teachers from Z. P. Primary school, Lokamanya High School Nimbavade, K. B. P. Junior College of Science, Devapur, Atpadi College Atpadi, Department of Chemistry, Shivaji University Kolhapur.

I would like to acknowledge the people who mean world to me, my parents and other family members. I don't imagine a life without their love and blessings.

I would like to express my thanks to all others who helped and supported me directly or indirectly.

Finally I would like to express my thanks to IIT Indore for infrastructure and Ministry of Human Resource Development (MHRD), New Delhi for my Fellowship.

PATIL YUVRAJ ANANDA
IIT INDORE

DEDICATED TO
MY FAMILY

–Yuvraj

SYNOPSIS

Diketopyrrolopyrrole (DPP) is a 8π electron bicyclic system containing two lactam units. DPP is an electron acceptor building block widely used in the field of organic photovoltaics. DPP derivatives often exhibit broad optical absorption, high thermal stability and have been used for various applications including aggregation induced emission, solar cells, photodynamic therapy, bioimaging, laser dyes, conductive polymers, photoconductive materials and fluorescent sensors. The substitution of the donors and acceptors at 3- and 6-position of the DPP perturbs the photonic properties of DPP based molecular systems significantly. The donor-acceptor (D–A) architectures with strong absorption in visible to near-infrared (NIR) region and low HOMO–LUMO gap are used as potential candidates for organic photovoltaics. In order to improve the absorption towards NIR region and lower the HOMO–LUMO gap, DPP unit has been functionalized with various donors, acceptors and linkers in symmetrical and unsymmetrical way. The effect of substitution of various donor and acceptor units on the photonic, thermal and electrochemical properties was investigated. The photophysical, electrochemical properties and HOMO–LUMO gap of DPP based D–A systems can be tuned either by altering the strength of donor or acceptor units.

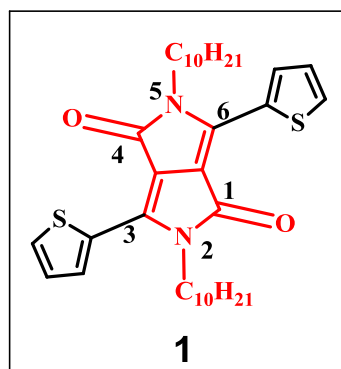


Figure 1. Diketopyrrolopyrrole (DPP).

We have explored variety of donor (carbazole, triphenylamine, ferrocene *etc.*) and acceptor (TCBD) functionalized DPP based D–A systems and investigated their photophysical, thermal, electrochemical and computational properties which indicate their applicability for photovoltaic applications. The DPPs in this work have been classified as symmetrical (**DPPs 2–4**) and unsymmetrical (**DPPs 5–7**) on the basis of functionalization at the 3- and 6- positions of DPP. The substitution of same donor or acceptor units on both the positions on the DPP and by making dimers will

Chapter 1: Introduction

This chapter describes the synthesis and functionalization approaches of DPP derivatives, and their applications in various fields.

Chapter 2: Materials and experimental techniques

This chapter summarizes the general experimental methods, characterization techniques and details of instruments used for characterization.

Chapter 3: *N*-phenyl carbazole functionalized diketopyrrolopyrroles

In chapter 3, we have designed and synthesized ethyne bridged *N*-phenyl carbazole substituted DPPs (**DPPs 8 and 9**) and their TCBD derivatives (**10 and 11**) by the Pd-catalyzed Sonogashira cross-coupling and [2+2] cycloaddition-retroelectrocyclization reactions respectively. The effect of incorporation of tetracyanobutadiene (TCBD) unit on photophysical, thermal and electrochemical properties of *N*-phenyl carbazole functionalized DPPs was investigated, which show substantial donor-acceptor interaction between carbazole and DPP. The *N*-phenyl carbazole substituted DPPs exhibit excellent thermal stability. The TCBD derivatives of DPP **10** and **11** show red shifted broad charge-transfer (CT) bands in the visible region with low HOMO – LUMO gap compared to ethyne bridged *N*-phenyl carbazole substituted **DPPs 8 and 9** (Figure 3). The electrochemical study reveals, additional reduction waves in **10** and **11** at low voltage corresponding to the TCBD moiety.

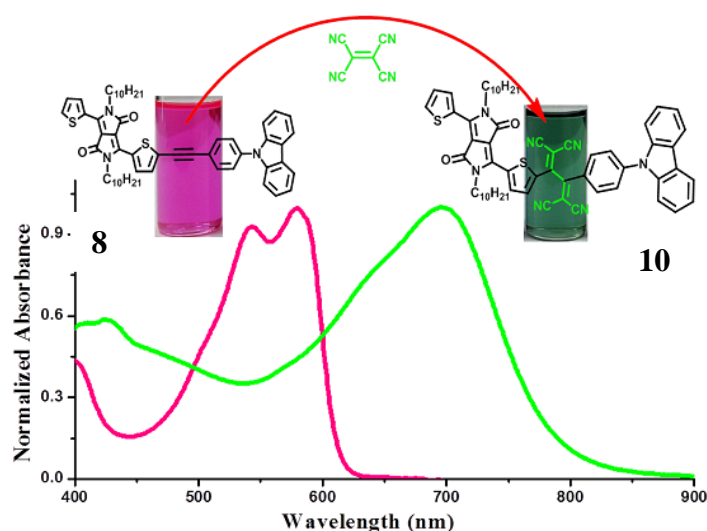


Figure 3. Absorption spectra of *N*-phenyl carbazole functionalized DPPs.

Chapter 4: Triphenylamine functionalized diketopyrrolopyrroles

In Chapter 4, a set of triphenylamine (TPA) based unsymmetrical and symmetrical diketopyrrolopyrroles (DPPs) **12** and **13** were designed and synthesized by the Pd-catalyzed Sonogashira cross-coupling reaction. The [2+2] cycloaddition-retroelectrocyclization reaction of DPPs **12** and **13** with tetracyanoethylene (TCNE) resulted in tetracyanobutadiene (TCBD) derivatives DPPs **14** – **16** respectively. The effect of TPA as donor and TCBD as acceptor on the photophysical properties of DPP and their donor-acceptor interaction was evaluated. The photophysical, thermal and electrochemical properties of TPA based DPPs **12** and **13** were compared with their TCBD derivatives **14** – **16**. The TCBD derivatives DPPs **14** – **16** show red shifted absorption (Figure 4), decrease in thermal stability and increase in strength of D – A interaction compared to DPPs **12** and **13**.

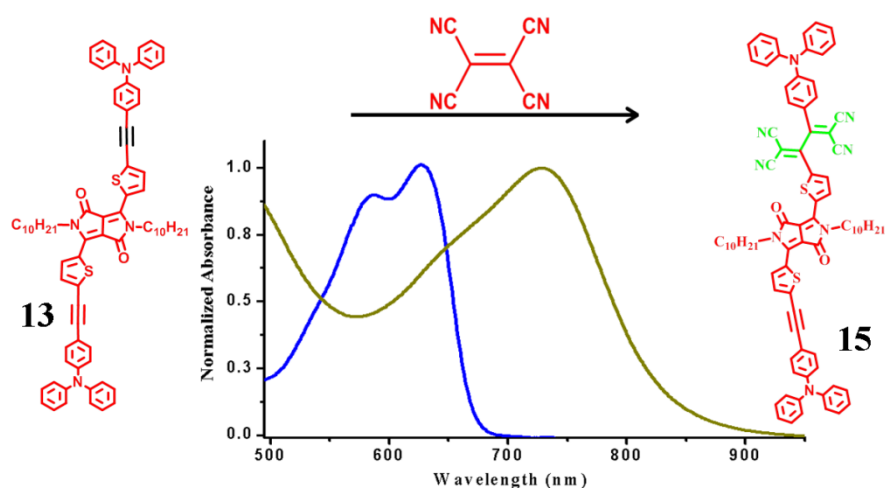


Figure 4. Electronic absorption spectra of triphenylamine functionalized DPPs.

Chapter 5: Ferrocenyl functionalized diketopyrrolopyrroles

Chapter 5 describes the synthesis of unsymmetrical and symmetrical ferrocenyl diketopyrrolopyrroles **17** and **18** by Sonogashira cross-coupling and their TCBD derivatives DPPs **19**–**21** by [2+2] cycloaddition-retroelectrocyclization reaction respectively. The incorporation of TCBD in ferrocenyl DPPs facilitate the reduction and show low HOMO – LUMO gap. The TCBD substituted DPPs show systematic red shift in absorption (Figure 5) with enhanced thermal stability. The photophysical, electrochemical, and computational studies show substantial donor–acceptor interaction. High thermal stability and low HOMO – LUMO gap of

ferrocenyl DPPs (**17–21**) makes them a potential candidate for organic photovoltaics.

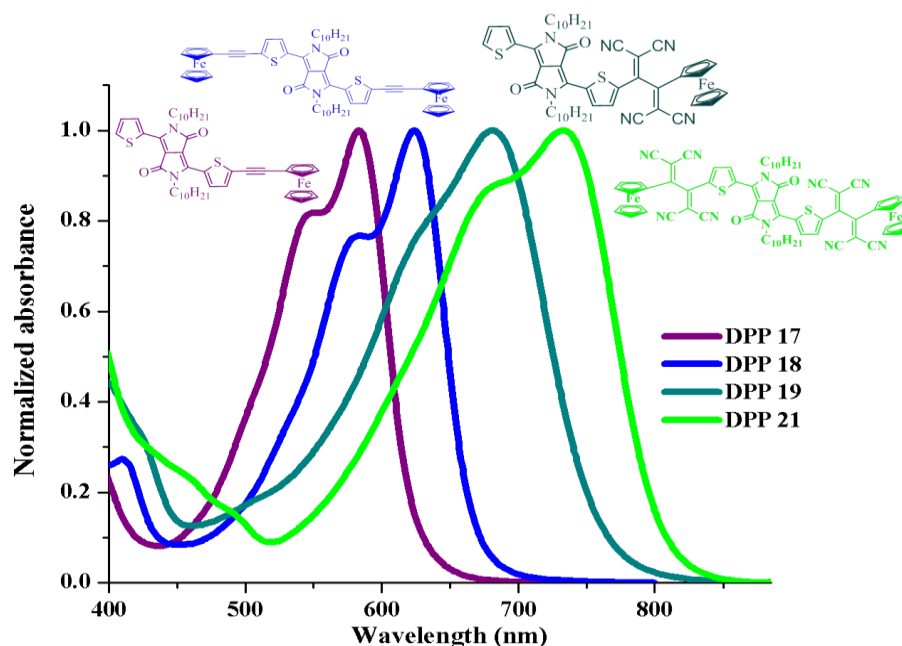


Figure 5. Electronic absorption spectra of ferrocenyl functionalized DPPs.

Chapter 6: Metal functionalized diketopyrrolopyrroles

In chapter 6, a symmetrical cobalt-dithiolene functionalized diketopyrrolopyrrole (DPP) **Co-DPP-Co** was designed and synthesized. Its photophysical, thermal, electrochemical and computational studies were compared with symmetrical ferrocenyl **Fc-DPP-Fc**. The electronic absorption spectrum of **Co-DPP-Co** exhibited absorption in Vis-NIR region with shoulder band in longer wavelength region (Figure 6). The thermogravimetric analysis shows good thermal stability of **Co-DPP-Co**. The density functional theory (DFT) investigation exhibited the cis geometry of cobalt-dithiolene ring with respect to DPP in **Co-DPP-Co** whereas trans geometry was observed for ferrocenyl unit in **Fc-DPP-Fc**.

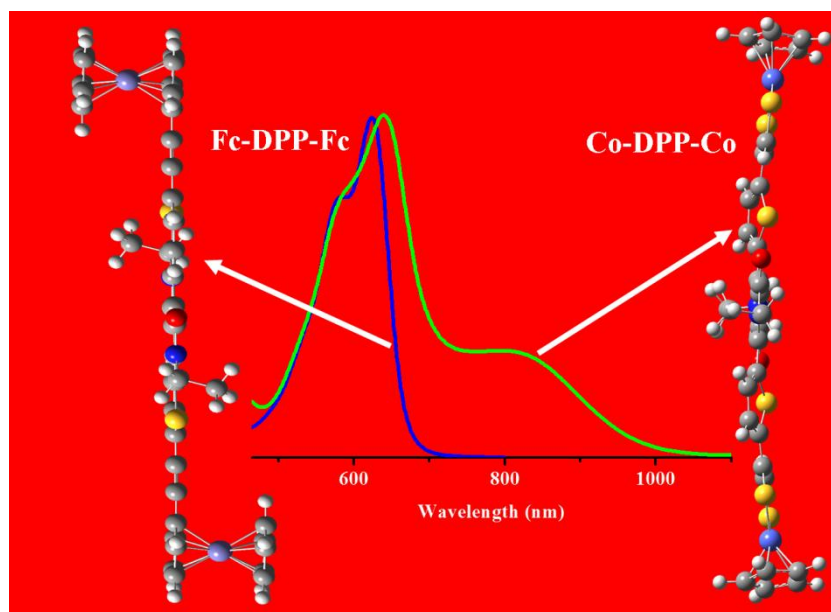


Figure 6. Absorption spectra of metal functionalized DPPs.

Chapter 7: Diketopyrrolopyrrole based monomer, dimers and trimer

In chapter 7, we have designed and synthesized diketopyrrolopyrrole (DPP) based monomer (**22**), dimers (**23** and **24**) and trimer (**25**) in order to see the effect of number of DPP units on the photophysical and electrochemical properties (Figure 7). The absorption spectra show that the red shift in the absorption after dimerization and trimerization of DPP, with broadening of absorption bands in dimer analogues (**23** and **24**). The TGA analysis shows the dimerization and trimerization of DPP improves the thermal stability. The electrochemical study exhibited additional oxidation peak in trimer **25** related to the oxidation of triphenylamine unit. The effect of connecting bridge between DPP units in dimers and trimer of DPP was investigated which reveals the ethene bridged dimer exhibit good electronic communication between two DPP units.

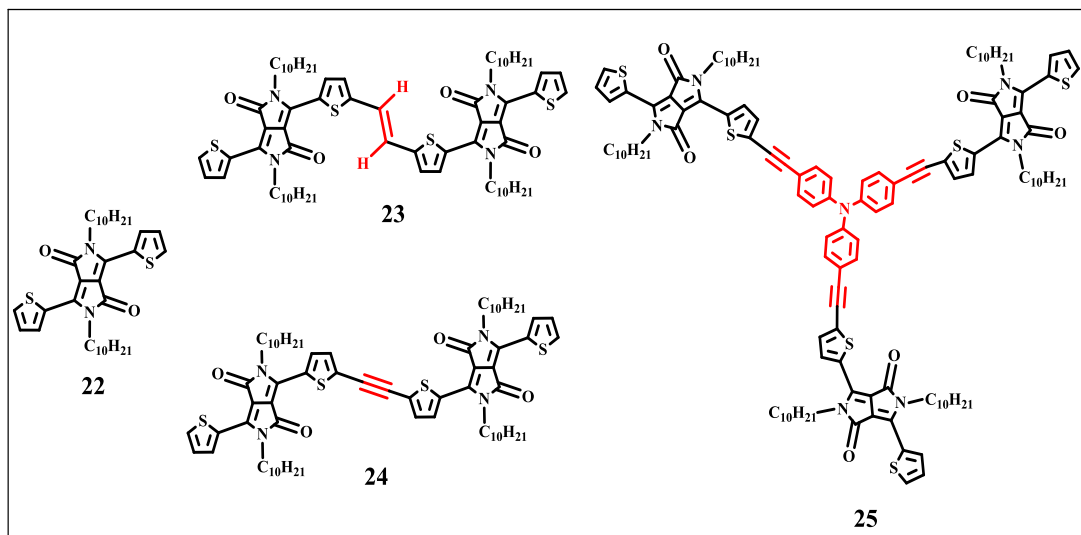


Figure 7. Chemical structures of DPP based monomer, dimers and trimer.

Chapter 8: Conclusions and future scope

This chapter summarizes the salient features of the work and future prospective to develop new materials for optoelectronic applications.

List of Publications

1. **Patil, Y.**, Jadhav, T., Dhokale, B., Misra, R.* (2016), Tuning of the HOMO–LUMO Gap of Symmetrical and Unsymmetrical Ferrocenyl-Substituted Diketopyrrolopyrroles. *Eur. J. Org. Chem.*, 2016, 733–738 (DOI:10.1002/ejoc.201501123).† (Impact Factor = 3.068)
2. **Patil, Y.**, Misra, R.,* Keshtov, M. L., Sharma, G. D. (2016), 1,1,4,4-Tetracyanobuta-1,3-diene Substituted Diketopyrrolopyrroles: An Acceptor for Solution Processable Organic Bulk Heterojunction Solar Cells. *J. Phys. Chem. C*, 120, 6324–6335 (DOI: 10.1021/acs.jpcc.5b12307).† (Impact Factor = 4.509)
3. **Patil, Y.**, Jadhav, T., Dhokale, B., Misra, R.* (2016), Design and Synthesis of Low HOMO–LUMO Gap *N*-phenyl carbazole-Substituted Diketopyrrolopyrroles. *Asian J. Org. Chem.* 5, 1008–1014 (DOI: 10.1002/ajoc.201600194).† (Impact Factor = 3.275)
4. **Patil, Y.**, Misra, R.,* Sharma, A., Sharma, G. D. (2016), D-A-D- π -D-A-D Type Diketopyrrolopyrrole Based Small Molecule Electron Donor for Bulk Heterojunction Organic Solar Cells. *Phys. Chem. Chem. Phys.*, 18, 16950–16957 (DOI: 10.1039/C6CP02700H).† (Impact Factor = 4.449)
5. **Patil, Y.**, Misra, R.,* Chen, F. C., Keshtov, M. L., Sharma, G. D. (2016), Symmetrical and Unsymmetrical Triphenylamine based Diketopyrrolopyrroles and their use as Donor for Solution Processed Bulk Heterojunction Organic Solar Cells. *RSC Adv.*, 6, 99685–99694 (DOI: 10.1039/C6RA10442H).† (Impact Factor = 3.287)
6. **Patil, Y.**, Shinde, J. S., Misra, R.* (2017), Near-infrared absorbing metal functionalized diketopyrrolopyrroles. *J. Organomet. Chem.*, 852, 48–53 (DOI: doi.org/10.1016/j.jorganchem.2017.10.014).† (Impact Factor = 2.173)
7. **Patil, Y.**, Popli, C. Misra, R.* (2018), Near-infrared absorbing tetracyanobutadiene bridged diketopyrrolopyrroles. *New J. Chem.*, 42, 3892–3899 (DOI: 10.1039/C7NJ05162J).† (Impact Factor = 3.277)
8. **Patil, Y.**, Misra, R.,* Keshtov, M. L., Singhal, R., Sharma, G. D. (2017), Ferrocene-diketopyrrolopyrrole based non-fullerene acceptors for bulk

- heterojunction polymer solar cells. (2017), *J. Mater. Chem. A*, 5, 13625-13633 (DOI: 10.1039/C7TA03322B). (Impact Factor = 8.867)
9. **Patil, Y.,** Misra, R.,* Keshtov, M. L., Sharma, G. D. (2017), Small molecule carbazole-based diketopyrrolopyrroles with tetracyanobutadiene acceptor unit as a non-fullerene acceptor for bulk heterojunction organic solar cells. *J. Mater. Chem. A*, 5, 3311–3319 (DOI: 10.1039/C6TA09607G). (Impact Factor = 8.867)
10. **Patil, Y.,** Misra, R.* (2018), Small Molecule Based Non-Fullerene Acceptors: A Comparative Study, *Chem. Rec.*, 18, 1350–1364 (DOI:10.1002/tcr.201800037). (Impact Factor = 4.891)
11. **Patil, Y.,** Misra, R.* (2018), Diketopyrrolopyrrole-based and tetracyano-bridged small molecules for bulk heterojunction organic solar cells. *Chem. Asian J.*, 13, 220 – 229 (DOI: 10.1002/asia.201701493). (Impact Factor = 4.083)
12. **Patil, Y.,** Misra, R.,* Singh, M. K., Sharma, G. D. (2017), Ferrocene-diketopyrrolopyrrole based small molecule donors for bulk heterojunction solar cells. *Phys. Chem. Chem. Phys.*, 19, 7262–7269 (DOI: 10.1039/C7CP00231A). (Impact Factor = 4.123)
13. **Patil, Y.,** Misra, R.,* Chen, F. C., Sharma, G. D. (2016), Small molecules based *N*-phenyl carbazole Substituted Diketopyrrolopyrroles as donor for solution processed bulk heterojunction organic solar cells. *Phys. Chem. Chem. Phys.*, 18, 22999-23005 (DOI: 10.1039/C6CP03767D). (Impact Factor = 4.123)
14. **Patil, Y.,** Misra, R.* (2017), Tetracyanobutadiene bridged Ferrocene and Triphenylamine functionalized Pyrazabole dimers. *J. Organomet. Chem.*, 840, 23–29 (DOI:10.1016/j.jorganchem.2017.03.048). (Impact Factor = 2.173)
15. **Patil, Y.,** Jadhav, T., Dhokale, B., Butenschön, H., Misra, R.* (2017), Donor Substituted Pyrazabole Monomers and Dimers: Design, Synthesis and Properties *ChemistrySelect*, 2, 415–420 (DOI: 10.1002/slct.201601704). (Impact Factor = 1.505)

†Papers pertaining to the thesis.

TABLE OF CONTENTS

1. List of Figures	xxvii
2. List of Schemes	xxix
3. List of Charts	xxx
4. List of Tables	xxx
5. Acronyms	xxxiii
6. Nomenclature	xxxiv

Chapter 1: Introduction

1.1.	General Introduction	1
1.2.	Donor-Acceptor systems	1
1.3.	Diketopyrrolopyrrole (DPP)	3
1.4.	Synthesis of diketopyrrolopyrrole	4
1.4.1.	Reformatsky Route	4
1.4.2.	Succinic ester route	5
1.4.3.	Condensation of Nitrile with 3-Alkyloxycarbonyl- 2-pyrroline-5-one	6
1.4.4.	Synthesis of DPPs by 2, 5-Dihydrofuro[4,3-c]furan-1,4- diones (DFFs)	7
1.5.	Absorption Spectra of diketopyrrolopyrrole	8
1.6.	Reactions of diketopyrrolopyrrole	8
1.6.1.	Alkylation and bromination	8
1.6.2.	Cross-coupling of diketopyrrolopyrrole	9
1.6.2.1.	Heck and Suzuki Coupling	9
1.6.2.2.	Sonogashira Coupling	10
1.6.2.3.	Stille Coupling	11
1.6.3.	Metal functionalized diketopyrrolopyrroles	11
1.6.4.	[2+2] cycloaddition–retroelectrocyclization	12
1.7.	Applications of diketopyrrolopyrroles	12
1.7.1.	Photothermal cancer therapy	12
1.7.1.	Dye sensitized solar cells (DSSCs)	13
1.7.3.	Bulk heterojunction (BHJ) solar cells	14

1.7.3.1.	As donor in bulk heterojunction organic solar cells	14
1.7.3.2.	As Acceptor in bulk heterojunction organic solar cells	15
1.7.4.	Perovskite solar cells	15
1.7.5.	Organic Light Emitting Diodes	16
1.7.6.	Organic Field effect transistors	17
1.7.7.	Fluorescent sensors	17
1.8.	Current Work	18
1.9.	Organization of thesis	19
1.10.	References	21

Chapter 2: Materials and experimental techniques

2.1.	Introduction	29
2.2.	Chemicals for synthesis	29
2.3.	Spectroscopic measurements	29
2.3.1.	NMR spectroscopy	29
2.3.2.	Mass spectrometry	30
2.3.3.	UV–vis spectroscopy	30
2.3.4.	Fluorescence spectroscopy	30
2.4.	Electrochemical studies	30
2.5.	Computational calculations	30
2.6.	References	30

Chapter 3: *N*-phenyl carbazole functionalized diketopyrrolopyrroles

3.1.	Introduction	33
3.2.	Results and discussion	34
3.3.	Photophysical properties	35
3.4.	Thermal properties	38
3.5.	Electrochemical properties	38
3.6.	Density Functional Theory Calculations	41
3.7.	Application in Photovoltaics	43
3.7.	Experimental section	43
3.8.	Conclusions	46
3.9.	References	46

Chapter 4: Triphenylamine functionalized diketopyrrolopyrroles

4.1.	Introduction	55
4.2.	Results and discussion	56

4.3.	Photophysical properties	57
4.4.	Thermogravimetric analysis	58
4.5.	Electrochemical properties	59
4.6.	Theoretical calculations	61
4.7.	Application in Photovoltaics	63
4.8.	Experimental section	63
4.9.	Conclusions	66
4.10.	References	66

Chapter 5: Ferrocenyl functionalized diketopyrrolopyrroles

5.1.	Introduction	71
5.2.	Results and discussion	72
5.3.	Photophysical properties	73
5.4.	Thermogravimetric properties	75
5.5.	Electrochemical properties	76
5.6.	Density Functional Theory calculation	78
5.7.	Application in Photovoltaics	81
5.8.	Experimental details	81
5.9.	Conclusions	84
5.10.	References	85

Chapter 6: Metal functionalized diketopyrrolopyrroles

6.1.	Introduction	91
6.2.	Results and discussion	92
6.3.	Photophysical properties	92
6.4.	Thermal properties	94
6.5.	Electrochemical properties	94
6.6.	Theoretical calculations	95
6.7.	Experimental section	98
6.8.	Conclusions	99
6.9.	References	99

Chapter 7: Diketopyrrolopyrrole based monomer, dimers and trimer: A comparative study

7.1.	Introduction	105
7.2.	Results and discussion	106
7.3.	Photophysical properties	107

7.4.	Thermal properties	109
7.5.	Electrochemical properties	109
7.6.	Theoretical calculations	111
7.7.	Application in Photovoltaics	113
7.7.	Experimental section	113
7.8.	Conclusions	116
7.9.	References	116
Chapter 8: Conclusions and future scope		
8.1.	Conclusions	123
8.2.	Scope for future work	125
8.3.	References	125

LIST OF FIGURES

Chapter 1. Introduction

- Figure 1.1.** Schematic representation of HOMO and LUMO energy levels in D–A system. 3
- Figure 1.2.** Chemical structure of diketopyrrolopyrrole. 4
- Figure 1.3.** UV/vis absorption and photoluminescence spectra of diphenyl DPP. 8
- Figure 1.4.** Chemical structure of **PCBTDP**. 16
- Figure 1.5.** General classification of DPPs in this work. 19
- ### Chapter 3. *N*-phenyl carbazole functionalized diketopyrrolopyrroles
- Figure 3.1.** Normalized electronic absorption spectra and photograph of **DPPs 5 – 8** in dichloromethane. 36
- Figure 3.2.** The fluorescence spectra of **DPPs 5 – 8** in dichloromethane. 37
- Figure 3.3.** Thermogravimetric analysis of **DPPs 5 – 8** measured at a heating rate of 10 °C min⁻¹ under nitrogen atmosphere. 38
- Figure 3.4.** CV (red line) and DPV (black line) oxidation plots of (a) **DPP 5**, (b) **DPP 6**, (c) **DPP 7**, and (d) **DPP 8**. 39
- Figure 3.5.** CV (red line) and DPV (black line) oxidation plots of (a) **DPP 5**, (b) **DPP 6**, (c) **DPP 7**, and (d) **DPP 8**. 40
- ### Chapter 4. Triphenylamine functionalized diketopyrrolopyrroles
- Figure 4.1.** Electronic absorption spectra of **DPPs 3 – 7** in DCM solution. 57
- Figure 4.2.** Thermogravimetric analysis of **DPPs 3 – 7** measured at heating rate of 10 °C / min under nitrogen atmosphere. 59
- Figure 4.3.** CV (red line) and DPV (black line) plots of TPA based **DPP3** (a), **DPP4** (b), **DPP5** (c), **DPP6** (d) and **DPP7** (e). 60
- Figure 4.4.** The frontier molecular orbitals of **DPPs 3 - 7** estimated by DFT calculation at B3LYP level. 62
- ### Chapter 5. Ferrocenyl functionalized diketopyrrolopyrroles
- Figure 5.1.** Photograph of **DPPs (5–7 and 9)** in dichloromethane. 73
- Figure 5.2.** Electronic absorption spectra of **DPPs 5 – 9** in dichloromethane solution. 74
- Figure 5.3.** Thermogravimetric analysis of **DPPs 5 – 8** measured at a heating rate of 10 °C / min under nitrogen atmosphere. 76

Figure 5.4.	CV (red line) and DPV (black line) plots of (a) DPP 5 , (b) DPP 6 , (c) DPP 7 (d) DPP 8 and DPP 9 .	77
Figure 5.6.	The frontier molecular orbitals of DPPs 5–9 estimated by DFT calculations.	79
Figure 5.7.	Absorption curves of DPPs 5 – 7 and DPP9 in different solvents.	81
Chapter 6.	Metal functionalized diketopyrrolopyrroles	
Figure 6.1.	Chemical structures of metal coordinated DPPs.	92
Figure 6.2.	Normalized electronic absorption spectra of Co-DPP-Co and Fc-DPP-Fc in dichloromethane solution.	93
Figure 6.3.	TGA of Co-DPP-Co and Fc-DPP-Fc .	94
Figure 6.4.	CV (red line) and DPV (black line) oxidation plots of a) Co-DPP-Co and b) Fc-DPP-Fc .	95
Figure 6.5.	CV (red line) and DPV (black line) reduction plots of (a) Fc-DPP-Fc and (b) Co-DPP-Co .	95
Figure 6.6.	The frontier molecular orbitals of Co-DPP-Co and Fc-DPP-Fc .	96
Figure 6.7.	The frontier molecular orbitals of Co-DPP-Co and Fc-DPP-Fc at B3LYP/6-31G(d) level.	97
Chapter 7.	Diketopyrrolopyrrole based monomer, dimers and trimer: A comparative study	
Figure 7.1.	Chemical structures of DPP based monomer (1), dimers (2 and 3) and trimer (4).	106
Figure 7.2.	Normalized electronic absorption spectra of DPP based monomer (1), dimers (2 and 3) and trimer (4) in dichloromethane solution.	108
Figure 7.3.	TGA of DPP based monomer (1), dimers (2 and 3) and trimer (4).	109
Figure 7.4.	CV (red line) and DPV (black line) oxidation plots of DPP based monomer (1), dimers (2 and 3) and trimer (4).	110
Figure 7.5.	CV (red line) and DPV (black line) reduction plots of DPP based monomer (1), dimers (2 and 3) and trimer (4).	110
Figure 7.6.	Frontier molecular orbitals of the DPP based monomer (1),	

	dimers (2 and 3) and trimer (4) estimated by DFT calculation.	111
Figure 7.7.	Frontier molecular orbital of the DPP based trimer (4) estimated by DFT calculation.	112

LIST OF SCHEMES

Chapter 1. Introduction

Scheme 1.1.	Farnum's synthesis of DPP.	5
Scheme 1.2.	Farnam's postulated mechanism of DPP formation <i>via</i> Reformatsky conditions.	5
Scheme 1.3.	Succinic ester route of DPP synthesis.	6
Scheme 1.4.	Preparation of DPP <i>via</i> the succinic ester route.	6
Scheme 1.5.	Mixed condensation of different aromatic nitriles with a succinic acid ester.	7
Scheme 1.6.	Synthesis of DPPs from 2, 5-Dihydrofuro[4,3-c]furan-1,4-diones.	7
Scheme 1.7.	Synthesis of alkyl-substituted bromo- DPPs 3 and 4 .	9
Scheme 1.8.	Synthesis of DPPs 2 – 5 .	10
Scheme 1.9.	Synthesis of DPPEZnP-THE .	11
Scheme 1.10.	Synthesis of PDPP3T .	11
Scheme 1.11.	Synthesis of tetracyanobutadiene (TCBD) bridged DPP 3 .	12
Scheme 1.12.	Synthesis of BDT-2DPP .	15
Scheme 1.13.	Synthesis of DPP-Cy .	17
Scheme 1.14.	Synthesis of PDTDPPTe .	17
Chapter 3.	<i>N</i>-phenyl carbazole functionalized diketopyrrolopyrroles	
Scheme 3.1.	Synthesis of <i>N</i> -phenyl carbazole substituted DPPs 5 and 6 .	34
Scheme 3.2.	Synthesis of <i>N</i> -phenyl carbazole substituted TCBD derivatives 7 and 8 .	35
Chapter 4.	Triphenylamine functionalized diketopyrrolopyrroles	
Scheme 4.1.	Scheme 4.1: Synthesis of TPA based DPPs 3 and 4 .	56
Scheme 4.2.	Synthesis of TPA based TCBD bridged DPPs 5–7 .	57
Chapter 5.	Ferrocenyl functionalized diketopyrrolopyrroles	
Scheme 5.1.	Synthesis of ethyne bridged ferrocenyl DPPs 5 and 6 .	72
Scheme 5.2.	Synthesis of TCBD based ferrocenyl DPPs 7 – 9 .	73

Chapter 6.	Metal functionalized diketopyrrolopyrroles	
Scheme 6.1.	Synthesis of Co-DPP-Co.	92
Chapter 7.	Diketopyrrolopyrrole based monomer, dimers and trimer: A comparative study	
Scheme 7.1.	Synthesis of DPP based monomer (1), dimers (2 and 3) and trimer (4).	107

LIST OF CHARTS

Chart 1.1.	Chemical structures of electron donor units.	2
Chart 1.2.	Chemical structures of electron acceptor units.	2
Chart 1.3.	Chemical structures of metal functionalized DPPs Pt-DPP-Pt-1 and Pt-DPP-Pt-2.	11
Chart 1.4.	Chemical structures of DPP-TPA and DPPCN-Fc.	13
Chart 1.5.	Chemical structures of DPPs 1 and 2.	14
Chart 1.6.	Chemical structures of SM1 and SM2.	15
Chart 1.7.	Chemical structures of DPP-Py1 and DPP-Py2.	17

LIST OF TABLES

Chapter 3.	N-phenyl carbazole functionalized diketopyrrolopyrroles	
Table 3.1.	Photophysical, thermal and computational properties of DPPs 5 – 8.	37
Table 3.2.	Electrochemical properties of DPPs 5 – 8.	40
Table 3.3.	The frontier molecular orbitals of DPPs 5 – 8 estimated from DFT calculations.	41
Table 3.4.	Calculated Electronic Transitions for DPPs 5 – 8 in the Gas phase.	42
Chapter 4.	Triphenylamine functionalized diketopyrrolopyrroles	
Table 4.1.	Photophysical and thermal properties of DPPs 3 – 7.	58
Table 4.2.	Electrochemical properties of DPPs 3 – 7.	61
Table 4.3.	The main electronic transitions with composition and oscillator Strengths for DPPs 3 – 7.	63
Chapter 5.	Ferrocenyl functionalized diketopyrrolopyrroles	

Table 5.1.	Photophysical properties of DPPs 5 – 9.	78
Table 5.2.	Electrochemical properties of DPPs 5 – 9.	79
Table 5.3.	Calculated major electronic transitions for DPPs 5 – 9 in the gas phase.	80
Table 5.4.	Absorption maxima of DPPs 5 – 7 and 9 in different solvents.	80
Chapter 6.	Metal functionalized diketopyrrolopyrroles	
Table 6.1.	Photophysical, thermal and electrochemical properties of Co-DPP-Co and Fc-DPP-Fc.	93
Table 6.2.	Calculated electronic transitions Co-DPP-Co for and Fc-DPP-Fc in the gas phase.	98
Chapter 7.	Diketopyrrolopyrrole based monomer, dimers and trimer: A comparative study	
Table 7.1.	Photophysical, thermal and electrochemical properties of DPP based monomer (1), dimers (2 and 3) and trimer (4).	108
Table 2.	The major electronic transitions calculated from TD-DFT for DPP based monomer (1), dimers (2 and 3) and trimer (4) in the gas phase.	113

ACRONYMS

D-A	Donor-acceptor
NMR	Nuclear Magnetic Resonance
PPh ₃	Triphenylphosphine
DMF	Dimethylformamide
DCM	Dichloromethane
DCE	Dichloroethane
TGA	Thermogravimetric Analysis
IR	Infrared
UV-Vis	UV-Visible Spectroscopy
Calcd.	Calculated
CDCl ₃	Chloroform-d
ESI-MS	Electrospray Ionization- Mass Spectrometry
MeOH	Methanol
THF	Tetrahydrofuran
TLC	Thin Layer Chromatography
TEA	Triethylamine

NOMENCLATURE

λ	Wavelength
ε	Extinction coefficient
π	Pi
\AA	Angstrom
nm	Nanometer
cm	Centimeter
$^{\circ}$	Degree
$^{\circ}\text{C}$	Degree Centigrade
mmol	Millimol
mL	Milliliter
μL	Microliter
a. u.	Arbitrary Unit

Chapter 1

Introduction

1.1. General Introduction

The growing requirement of energy has captured the attention of scientific community towards generation of clean and renewable energy sources at low cost. The generation of energy from sunlight using solar cell devices is one of the most significant long-term solution. The π -conjugated polymers and small molecules are of significant interest due to their number of applications such as organic light-emitting diodes (OLEDs), organic solar cells (OSCs), two photon absorption and organic field-effect transistors (OFETs).^[1,2] The thermal stability, broad absorption in the visible region and low HOMO-LUMO gap values in small organic molecules make them potential candidate for optoelectronics.^[3] Donor-acceptor (D-A) approach is one of the useful ways to design the materials with absorption in Vis-NIR region with low band gap.

1.2. Donor-Acceptor Systems

The donor-acceptor (D-A) system consists of combination of electron rich donor with electron deficient acceptor through appropriate spacer (Figure 1.1).

Donor

The molecule which possesses the ability to donate the electron to another molecule is known as donor, for example, the groups containing heteroatoms with lone pair of electrons, amines, alcohols, sulphides etc. The other examples of metallocene derivatives such as ferrocene, ruthenocene and aromatic carbocycles are well known donors (Chart 1.2). Ferrocene, carbazole and triphenylamine (TPA) are widely used donors for designing molecular systems with low HOMO-LUMO gap.

[4-6]

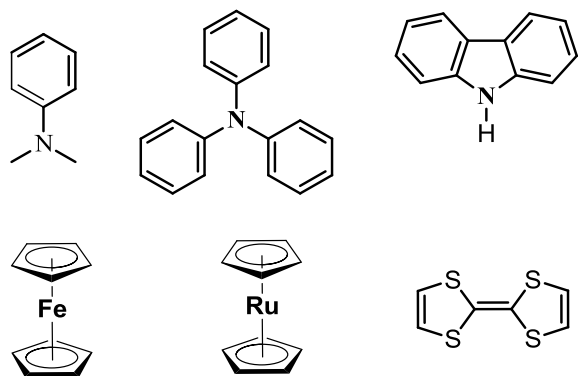


Chart 1.1. Chemical structures of electron donor units.

Acceptor

The molecule which possesses the ability to withdraw electrons from another molecule is known as acceptor. The acceptor strength of molecule to withdraw the electron depends on the lowest energy unoccupied molecular orbital (LUMO). Low lying the LUMO, stronger will be the accepting capacity of acceptor and *vice versa*. The examples of acceptors include amides, nitriles and esters, nitrogen rich heterocycles, boron complexes, ketones, tetracyano acceptors etc. (Chart 1.2).

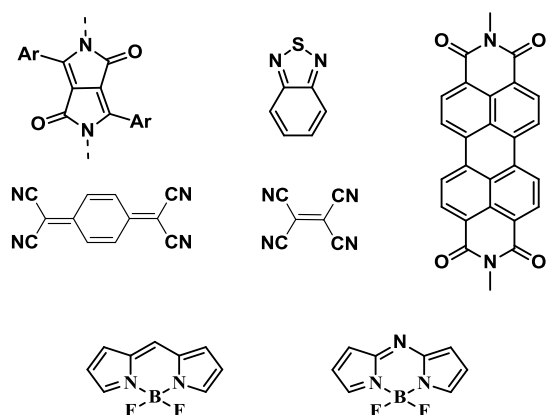


Chart 1.2. Chemical structures of electron acceptor units.

The LUMO of D-A system is stabilized as compared to individual donor and acceptor units, whereas the HOMO is destabilized as compared to that of individual donor and acceptor units (Figure 1.1). The combination of donor and acceptor with appropriate π -linker (such as double or triple bond, aromatic ring) results in red shift of the absorption spectra with lowering of HOMO-LUMO gap.

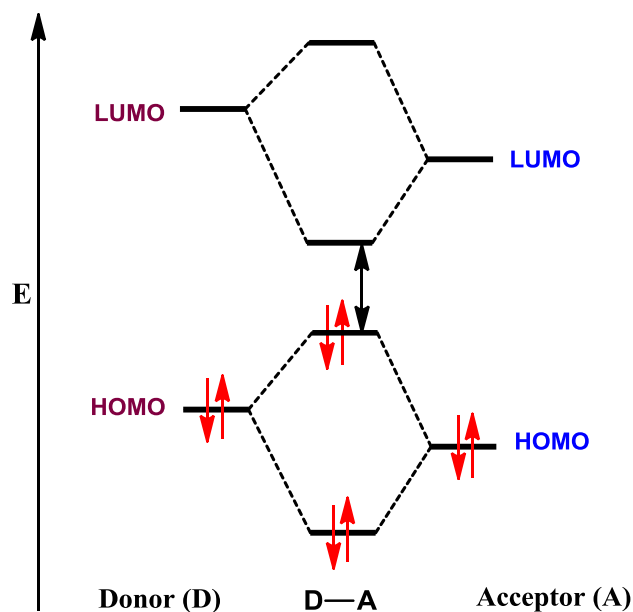


Figure 1.1. Schematic representation of HOMO and LUMO energy levels in D–A system.

The strength of D-A interaction depends on the strength of donor as well as strength of acceptor and the nature of π -linker also plays key role in determining the strength of D-A system.

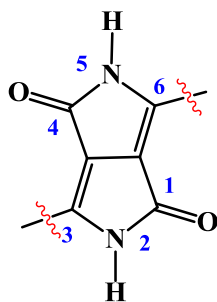
The D-A systems exhibit various applications in diverse fields^[7–9] such as;

- ❖ Organic Solar Cells (OSCs)
- ❖ Organic Light Emitting Diodes (OLEDs)
- ❖ Non-Linear Optics (NLO)
- ❖ Mechanochromism
- ❖ Organic Field Effect Transistors (OFETs)
- ❖ Photodynamic Therapy

1.3. Diketopyrrolopyrrole (DPP)

DPP is a 8π electron bicyclic system containing two lactam units. The diphenyl-DPPs have melting points over $350\text{ }^{\circ}\text{C}$ and possess very low solubility in most of the organic solvents. The alkyl chains were substituted on amidic nitrogen to improve the solubility in organic solvents. DPP possess excellent properties such as strong electron withdrawing nature, light absorption in visible region, highly conjugated and coplanar molecular structure, excellent photochemical and thermal

stability. DPP is one of attractive unit used for the designing of small molecule as well as polymer based efficient materials for OSCs.



Diketopyrrolopyrrole (DPP)

Figure 1.2. Chemical structure of diketopyrrolopyrrole (DPP).

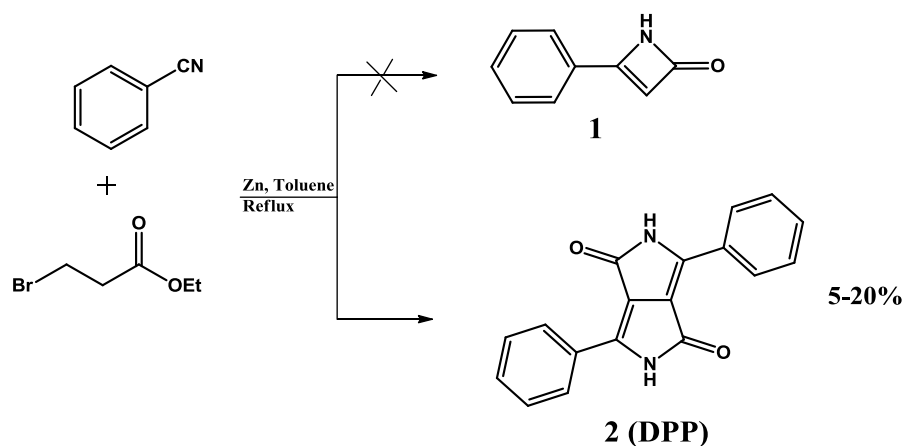
The dithienyl-DPP possesses planar structure due to the hydrogen bonding of oxygen in the DPP units with the β -hydrogens on the adjacent thiophenes which induces intermolecular interactions as well. The HOMO and LUMO energy levels of unsubstituted thienyl DPP are -5.3 eV and -3.4 eV respectively. The electron donors (P3HT and other polymer donors) generally used to fill the essential criterion of conjugated materials such as higher LUMO energy levels above -3.1 eV, for efficient exciton separations.

The simple synthesis, intense color, excellent stability, and low solubility exhibited by DPP, it has been used for the applications such as pigments in paints, varnishes, and high-quality printing. Farnum *et al.* in 1974 first reported the synthesis of the 3, 6-diphenyldihydropyrrolo[3,4-c]pyrrole-1,4-dione (DPP) in very low yield in an attempt of formation of 2 azetinone by Reformatsky reaction of benzonitrile, ethyl bromoacetate, and zinc (Scheme 1.1).^[10]

1.4. Synthesis of Diketopyrrolopyrrole

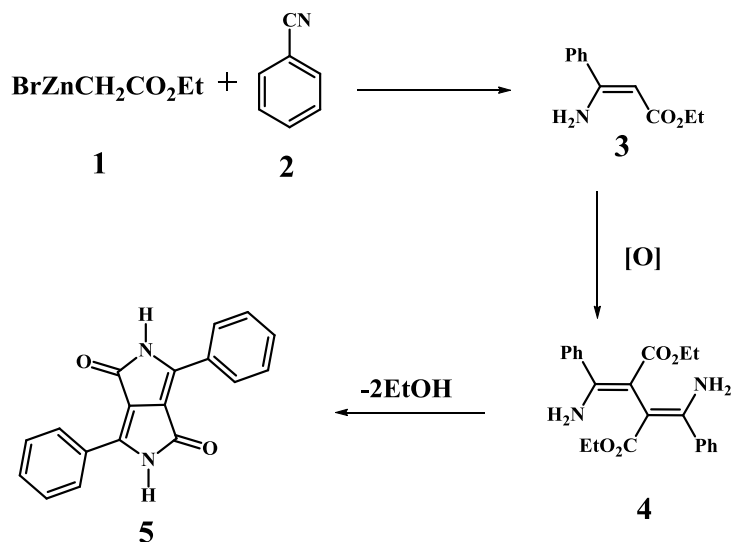
1.4.1. Reformatsky Route

Farnum *et al.* in 1974 tried to synthesize unsaturated β -lactam **1** by the reaction of benzonitrile with bromo-ethyl acetate in the presence of zinc *via* Reformatsky conditions but the attempt to get desired product was failed instead they obtained unknown dilactam **2** along with several by-products (Scheme 1.1). The authors observed properties like a bright red color and very low solubility of dilactam **2** and realized it could be organic pigment.



Scheme 1.1. Farnum's synthesis of DPP.

In order to explain the formation of dilactam **5**, Farnum has given mechanism which is shown in Scheme 1.2. The addition of organ zinc compound **1** to benzonitrile **2** is first step which gives ethyl 2-aminocinnamate **3**. Then intermediate compound **3** undergoes oxidative dimerization to obtain compound **4**, further the loss of two ethanol molecules led to final compound **5 (DPP)**.

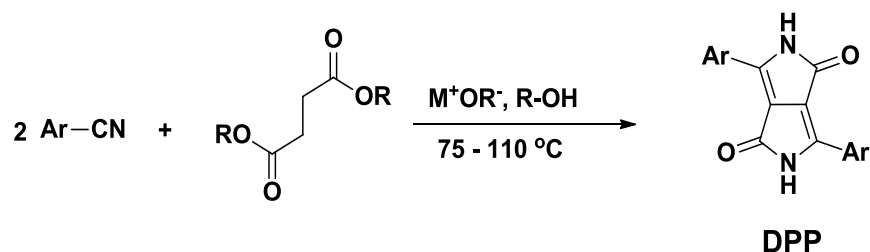


Scheme 1.2 Farnum's postulated mechanism of DPP formation *via* Reformatsky conditions.

1.4.2. Succinic Ester Route

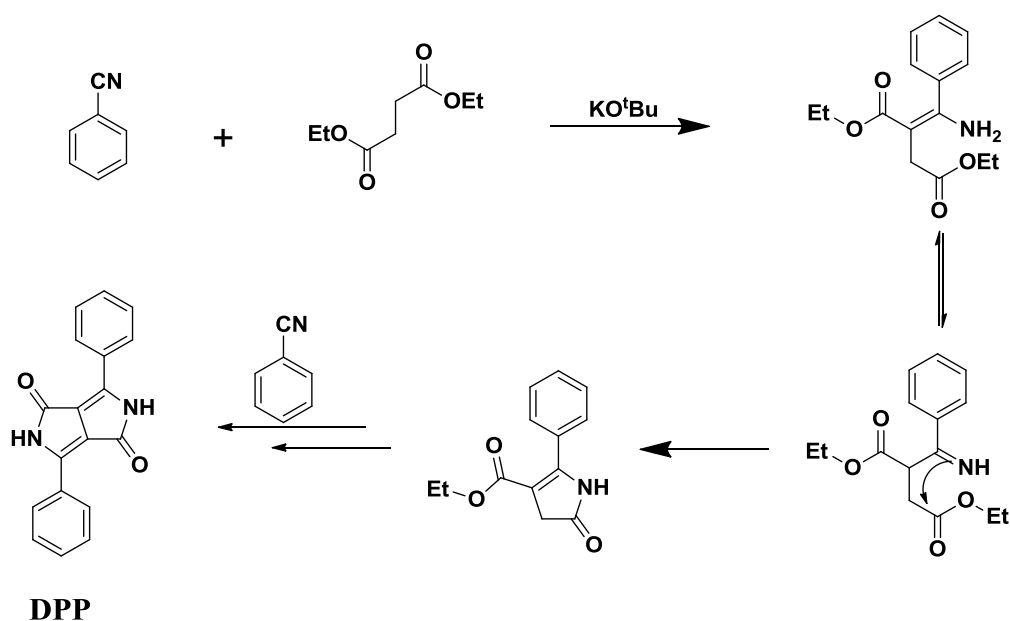
The researchers from Ciba-Geigy company developed method to synthesize DPP from benzonitrile and dialkyl succinate in the presence of base such as alkali metal alkoxides.^[11] This reaction proceeded through similar mechanism as like Reformatsky route but the only difference was that, DPP is made from the reaction

of aromatic nitrile with dialkyl succinate. They optimized procedure and showed that when succinates of starting materials from secondary or tertiary alcohols are used and use of tertiary alkoxides as bases along with solvents such as tertiary alcohol gives the best results.



Scheme 1.3 Succinic ester route of DPP synthesis.

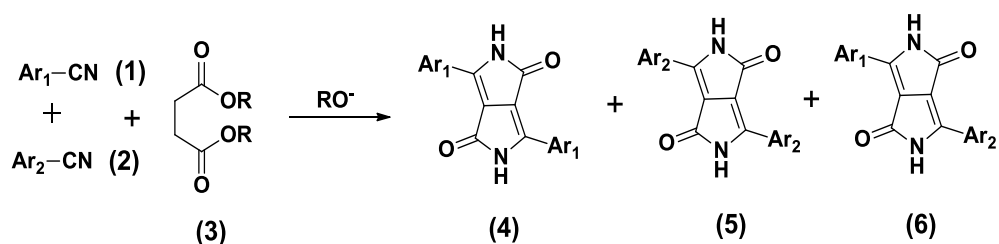
Mechanism



Scheme 1.4 Preparation of **DPP** *via* the succinic ester route.

1.4.3. Condensation of Nitrile with 3-Alkyloxycarbonyl-2-pyrroline-5-one

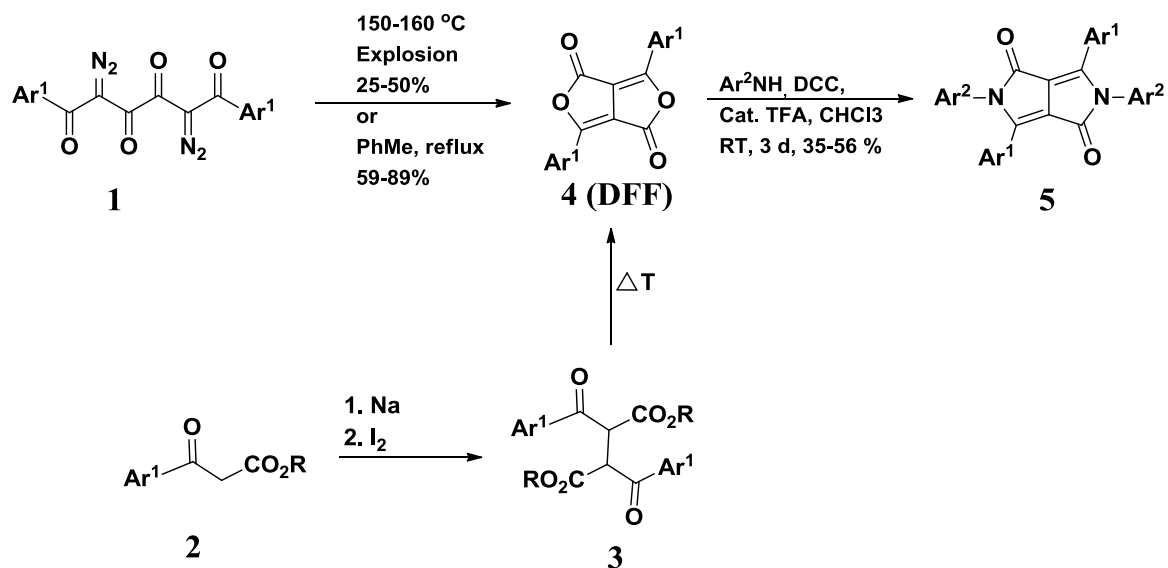
The DPPs have been generally synthesized by the succinic ester route but this method is restricted only to the synthesis of symmetrical DPPs.^[12] The two different aromatic nitriles were reacted with a succinic ester in order to synthesize the unsymmetrical DPP with different aryl substituents at 3- and 6- positions. In this reaction three products were obtained, one was unsymmetrical DPP **6** along with two symmetrical DPPs **4** and **5** (Scheme 1.5) but the separation of these DPPs was impossible due to very low solubility.



Scheme 1.5 Mixed condensation of different aromatic nitriles with a succinic ester.

1.4.4. Synthesis of DPP from 2, 5-Dihydrofuro[4,3-c]furan-1,4-diones (DFFs)

Rubin *et al.* in 1980 observed explosive decomposition of unstable bisdiazotetraketones by heating **1** resulted in the 3, 6-diaryl-2,5-dihydrofuro[4,3-c]furan-1,4-diones **4** (or diketofurofurans, DFFs), analogues of DPP.^[13] The **4** (DFF) can be readily transformed into *N,N*-diaryl DPP **5** through reactions with aromatic amines in the presence of DCC and a catalytic amount of trifluoroacetic acid (TFA). An alternative route to the synthesis of DFF is by the thermolysis of diacylsuccinates **3** which was formed by the reaction of β -ketoesters **2** with iodine under basic condition.



Scheme 1.6 Synthesis of DPP from 2, 5-Dihydrofuro[4,3-c]furan-1,4-diones.

The succinic ester route is regarded as the best one from all the routes. DPP possesses the good thermal stability as well as photo stability, high quantum yields and large Stokes shifts. The alkylation at *N*-position of lactam ring has been carried out to improve the solubility of DPP in organic solvents.

1.4. Absorption Spectra of diketopyrrolopyrrole

The diaryl DPP derivatives exhibit solution state absorption in the range of 470 nm to 520 nm and emission in the range of 508 nm to 540 nm.^[14] The solid state absorption is comparatively red shifted due to intermolecular interactions and π - π stacking.

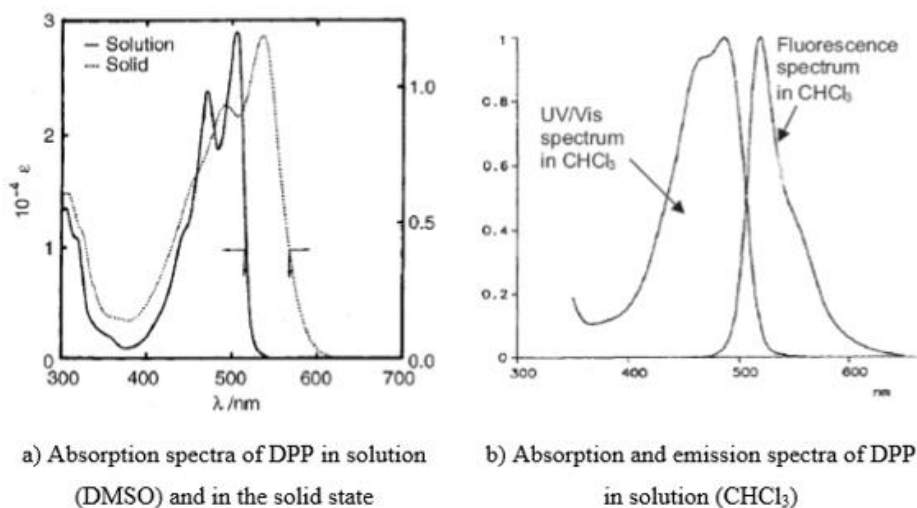
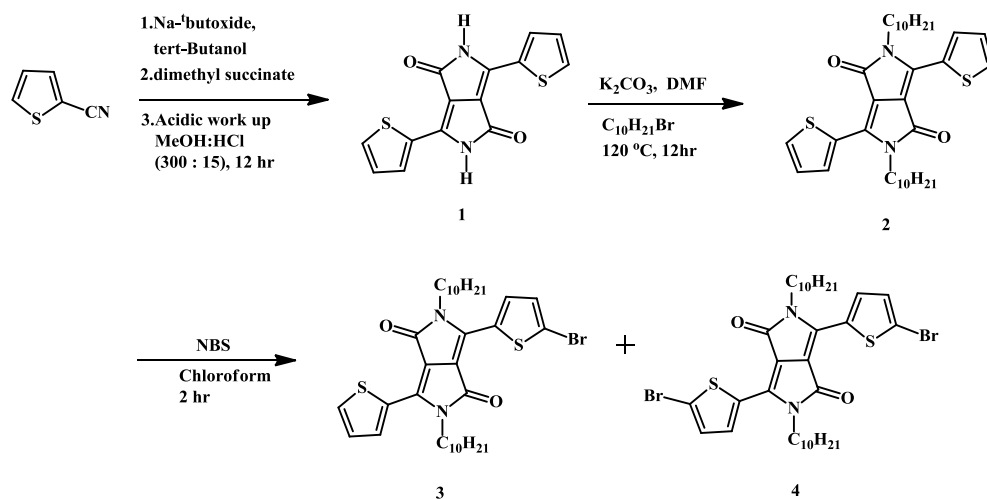


Figure 1.3. UV/vis absorption and photoluminescence spectra of diphenyl DPP.

1.6. Reactions of diketopyrrolopyrrole (DPP)

1.6.1. Alkylation and bromination (Synthesis of Mono- and di-bromo DPPs)

The starting precursor's monobromo-DPP **3** and dibromo-DPP **4** were synthesized by procedures as shown in Scheme 1.7. DPP **1** was synthesized by using procedure which involves the reaction of 2-thiophenecarbonitrile with half equivalent of dimethyl succinate in presence of strong base sodium *tert*-butoxide in *tert*-butanol at 120 °C for 12 hours under argon atmosphere and worked up by methanol: hydrochloric acid (300ml methanol: 15ml conc. HCl), filtered on Buchner funnel and finally washed with methanol yielded maroon solid with 65% yield. In order to make it soluble, DPP **1** was reacted with excess amount of 1-bromodecane in presence of base K₂CO₃ in *N,N*-dimethyl formamide (DMF) at 120 °C for 12 hours under argon atmosphere. The reaction contents were cooled to room temperature and solvent was removed under vacuum. The crude compound was purified by silica column-chromatography (eluted with 50% dichloromethane in hexane) yielded 23% shiny crystalline solid (DPP **2**).



Scheme 1.7. Synthesis of alkyl-substituted bromo-DPPs **3** and **4**.

Then DPP **2** was further brominated with *N*-bromosuccinimide (NBS) and mixture of mono- and di-brominated DPP (**3** and **4**) was obtained. Bromination reaction was carried out at room temperature in dry chloroform and compounds **3** and **4** were purified by the use of silica-column chromatography, eluted with 30–80% of dichloromethane in hexane yielded 90% of pure compounds.

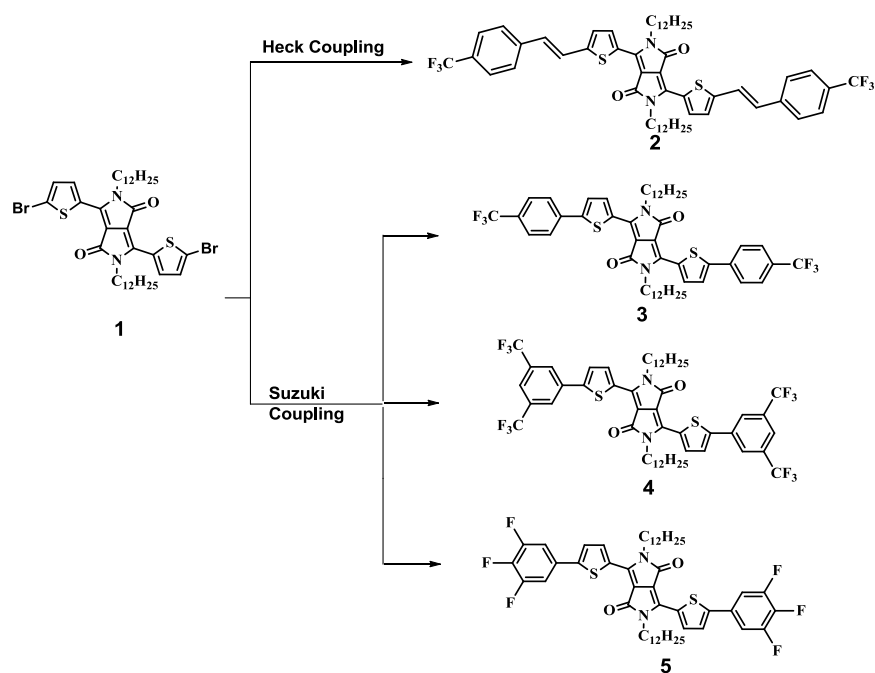
1.6.2. Cross-coupling Reactions of DPP:

The one of common pathway to design and synthesize D-A system based on DPP involves the cross-coupling reaction of the bromo DPP with different aryls in presence of Pd-catalyst. The various cross-coupling reactions of DPP include Suzuki coupling, Heck coupling, Sonogashira coupling and Stille coupling reactions.

1.6.2.1. Heck and Suzuki Coupling

This protocol involves the use of mono/dibromo derivative of DPP to react with boronic acid/ester, vinylic or acetylene substituted derivative in presence of Pd-catalyst such as tetrakis(triphenylphosphine)palladium(0) [Pd(PPh₃)₄]/bis(triphenylphosphine)palladium(II) dichloride [Pd(PPh₃)₂Cl₂] with triethylamine as a base. Heck coupling involves palladium-catalyzed C-C bond coupling between bromo DPP and vinyl halides in the presence of Pd-catalyst with base.

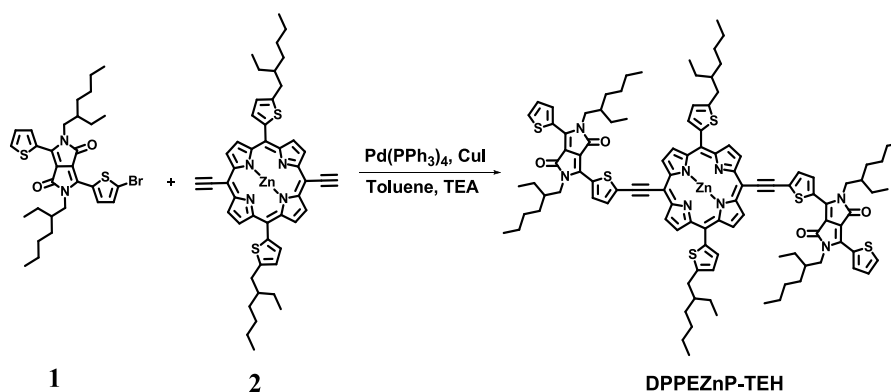
Sonar *et al.* enhanced electron affinity of DPP by functionalizing it with electron withdrawing fluorophenyl and trifluoromethylphenyl groups.^[15] The fluorophenyl and trifluoromethylphenyl substituted DPPs **3–5** were synthesized by the use of Suzuki coupling reaction whereas the vinyl bridged trifluoromethyl phenyl substituted DPP **2** was synthesized by Heck coupling reaction (Scheme 1.8).



Scheme 1.8. Synthesis of DPPs 2 – 5.

1.6.2.2. Sonogashira Coupling

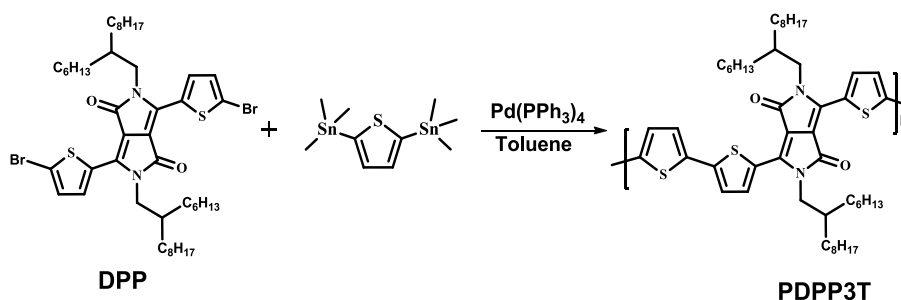
Russell *et al.* have designed and synthesized small molecule **DPPEZnP-TEH** containing porphyrin as a central core and DPP as end group by the Pd-catalyzed Sonogashira cross coupling reaction (Scheme 1.9).^[16] The Sonogashira coupling reaction of one equivalent of 5, 15-diethynyl-10, 20-bis(5-(2-ethylhexyl)-thienyl)-porphyrin zinc **2** with two equivalents of mono-bromo diketopyrrolopyrrole **1** resulted in the formation of **DPPEZnP-TEH**. The **DPPEZnP-TEH** exhibits broad light absorption in visible to NIR region with very low band gap of 1.37 eV. When used as a donor for BHJ OSCs, an open-circuit voltage of 0.78 V was obtained with a low energy loss of only 0.59 eV, which was the first report for energy losses <0.6 eV as small molecule.



Scheme 1.9. Synthesis of **DPPEZnP-TEH**.

1.6.2.3. Stille Coupling

Hong *et al.* used Pd-catalyzed Stille coupling reaction for the synthesis of DPP based polymer **PDPP3T** to study thermoelectric properties (Figure 1.10).^[17] When a di-bromo **DPP** reacts with bis(trimethylstannyl)thiophene in presence of Pd-catalyst [Pd(PPh₃)₄] in toluene for 16 hours resulted the polymer **PDPP3T** in 83% yield.



Scheme 1.10. Synthesis of **PDPP3T**.

1.6.3. Metal Functionalized DPPs

The synthesis of organic chromophores with strong absorption in the near infrared (NIR) region has gained considerable attention of the scientific community due to their applications in optoelectronics and in biomedical imaging.^[18,19] The NIR absorbing small molecules possess low HOMO-LUMO gap, larger dielectric constant, high dipole moment, and lower exciton binding energy which are promising features for generating efficient materials for optoelectronic applications.^[20,21] In this regard Schanze *et al.* reported the synthesis and photophysical properties of chromophores containing ortho-metalated 2-thienylpyridinyl (platinum) end groups, **Pt-DPP-Pt-1** and platinum acetylide derivative, **Pt-DPP-Pt-2** of the DPP (Chart 1.3)^[22] They observed that the metal auxochromes have a

pronounced effect on the chromophores' photophysical properties. The reduction in the fluorescence was observed due to a spin-orbit coupling induced by the metal centers which is more pronounced in **Pt-DPP-Pt-2**.

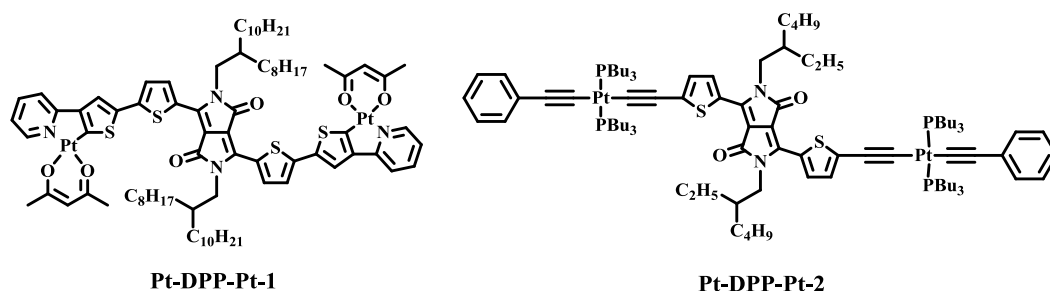
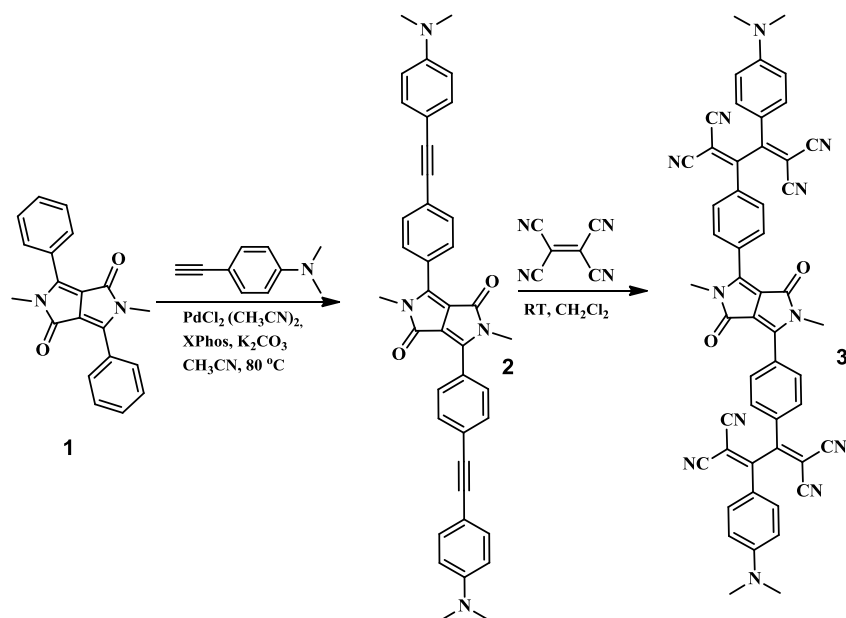


Chart 1.3. Chemical structures of metal functionalized DPPs **Pt-DPP-Pt-1** and **Pt-DPP-Pt-2**.

1.6.4. [2+2] cycloaddition–retroelectrocyclization reaction

An efficient strategy to improve the strength of D-A interaction by incorporation of electron deficient tetracyanoethylene (TCNE) through [2+2] cycloaddition–retroelectrocyclization reaction has been explored by Diederich *et al.*^[23–25] In order to lower the LUMO level of the DPP, electron-withdrawing groups has been incorporated.



Scheme 1.11. Synthesis of tetracyanobutadiene (TCBD) bridged DPP **3**.

The electron accepting ability of DPP has been improved by introducing electron withdrawing pentafluorophenyl and tetracyanobutadiene (TCBD) groups^[26] (Scheme 1.11). The TCBD derivative **3** exhibited broad absorption in visible

region corresponds to π - π^* transition of DPP core, charge transfer from the *N,N*-dimethyl aniline to TCBD and DPP core and showed reversible reduction peaks.

1.7. Applications of Diketopyrrolopyrroles

The DPP based D-A molecular architectures have been explored for various applications. Some of the important applications are discussed here,

1.7.1. Photothermal cancer therapy

Photothermal therapy for cancer treatment is gaining attention among other treatments, as it is highly selective and noninvasive therapeutic method by the use of NIR laser-induced ablation of tumor cells.^[27,28] Dong *et al.* recently reported the triphenylamine and ferrocenyl functionalized DPP based small molecules **DPP-TPA** and **DPPCN-Fc** as promising cancer theranostic agents for cancer therapy and achieved photothermal conversion efficiency of 34.5% and 59.1% respectively^[29,30](Chart 1.4).

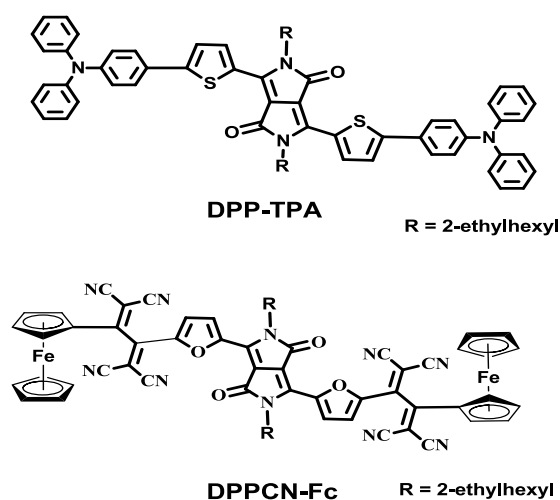


Chart 1.4. Chemical structures of **DPP-TPA** and **DPPCN-Fc**.

1.7.2. Dye sensitized solar cells (DSSCs):

Dye-sensitized solar cells (DSSCs) have gained attention of scientific community as it is one of the promising sources for renewable energy systems with high power conversion efficiency and low production cost.^[31] The two triphenylamine based DPP derivatives **1** and **2** were synthesized and used for DSSCs by Tian *et al.*^[32] (Chart 1.5). The photophysical and electrochemical properties

indicated that the energy levels can be tuned by alternating the π -conjugated systems. When DPPs **1** and **2** used for DSSC showed overall conversion efficiency of 4.14% with a short-circuit photocurrent density (J_{sc}) of 9.78 mA cm⁻² and a fill factor (FF) of 0.69.

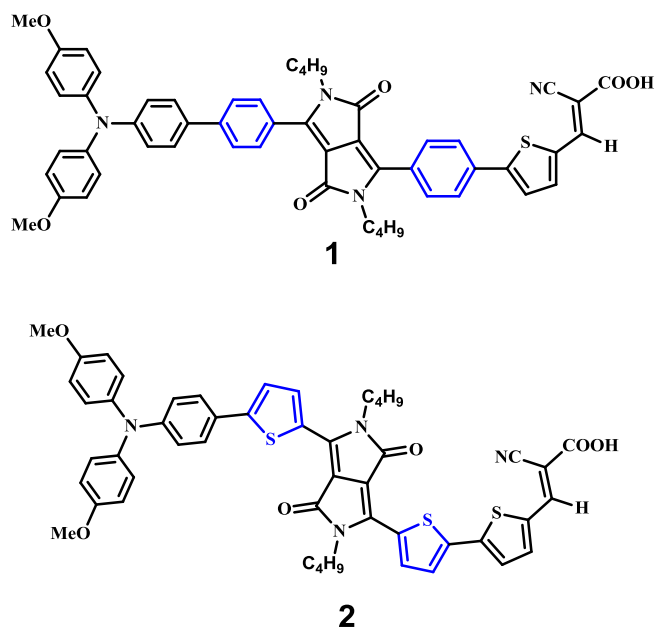


Chart 1.5. Chemical structures of DPPs **1** and **2**.

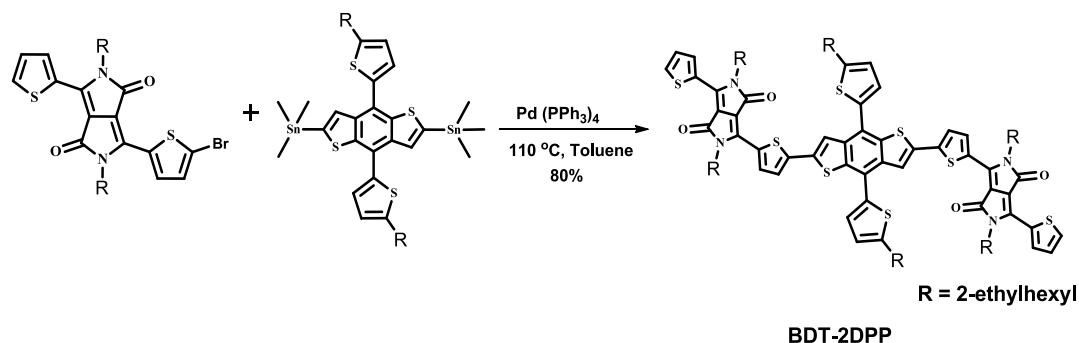
1.7.3. Bulk heterojunction (BHJ) organic solar cells:

Organic solar cells (OSCs) have been explored as a renewable energy source as it can convert sunlight into electricity at low cost.^[33] A substantial improvement in the performance of OSCs have been observed in based on bulk heterojunction (BHJ) containing a conjugated polymer as an electron donor and a fullerene as an electron acceptor.^[34] DPP possesses excellent properties such as strong electron affinity, light absorption in the visible region, highly conjugated coplanar molecular structure, and excellent photochemical stability.^[35] DPP is one of the widely used acceptor unit for the synthesis of small molecule based non-fullerene electron acceptors.^[36]

1.7.3.1. As donor in bulk heterojunction organic solar cells (BHJ-OSCs)

Zhan *et al.* reported linear small molecule **BDT-2DPP** based on 5-alkylthiophene-2-yl-substituted benzodithiophene as core and DPP as arms for BHJ OSCs (Scheme 1.12).^[37] **BDT-2DPP** possesses excellent thermal stability, broad absorption with low band gap and energy levels matched with PC₆₁BM.

When they used **BDT-2DPP** as donor along with PC₆₁BM acceptor in BHJ OSCs achieved a PCE of 4.09% and after thermal annealing treatment improved the PCE up to 5.79%.



Scheme 1.12. Synthesis of **BDT-2DPP**.

1.7.3.2. As Acceptor in bulk heterojunction organic solar cells (BHJ-OSCs)

Huang and coworkers reported two novel three-dimensional acceptor materials **SM1** and **SM2** with tetraphenylethylene (TPE) and 4,4'-spirobi[cyclopenta[2,1-b;3,4-b']dithiophene] (SCPDT) as the cores and dicyanovinyl (DCV) end-capped DPP as the arms (Chart 1.6).^[38] The introduction of DCV in DPP lowers the energy levels of the material which allow to use as acceptor with low energy-level donor materials such as **PTB7-TH** in solar cell devices. When blended with PTB7-TH, the **SM1** and **SM2** showed maximum PCE of 4.20% and 4.01% respectively.

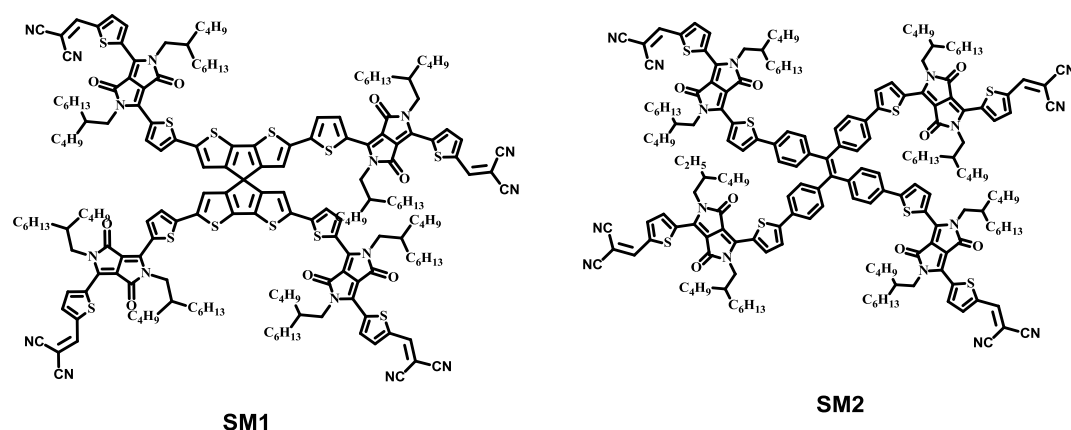


Chart 1.6. Chemical structures of **SM1** and **SM2**.

1.7.4. Perovskite solar cells

The DPP based hole transporting material (HTM) **PCBTDPP** was introduced by Qiu *et al.* in 2013 for hybrid solar cells (Figure 1.4).^[39] In this study they used **PCBTDPP** as the HTM to study solid state hybrid solar cells made up of the light harvester $\text{CH}_3\text{NH}_3\text{PbBr}_3$ -nanoparticles and TiO_2 (mp- TiO_2) as the electron transporting material (ETM).

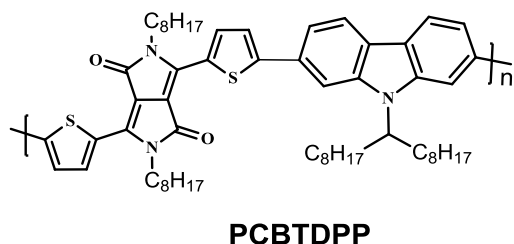
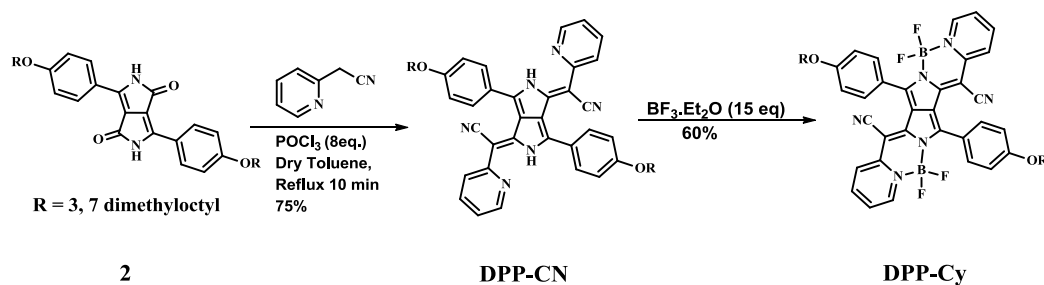


Figure 1.4. Chemical structure of **PCBTDPP**.

The devices showed a 3.04% of PCE along with open circuit voltage (V_{oc}) of -1.15 V. They further used $\text{CH}_3\text{NH}_3\text{PbI}_3$ by replacing $\text{CH}_3\text{NH}_3\text{PbBr}_3$ as the light harvester, and achieved a higher PCE of 5.55%.

1.7.5. Organic Light Emitting Diodes (LEDs)

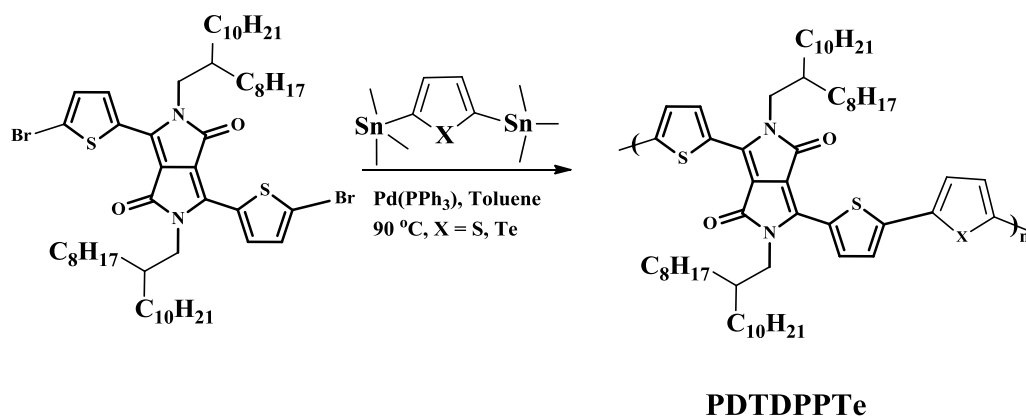
Organic light emitting diodes (OLEDs) operating in the NIR region are getting attention of scientific community due to various applications including flexible self-medicated pads for photodynamic therapy, lab-on-chip platforms for medical diagnostics, night vision and plastic-based telecommunications. Beverina *et al.* reported the first example of NIR-OLEDs based on a NIR emitting DPP-borondifluoride cyanine emitter **DPP-Cy**^[40] (Scheme 1.13). **DPP-Cy** represents an alternative to existing NIR chromophores for all-organic NIR-OLEDs emitting in the transparency window of biological tissues, which is particularly interesting for bioimaging and photodynamic therapy technologies. The incorporation of DPP derivative to conductive polymer matrix they achieved a 0.55% of external quantum efficiency (EQE). Herein they incorporated the functionalized DPP which emits at ~760 nm to active matrix of poly(9,9-dioctylfluorene-altbenzothiadiazole) and achieved 0.5% efficiency without use of complex light out-coupling or encapsulation.



Scheme 1.13. Synthesis of **DPP-Cy**.

1.7.6. Organic Field effect transistors (OFET)

DPP derivatives have been widely used for high mobility semiconductors for OTFTs^[41,42] since it strengthens π - π intermolecular interactions. Choi *et al.* reported the design and synthesis of a DPP-based polymer containing tellurophene **PDTDPPTe** for OTFTs^[43] (Scheme 1.14). They reported the synthesis of a DPP and tellurophene based polymer using the Pd-catalysed Stille coupling reaction in 88% yield. The **PDTDPPTe** polymer exhibited a high hole mobility of $\mu_{\max} = 1.78 \text{ cm}^2 \text{ V}^{-1} \text{ s}^{-1}$, due to the polymer chains exhibited better edge-on orientation and the strong donor capacity of the tellurophene.

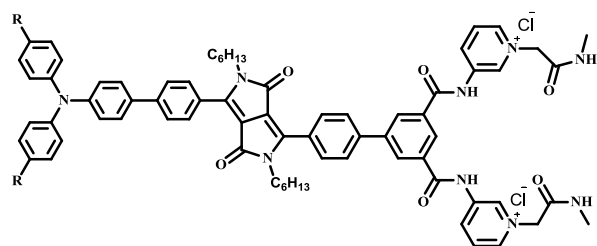


Scheme 1.14. Synthesis of **PDTDPPTe**.

1.7.7. Fluorescent sensors

Two DPP based fluorescent chemosensors **DPP-Py1** and **DPP-Py2** were reported using symmetrical diamides as recognition groups for selective and fast detection of citrate in the near-infrared region^[44] (Chart 1.7). It has been observed that **DPP-Py1** has higher accuracy and sensitivity with a relatively lower detection

limit ($1.8 \times 10^{-7} \text{M}$) and better stability in different pH buffers compared to that of **DPP-Py2**. The various measurements like scanning electron microscopy, ^1H NMR titration, 2D-NOESY NMR, and dynamic light scattering analyses indicated the fluorescence increment of the probes **DPP-Py1** and **DPP-Py2** for citrate was probably originated from aggregation-induced emission (AIE) on the basis of the complexation of the pyridinium-based symmetrical diamides, DPPs, with carboxyl anions of citrate.



DPP-Py1, R= H

DPP-Py2, R = OMe

Chart 1.7. Chemical structures of **DPP-Py1** and **DPP-Py2**.

1.8. Current Work

The donor-acceptor (D–A) architectures with strong absorption in visible to near-infrared (NIR) region and low HOMO–LUMO gap are used as potential candidates for organic photovoltaics. In order to improve the absorption towards NIR region and lower the HOMO–LUMO gap, DPP unit has been functionalized with various donors, acceptors and linkers in symmetrical and unsymmetrical way. The effect of substitution of various donor and acceptor units on the photonic, thermal and electrochemical properties was investigated. The photophysical, electrochemical properties and HOMO–LUMO gap of DPP based D–A systems can be tuned either by altering the strength of donor or acceptor units.

We have explored variety of donor (carbazole, triphenylamine, ferrocene *etc.*) and acceptor (TCBD) functionalized DPP based D–A systems and investigated their photophysical, thermal, electrochemical and computational properties which indicate their applicability for photovoltaic applications. The DPPs classified as symmetrical (**DPPs 2–4**) and unsymmetrical (**DPPs 5–7**) on the basis of functionalization at the 3- and 6- positions of DPP. The substitution of same donor

1.9. Organization of thesis

Chapter 1 gives the detailed introduction about the historical development of various synthetic, functionalization strategies, reactivity and utility of DPPs in diverse fields. The recent functionalization strategies have been summarized and further explored in D-A systems in the subsequent chapters.

Chapter 2 Summarizes the instrumentation and general methods used for the present study.

In **Chapter 3** a donor-acceptor *N*-phenyl carbazole functionalized DPPs and their TCBD derivatives were designed, and synthesized *via* palladium catalysed Sonogashira cross-coupling and [2+2] cycloaddition-retroelectrocyclization reaction respectively. The effect of *N*-phenyl carbazole on the photophysical, electrochemical properties of DPP and further effect of electron accepting TCBD on *N*-phenyl carbazole functionalized DPPs derivatives were studied.

In **Chapter 4**, a set of triphenylamine substituted DPPs and their TCBD derivatives were synthesized *via* palladium catalysed Sonogashira cross-coupling and [2+2] cycloaddition-retroelectrocyclization reaction respectively. The effect of triphenylamine donor on the photophysical, electrochemical properties of DPPs and further effect of electron accepting TCBD on ferrocenyl derivatives were studied.

In **Chapter 5** ferrocenyl substituted DPPs and their TCBD derivatives have been designed, and synthesized *via* palladium catalysed Sonogashira cross-coupling and [2+2] cycloaddition-retroelectrocyclization reaction respectively. The effect of ferrocenyl group on the photophysical, electrochemical properties of DPPs and further effect of electron accepting TCBD on ferrocenyl derivatives were studied.

Chapter 6 includes synthesis, photophysical, thermal and electrochemical properties of a symmetrical cobalt-dithiolene functionalized diketopyrrolopyrrole (DPP) **Co-DPP-Co** and its comparison with earlier reported ferrocenyl based **Fc-DPP-Fc**.

In **Chapter 7** we have designed and synthesized DPP based monomer (**1**), dimers (**2** and **3**) and trimer (**4**) and studied their photophysical, thermal and

electrochemical properties, in order to investigate the effect of number of DPP units and connecting bridge on photophysical and electrochemical properties.

Chapter 8 summarizes the salient features of the work and future prospectus to develop the new materials for optoelectronic applications.

1.10. References

- [1] (a) Liangwab, M., Chen, J. (2013), Arylamine organic dyes for dye sensitized solar cells, *Chem. Soc. Rev.*, 42, 3453-3488 (DOI:10.1039/C3CS35372A). (b) Mishra, A., Fischer, M. K. R., Bauerle, P. (2009), Metal-free organic dyes for dye-sensitized solar cells: from structure: property relationships to design rules, *Angew. Chem., Int. Ed.*, 48, 2474-2499 (DOI: 10.1002/anie.200804709).
- [2] (a) Thomas, K. R. J., Lin J. T., Velusamy, M., Tao, Y. T., Chuen, C. H. (2004), Color tuning in benzo[1,2,5]thiadiazole-based small molecules by amino conjugation/deconjugation: bright red-light-emitting diodes, *Adv. Funct. Mater.*, 14, 83-90 (DOI: 10.1002/adfm.200304486). (b) Omer, K. M., Ku, S. Y., Wong, K. T., Bard, A. J. (2009), Green electrogenerated chemiluminescence of highly fluorescent benzothiadiazole and fluorene derivatives, *J. Am. Chem. Soc.*, 131, 10733-10741 (DOI:10.1021/ja904135y). (c) Yasuda, T., Shinohara, Y., Matsuda, T., Han, L., Ishi-i., T. (2012), Improved power conversion efficiency of bulk-heterojunction organic solar cells using a benzothiadiazole–triphenylamine polymer, *J. Mater. Chem.*, 22, 2539-2544 (DOI: 10.1039/c2jm14671a).
- [3] Ostroverkhova, O. (2016), Organic Optoelectronic Materials: Mechanisms and Applications, *Chem. Rev.*, 116, 13279–13412 (DOI:10.1021/acs.chemrev.6b00127).
- [4] (a) Mochida, T., Yamazaki, S. (2002), Mono- and diferrocenyl complexes with electron-accepting moieties formed by the reaction of ferrocenylalkynes with tetracyanoethylene, *J. Chem. Soc. Dalton Trans.*, 0, 3559-3564 (DOI: 10.1039/B204168E.) (b) Michinobu, T. (2010), Click synthesis of donor–acceptor-type aromatic polymers, *Pure Appl. Chem.*, 82, 1001 (DOI: <https://doi.org/10.1351/PAC-CON-09-09-09>). (c) Maligaspe, E., Pundsack, T. J., Albert, L. M., Zatsikha, Y. V., Solntsev, P. V., Blank, D. A., Nemykin, V. N. (2015), Synthesis and charge-transfer dynamics in a ferrocene-containing organoboryl aza-BODIPY donor-acceptor triad with boron as the hub, *Inorg. Chem.*, 54, 4167–4174 (DOI: 10.1021/acs.inorgchem.5b00494).

- [5] (a) Michinobu, T., Satoh, N., Cai, J., Lia, Y., Han, L. (2014), Novel design of organic donor–acceptor dyes without carboxylic acid anchoring groups for dye-sensitized solar cells, *J. Mater. Chem. C*, 2, 3367 (DOI: 10.1039/c3tc32165g). (b) Leliège, A., Blanchard, P., Rousseau, T., Roncali, J. (2011), Triphenylamine/Tetracyanobutadiene-Based D-A-D π -Conjugated Systems as Molecular Donors for Organic Solar Cells, *Org. Lett.*, 13, 3098–3101 (DOI: 10.1021/ol201002j).
- [6] Zhang, L., Zeng S., Yin L., Ji C., Li, K., Li Y., Wang Y. (2013), The synthesis and photovoltaic properties of A–D–A-type small molecules containing diketopyrrolopyrrole terminal units, *New J. Chem.*, 37, 632. (DOI: 10.1039/C2NJ40963A)
- [7] (a) Liangwab, M., Chen, J. (2013), Arylamine organic dyes for dyesensitized solar cells, *Chem. Soc. Rev.*, 42, 3453-3488 (DOI:10.1039/C3CS35372A). (b) Thomas, K. R. J., Lin, J. T., Velusamy, M., Tao, Y. T., Chuen, C. H. (2004), Color tuning in benzo[1,2,5]thiadiazole-based small molecules by amino conjugation/deconjugation: bright red-light-emitting diodes, *Adv. Funct. Mater.*, 14, 83-90 (DOI: 10.1002/adfm.200304486).
- [8] Mishra, A., Fischer, M. K. R., Bauerle, P. (2009), Metal-free organic dyes for dye-sensitized solar cells: from structure: property relationships to design rules, *Angew. Chem., Int. Ed.*, 48, 2474-2499 (DOI: 10.1002/anie.200804709).
- [9] Omer, K. M., Ku, S. Y., Wong, K. T., Bard, A. J. (2009), Green electrogenerated chemiluminescence of highly fluorescent benzothiadiazole and fluorene derivatives, *J. Am. Chem. Soc.*, 131, 10733-10741 (DOI:10.1021/ja904135y).
- [10] Farnum, D. G. ; Mehta , G. ; Moore , G. G. I. ; Siegal , F. P (1974), Attempted reformatskii reaction of benzonitrile, 1,4-diketo-3,6-diphenylpyrrolo[3,4-C]pyrrole. A lactam analogue of pentalene, *Tetrahedron Lett.*, 29, 2549 (DOI: [https://doi.org/10.1016/S0040-4039\(01\)93202-2](https://doi.org/10.1016/S0040-4039(01)93202-2)).
- [11] Iqbal, A., Jost, M., Kirchmayr, R., Pfenninger, J., Rochat, A., Wallquist, O. (1988), The synthesis and properties of 1,4-diketo-pyrrolo[3,4-C]pyrroles, *Bull. Soc. Chim. Belges*, 97, 615–644 (DOI:10.1002/bscb.19880970804).
- [12] Rochat, A. C., Cassar, L., Iqbal, A. (1983), (Ciba-Geigy Ltd.), *Eur. Patent*, 9 94911.

- [13] Rubin, M. B., Barqurie, M., Kosti, S., Kaftory, M. (1980), Synthesis and reactions of 1,6-diaryl-2,5-bis(diazo)-1,3,4,6-tetraoxohexanes, *J. Chem. Soc., Perkin Trans.*, 1, 2670 (DOI: 10.1039/P19800002670).
- [14] (a) Mizuguchi, J., Wooden, G. (1991), A Large Bathochromic Shift from the Solution to the Solid-State in 1,4-Diketo-3,6-Diphenyl-Pyrrolo-[3,4-C]-Pyrrole, *Berichte der Bunsen-Gesellschaft-Physical Chemistry Chemical Physics*, 95 (10), 1264-1274 (DOI: 10.1002/bbpc.19910951016). (b) Langhals, H., Grundei T., Potrawa, T., Polborn, K. (1996), Highly photostable organic fluorescent pigments - A simple synthesis of *N*-arylpyrrolopyrrolediones (DPP), *Liebigs Annalen*, 5, 679-682 (DOI: 10.1002/jlac.199619960506).
- [15] Sonar, P., Ng, G. M., Lin, T. T., Dodabalapur, A., Chen, Z. K. (2010), Solution processable low bandgap diketopyrrolopyrrole (DPP) based derivatives: novel acceptors for organic solar cells, *J. Mater. Chem.*, 20, 3626 (DOI: 10.1039/b924404b).
- [16] Gao K., Li L., Lai T., Xiao L., Huang Y., Huang F., Peng J., Cao Y., Liu F., Russell T. P. (2015), Deep absorbing porphyrin small molecule for high-performance organic solar cells with very low energy losses, *J. Am. Chem. Soc.*, 137, 7282 (DOI: 10.1021/jacs.5b03740).
- [17] Jung, I. H., Hong, C. T., Lee, U.-H., Kang, Y. H., Jang, K.-S., Cho, S. Y., (2017), High Thermoelectric Power Factor of a Diketopyrrolopyrrole-Based Low Bandgap Polymer via Finely Tuned Doping Engineering, *Scientific Reports*, 7, 44704 (DOI:10.1038/srep44704).
- [18] (a) Wang, H., Xiao, L., Yan, L., Chen, S., Zhu, X., Peng, X., Wang, X., Wong, W.-K., Wong, W.-Y. (2016), Structural engineering of porphyrin-based small molecules as donors for efficient organic solar cells, *Chem. Sci.*, 7, 4301-4307 (DOI: 10.1039/C5SC04783H). (b) Qin, C., Fu, Y., Chui, C.-H., Kan, C.-W., Xie, Z., Wang, L., Wong, W.-Y. (2011), Tuning the Donor–Acceptor Strength of Low-Bandgap Platinum-Acetylide Polymers for Near-Infrared Photovoltaic Applications, *Macromol. Rapid Commun.*, 32, 1472–1477 (DOI: 10.1002/marc.201100247).
- [19] (a) Qin, C., Wong, W.-Y., Han, L. (2013), Squaraine Dyes for Dye-Sensitized Solar Cells: Recent Advances and Future Challenges, *Chem. Asian J.*, 8, 1706–1719 (DOI:10.1002/asia.201300185). (b) Yuan, L., Lin, W., Zheng, K., He, L., Huang, W. (2013), Far-red to near infrared analyte-responsive fluorescent

- probes based on organic fluorophore platforms for fluorescence imaging, *Chem. Soc. Rev.*, 42 622–661 (DOI: 10.1039/C2CS35313J).
- [20] (a) Li, G., Zhu, R., Yang, Y. (2012), Polymer solar cells, *Nat. Photonics*, 6 153–161 (DOI:10.1038/nphoton.2012.11). (b) Janssen, R. A. J., Nelson, J. (2013), Factors limiting device efficiency in organic photovoltaics. *Adv. Mater.*, 25, 1847–1858 (DOI:10.1002/adma.201202873). (c) Zhao, Y., Guo, Y., Liu, Y. (2013), 25th anniversary article: recent advances in n-type and ambipolar organic field-effect transistors. *Adv. Mater.*, 25, 5372–5391 (DOI:10.1002/adma.201302315). (d) You, J., Dou, L., Yoshimura, K., Kato, T., Ohya, K., Moriarty, T., Emery, K., Chen, C.-C., Gao, J., Li, G., Yang, Y. (2013), A polymer tandem solar cell with 10.6% power conversion efficiency, *Nat. Commun.*, 4, 1446 (DOI:10.1038/ncomms2411).
- [21] (a) Dou, L., Liu, Y., Hong, Z., Li, G., Yang, Y. (2015), Low-Bandgap Near-IR Conjugated Polymers/Molecules for Organic Electronics, *Chem. Rev.*, 115 12633–12665 (DOI: 10.1021/acs.chemrev.5b00165). (b) Chen, S., Xiao, L., Zhu, X., Peng, X., Wong, W.-K., Wong, W.-Y. (2015), *Chem. Commun.*, 51, 14439–14442 (DOI: 10.1039/C5CC05807D).
- [22] Goswami, S., Winkel, R. W., Alarousu, E., Ghiviriga, I., Mohammed, O. F., Schanze, K. S. (2014), Photophysics of Organometallic Platinum (II) Derivatives of the Diketopyrrolopyrrole Chromophore, *J. Phys. Chem. A*, 118, 11735–11743 (DOI: 10.1021/jp509987p).
- [23] (a) Michinobu, T., May, J. C., Lim, J. H., Boudon, C., Gisselbrecht, J., Seiler, P., Gross, M., Biaggio, I., Diederich, F. (2005), A new class of organic donor–acceptor molecules with large third-order optical nonlinearities, *Chem. Commun.*, 737–739 (DOI: 10.1039/B417393G). (b) Kivala, M., Boudon, C., Gisselbrecht, J., Seiler, P., Gross, M., Diederich, F. (2007), A novel reaction of 7,7,8,8-tetracyanoquinodimethane (TCNQ): charge-transfer chromophores by [2+2] cycloaddition with alkynes, *Chem. Commun.*, 4731–4733 (DOI: 10.1039/B713683H).
- [24] (a) Michinobu, T., Boudon, C., Gisselbrecht, J. P., Seiler, P., Frank, B., Moonen, N. N. P., Gross, M., Diederich, F. (2006), Donor-Substituted 1,1,4,4-Tetracyanobutadienes (TCBDs): New Chromophores with Efficient Intramolecular Charge-Transfer Interactions by Atom-Economic Synthesis, *Chem. Eur. J.*, 12, 1889–1905 (DOI: 10.1002/chem.200501113). (b) Kivala,

- M., Diederich, F. (2009), Acetylene-Derived Strong Organic Acceptors for Planar and Nonplanar Push–Pull Chromophores, *Acc. Chem. Res.*, 42, 235–248 (DOI: 10.1021/ar8001238). (c) Kato, S. I., Diederich, F. Non-planar push–pull chromophores, (2010), *Chem. Commun.*, 1994–2006 (DOI: 10.1039/B926601A).
- [25] (a) Stefko, M., Tzirakis, M. D., Breiten, B., Ebert, M. O., Dumele, O., Schweizer, W. B., Gisselbrecht, J. P., Boudon, C., Beels, M. T., Biaggio, I., Diederich, F. (2013), Donor–Acceptor (D–A)-Substituted Polyene Chromophores: Modulation of Their Optoelectronic Properties by Varying the Length of the Acetylene Spacer, *Chem. Eur. J.*, 19, 12693–12704 (DOI: 10.1002/chem.201301642). (b) Wu, Y., Stuparu, M. C., Boudon, C., Gisselbrecht, J., Schweizer, W. B., Baldrige, K. K., Siegel, J. S., Diederich, F. (2012), Structural, Optical, and Electrochemical Properties of Three-Dimensional Push–Pull Corannulenes, *J. Org. Chem.*, 77, 11014–11026 (DOI: 10.1021/jo302217n).
- [26] (a) Yamagata, T., Kuwabara, J., Kanbara, T. (2012), Synthesis and Characterization of Dioxopyrrolopyrrole Derivatives Having Electron-Withdrawing Groups, *Eur. J. Org. Chem.*, 5282–5290 (DOI: 10.1002/ejoc.201200761). (b) Heyer, E., Ziessel, R. (2015), Panchromatic Push–Pull Dyes of Elongated Form from Triphenylamine, Diketopyrrolopyrrole, and Tetracyanobutadiene Modules, *Synlett.*, 26, 2109–2116 (DOI: 10.1055/s-0034-1378818).
- [27] (a) Wang, J., Yan, R., Guo, F., Yu, M., Tan, F., Li, N. (2016), Targeted lipid–polyaniline hybrid nanoparticles for photoacoustic imaging guided photothermal therapy of cancer, *Nanotechnology*, 27, 285102. (b) Sun, M., Liu, F., Zhu, Y., Wang, W., Hu, J., Liu, J., Dai, Z., Wang, K., Wei, Y., Bai, J. (2016), Salt-induced aggregation of gold nanoparticles for photoacoustic imaging and photothermal therapy of cancer, *Nanoscale*, 8, 4452–4457 (DOI: 10.1039/C6NR00056H).
- [28] (a) Huang, P., Gao, Y., Lin, J., Hu, H., Liao, H.-S., Yan, X., Tang, Y., Jin, A., Song, J., Niu, G. (2015), Tumor-Specific Formation of Enzyme-Instructed Supramolecular Self-Assemblies as Cancer Theranostics, *ACS Nano*, 9, 9517–9527 (DOI: 10.1021/acsnano.5b03874). (b) Huang, P., Lin, J., Li, W., Rong, P., Wang, Z., Wang, S., Wang, X., Sun, X., Aronova, M., Niu, G., Leapman,

- R. D., Nie, Z., Chen, X. (2013), Biodegradable Gold Nanovesicles with an Ultrastrong Plasmonic Coupling Effect for Photoacoustic Imaging and Photothermal Therapy. *Angew. Chem.*, 125, 14208–14214 (DOI:10.1002/ange.201308986).
- [29] Cai, Y., Liang, P., Tang, Q., Yang, X., Si, W., Huang, Wei., Zhang, Q., Dong, X., (2017), Diketopyrrolopyrrole–Triphenylamine Organic Nanoparticles as Multifunctional Reagents for Photoacoustic Imaging-Guided Photodynamic/Photothermal Synergistic Tumor Therapy, *ACS Nano*, 11, 1054–1063 (DOI: 10.1021/acsnano.6b07927).
- [30] Liang, P., Tang, Q., Cai, Y., Liu, G., Si, W., Shao, J., Huang, W., Zhang, Q., Dong, X. (2017), Self-quenched ferrocenyl diketopyrrolopyrrole organic nanoparticles with amplifying photothermal effect for cancer therapy, *Chem. Sci.*, 8, 7457-7463 (DOI: 10.1039/C7SC03351F).
- [31] (a) O'Regan, B., Grätzel, M. (1991), A low-cost, high-efficiency solar cell based on dye-sensitized colloidal TiO₂ films, *Nature*, 353, 737–740 (DOI:10.1038/353737a0). (b) Grätzel, M. (2005), Solar Energy Conversion by Dye-Sensitized Photovoltaic Cells, *Inorg. Chem.*, 44, 6841–6851 (DOI: 10.1021/ic0508371).
- [32] Qu, S., Wu, W., Hua, J., Kong, C., Long, Y., Tian, H. (2010), New Diketopyrrolopyrrole (DPP) Dyes for Efficient Dye-Sensitized Solar Cells, *J. Phys. Chem. C*, 114, 1343–1349 (DOI: 10.1021/jp909786k).
- [33] (a) Forrest, S. R. (2004), The path to ubiquitous and low-cost organic electronic appliances on plastic, *Nature*, 428, 911-918 (DOI:10.1038/nature02498). (b) Ginley, D., Green, M. A., Collins, R. (2008), Solar energy conversion toward 1 terawatt *MRS Bull.*, 33, 355–364 (<https://doi.org/10.1557/mrs2008.71>). (c) Espinosa, N., Hosel, M., Angmo, D., Krebs, F. C. (2012), Solar cells with one-day energy payback for the factories of the future, *Energy Environ Sci.*, 5, 5117-5132 (DOI: 10.1039/C1EE02728J).
- [34] (a) Lin, Y. Z., Li, Y. F., Zhan, X. W. (2012), Small molecule semiconductors for high-efficiency organic photovoltaics, *Chem. Soc. Rev.*, 41, 4245–4272 (DOI: 10.1039/C2CS15313K). (b) Cheng, Y. J., Yang, S. H., Hsu, C. S. (2009), Synthesis of Conjugated Polymers for Organic Solar Cell Applications, *Chem. Rev.*, 109, 5868 –5923 (DOI: 10.1021/cr900182s).

- [35] Grzybowski, M., Gryko, D. T. (2015), Diketopyrrolopyrroles: Synthesis, Reactivity, and Optical Properties. *Adv. Opt. Mater.*, 3, 280–320. (DOI:10.1002/adom.201400559).
- [36] Tang, A., Zhan, C., Yao, J., Zhou, E. (2017), Design of Diketopyrrolopyrrole (DPP)-Based Small Molecules for Organic-Solar-Cell Applications, *Adv. Mater.*, 29, 1600013 (DOI: 10.1002/adma.201600013).
- [37] Lin, Y., Ma, L., Li, Y., Liu, Y., Zhu, D., Zhan, X. (2013), A Solution-Processable Small Molecule Based on Benzodithiophene and Diketopyrrolopyrrole for High-Performance Organic Solar Cells. *Adv. Energy Mater.*, 3, 1166–1170 (DOI:10.1002/aenm.201300181).
- [38] Sun, P., Sun, H., Li, X., Wang, Y., Shan, H., Xu, J., Zhang, C., Xu, Z., Chen, Z.-K., Huang, W. (2017), Three dimensional multi-arm acceptors based on diketopyrrolopyrrole with (hetero)aromatic cores for non-fullerene organic solar cells without additional treatment, *Dyes Pigm.*, 139, 412-419 (doi.org/10.1016/j.dyepig.2016.11.049).
- [39] Cai, B., Xing, Y., Yang, Z., Zhang, W.-H., Qiu, J. (2013), High performance hybrid solar cells sensitized by organolead halide perovskites, *Energy Environ. Sci.*, 6, 1480–1485 (DOI: 10.1039/C3EE40343B).
- [40] Sassi, M., Buccheri, N., Rooney, M., Botta, C., Bruni, F., Giovanella, U., Brovelli, S., Beverina, L. (2016), Near-infrared roll-off-free electroluminescence from highly stable diketopyrrolopyrrole light emitting diodes, *Scientific Reports*, 6, 34096 (DOI: 10.1038/srep34096).
- [41] Shahid, M., Ashraf, R. S., Huang, Z., Kronemeijer, A. J., McCarthy-Ward, T., McCulloch, I., Durrant, J. R., Sringhaus, H., Heeney, M. (2012), Photovoltaic and field effect transistor performance of selenophene and thiophene diketopyrrolopyrrole co-polymers with dithienothiophene, *J. Mater. Chem.*, 22, 12817-12823 (DOI: 10.1039/C2JM31189E).
- [42] (a) Lin, H.-W., Lee, W.-Y., Lu, C., Lin, C.-J., Wu, H.-C., Lin, Y. W., Ahn, B., Rho, Y., Ree, M., Chen, W.-C. (2012), Biaxially extended quaterthiophene-thiophene and -selenophene conjugated polymers for optoelectronic device applications, *Polym. Chem.*, 3, 767-777 (DOI: 10.1039/C2PY00583B). (b) Lin, H.-W., Lee W.-Y., Chen, W.-C. (2012), Selenophene-DPP donor-acceptor conjugated polymer for high performance ambipolar field effect transistor and nonvolatile memory applications, *J. Mater. Chem.*, 22, 2120–

- 2128 (DOI: 10.1039/C1JM14640H). (c) Ha, J. S., Kim, K. H., Choi, D. H. (2011), 2,5-Bis(2-octyldodecyl)pyrrolo[3,4-c]pyrrole-1,4-(2H,5H)-dione-Based Donor–Acceptor Alternating Copolymer Bearing 5,5'-Di(thiophen-2-yl)-2,2'-biselenophene Exhibiting $1.5 \text{ cm}^2 \cdot \text{V}^{-1} \cdot \text{s}^{-1}$ Hole Mobility in Thin-Film Transistors, *J. Am. Chem. Soc.*, 133, 10364–10367 (DOI: 10.1021/ja203189h).
- [43] Kaur, M., Yang, D. S., Shin, J., Lee, T. W., Choi, K., Cho, M. J., Choi, D. H. (2013), A novel tellurophene-containing conjugated polymer with a dithiophenyl diketopyrrolopyrrole unit for use in organic thin film transistors, *Chem. Commun.*, 49, 5495–5497 (DOI: 10.1039/C3CC41250D).
- [44] Hang, Y., Wang, J., Jiang, T., Lu, N., Hua, J. (2016), Diketopyrrolopyrrole-Based Ratiometric/Turn-on Fluorescent Chemosensors for Citrate Detection in the Near-Infrared Region by an Aggregation-Induced Emission Mechanism, *Anal. Chem.*, 88, 1696–1703 (DOI: 10.1021/acs.analchem.5b03715).

Chapter 2

Materials and Experimental Techniques

2.1. Introduction

In this chapter the materials used, general synthetic procedures, characterization techniques and the instrumentation employed in this thesis are discussed.

2.2. Chemicals for synthesis

Common solvents used for syntheses were purified according to known procedures.^[1] 2-thiophene carbonitrile, sodium *tert*-butoxide, dimethyl succinate, conc. HCl, 1-bromodecane were obtained from Spectrochem India. Triethylamine, was obtained from S. D. Fine chem. Ltd., CuI, Pd(PPh₃)₄, PdCl₂(PPh₃)₂, ferrocene, tetrabutylammonium hexafluorophosphate (TBAF₆), Ethynyl ferrocene, were procured from Aldrich chemicals USA. Silica gel (100 – 200 mesh and 230 – 400 mesh) WAS purchased from Rankem chemicals, India. TLC pre-coated silica gel plates (Kieselgel 60F254, Merck) were obtained from Merck, India.

Dry solvents dichloromethane, chloroform, tetrahydrofuran (THF), *N,N*-dimethylformamide (DMF), *tert*-butanol and methanol were obtained from Spectrochem and S. D. Fine chem. Ltd. All oxygen or moisture sensitive reactions were performed under nitrogen/argon atmosphere using standard schlenk method.

The solvents and reagents were used as received unless otherwise indicated. The *N*-Bromosuccinimide was recrystallized from hot water before use. Photophysical and electrochemical studies were performed with spectroscopic grade solvents.

2.3. Spectroscopic Measurements

2.3.1. NMR Spectroscopy

¹H NMR (400 MHz), and ¹³C NMR (100 MHz) spectra were recorded on the Bruker Avance (III) 400 MHz, using CDCl₃ as solvent. Chemical shifts in ¹H, and ¹³C NMR spectra were reported in parts per million (ppm). In ¹H NMR chemical shifts are reported relative to the residual solvent peak (CDCl₃, 7.26 ppm).

Multiplicities are given as: s (singlet), d (doublet), t (triplet), q (quartet), m (multiplet), and the coupling constants J , are given in Hz. ^{13}C NMR chemical shifts are reported relative to the solvent residual peak (CDCl_3 , 77.02 ppm).

2.3.2. Mass Spectrometry

High resolution mass spectra (HRMS) were recorded on Bruker-Daltonics, micrOTOF-Q II mass spectrometer using positive and negative mode electrospray ionizations.

2.3.3. UV-Vis Spectroscopy

UV-Vis absorption spectra were recorded using a Varian Cary100 Bio UV-Vis and PerkinElmer LAMBDA 35 UV/Vis spectrophotometer.

2.3.4. Fluorescence Spectroscopy

Fluorescence emission spectra were recorded upon specific excitation wavelength on a Horiba Scientific Fluoromax-4 spectrophotometer. The slit width for the excitation and emission was set at 2 nm.

2.4. Electrochemical Studies

Cyclic voltammograms (CVs) and Differential Pulse Voltammograms (DPVs) were recorded on CHI620D electrochemical analyzer using Glassy carbon as working electrode and Pt wire as the counter electrode, Ag/Ag⁺ as the reference electrode. The scan rate was 100 mVs⁻¹. A solution of tetrabutylammonium hexafluorophosphate (TBAPF₆) in CH₂Cl₂ (0.1 M) was employed as the supporting electrolyte.

2.5. Computational Calculations

The density functional theory (DFT) calculation were carried out at the B3LYP/6-31G** level for B, F, C, N, O, H, and Lan12DZ level for Fe in the Gaussian 09 program.^[2]

2.6. References

- [1] (a) Vogel, A. I., Tatchell, A. R., Furnis, B. S., Hannaford, A. J., & Smith, P. W. G. (1996). *Vogel's Textbook of Practical Organic Chemistry (5th Edition)* (5th ed.); (b) Wei Ssberger, A. Proskraner, E. S. Riddick, J. A. Toppos Jr., E. F.

(1970). *Organic Solvents in Techniques of Organic Chemistry*, Vol. IV, 3rd Edition, Inc. New York.

- [2] (a) Frisch, M. J.; Trucks, G. W.; Schlegel, H. B.; Scuseria, G. E.; Robb, M. A.; Cheeseman, J. R.; Scalmani, G.; Barone, V.; Mennucci, B.; Petersson, G. A.; Nakatsuji, H.; Caricato, M.; Li, X.; Hratchian, H. P.; Izmaylov, A. F.; Bloino, J.; Zheng, G.; Sonnenberg, J. L.; Hada, M.; Ehara, M.; Toyota, K.; Fukuda, R.; Hasegawa, J.; Ishida, M.; Nakajima, T.; Honda, Y.; Kitao, O.; Nakai, H.; Vreven, T.; Montgomery, J. A. Jr.; Peralta, J. E.; Ogliaro, F.; Bearpark, M.; Heyd, J. J.; Brothers, E.; Kudin, K. N.; Staroverov, V. N.; Kobayashi, R.; Normand, J.; Raghavachari, K.; Rendell, A.; Burant, J. C.; Iyengar, S. S.; Tomasi, J.; Cossi, M.; Rega, N.; Millam, N. J.; Klene, M.; Knox, J. E.; Cross, J. B.; Bakken, V.; Adamo, C.; Jaramillo, J.; Gomperts, R.; Stratmann, R. E.; Yazyev, O.; Austin, A. J.; Cammi, R.; Pomelli, C.; Ochterski, J. W.; Martin, R. L.; Morokuma, K.; Zakrzewski, V. G.; Voth, G. A.; Salvador, P.; Dannenberg, J. J.; Dapprich, S.; Daniels, A. D.; Farkas, O.; Foresman, J. B.; Ortiz, J. V.; Cioslowski, J.; Fox, D. J. (2009). *Gaussian 09, revision A.02*; Gaussian, Inc.: Wallingford, CT. (b) Lee, C., Yang, W., & Parr, R. G. (1988). Development of the Colle-Salvetti correlation-energy formula into a functional of the electron density. *Physical Review B*, 37(2), 785–789. DOI: 10.1103/PhysRevB.37.785; (c) Becke, A. D. (1993). A new mixing of Hartree-Fock and local density-functional theories. *J. Chem. Phys.* 98, 1372–377. DOI: 10.1063/1.464304.

Chapter 3

N-phenyl carbazole functionalized diketopyrrolopyrroles

3.1. Introduction

The synthesis near infrared (NIR) absorbing small molecules has gained attention of the scientific community because of their applications in optoelectronic and biomedical imaging applications.^[1] The small molecules with extended π -conjugation have been widely used for organic solar cells (OSCs) as alternative for conjugated polymers because of their reproducible preparation, and easy functionalization.^[2] Our group is engaged in the design and synthesis of donor-acceptor (D – A) based small molecules for organic solar cells.^[3]

Diketopyrrolopyrrole (DPP) is strong electron acceptor unit with planar, well-conjugated lactam skeleton, which give rise to strong $\pi - \pi$ interactions. The derivatives of DPP are widely used for the applications in dyes, OSCs and high-quality printing.^[4] DPP derivatives possesses good solubility in common organic solvents and are photochemically as well as thermally stable.^[5] The functionalization of the DPP with electron donor moiety will results in D–A molecular system. We have recently reported the photonic and optical and electrochemical properties of ferrocenyl DPPs by varying strength and number of electron donor and acceptor units.^[6]

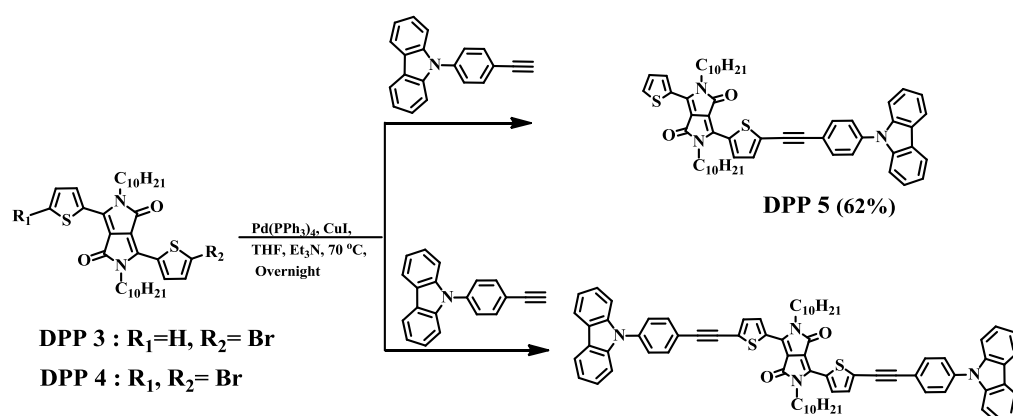
The *1,1,4,4*-tetracyanobutadiene (TCBD) is a strong electron-withdrawing group which can be incorporated into electron rich alkynes by [2+2] cycloaddition–retroelectrocyclization reaction.^[7,8] We have incorporated the TCBD acceptor in benzothiadiazoles (BTDs) and boron-dipyrrromethenes (BODIPY) for efficient tuning of D – A interaction.^[9] The electron accepting ability of DPP has been improved by introducing electron withdrawing pentafluorophenyl and TCBD groups.^[10]

The DPP attached with various positions of carbazole have been reported for various applications.^[11] Pyo *et al.* and Kim *et al.* have reported symmetrical *N*-phenyl carbazole substituted DPP for optoelectronic and solar cell applications.^[12] To the best of our knowledge there are no reports found in the literature on ethyne bridged *N*-phenyl carbazole substituted DPPs and their TCBD derivatives. The

motivation for choosing the *N*-phenyl carbazole as end-capping donor was its good electron-donating and charge transport capabilities^[13] and DPP as the electron acceptor core for its excellent electron affinity and broad absorption in the visible region.^[14] To understand the effect of acetylene linkage on the optoelectronic and structural properties of DPP, small molecules **DPPs 5** and **6** were designed and synthesized. The TCBD bridged **DPPs 7** and **8** were synthesized to investigate the effect of strong electron withdrawing TCBD unit on the optical, thermal and electrochemical properties of *N*-phenyl carbazole substituted DPPs.

In this chapter we wish to report the design and synthesis of ethyne and TCBD bridged *N*-phenyl carbazole substituted **DPPs 5–8** and their optical, thermal, electrochemical and computational properties.

3.2. Results and discussion

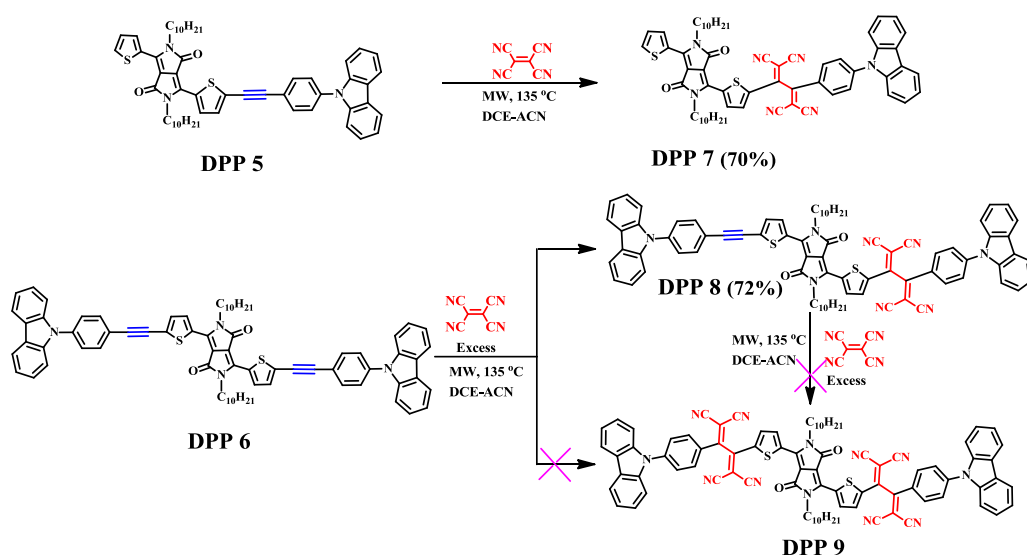


Scheme 3.1. Synthesis of *N*-phenyl carbazole substituted **DPPs 5** and **6**.

The *N*-phenyl carbazole substituted unsymmetrical **DPP 5** and symmetrical **DPP 6** were synthesized by the Pd-catalyzed Sonogashira cross-coupling reaction of monobromo **DPP 3** and dibromo **DPP 4** with 1.1 and 2.2 equivalents of *N*-(4-Ethynylphenyl) carbazole in 62% and 68% yield respectively (Scheme 3.1). The [2+2] cycloaddition-retroelectrocyclization reaction of *N*-phenyl carbazole substituted **DPPs 5** and **6** with excess equivalents of TCNE at 135 °C under microwave reaction condition for 4 hours resulted in TCBD substituted **DPPs 7** and **8** in 70% and 72% yield respectively (Scheme 3.2). The [2+2] cycloaddition-retroelectrocyclization reaction of strong electron withdrawing TCNE reacts with electron rich alkyne (in **DPPs 5** and **6**) result in the formation of TCBD bridged derivatives (**DPPs 7** and **8**). Here, carbazole is strong electron donor moiety but after incorporating with electron withdrawing DPP, its electron

donating capacity is decreased due to charge transfer and donor-acceptor interaction. After addition of first TCNE moiety in whole system is more electron deficient compared to starting material and due to which reactivity towards next TCNE is decreased or vanished and reaction stops after the addition of one TCNE. The reaction of symmetrical **DPP 6** with excess equivalents of TCNE at 135 °C under microwave reaction condition results exclusively mono-TCBD substituted unsymmetrical **DPP 8** and not di-TCBD substituted symmetrical **DPP 9** which may be due to increase in the acceptor strength of DPP after incorporation of first TCBD in **DPP 8**. The attempt to synthesize **DPP 9** from **DPP 8** with excess equivalents of TCNE at 135 °C under microwave reaction condition also results in failure of reaction. The precursors monobromo **DPP 3** and dibromo **DPP 4** were synthesized by following the reported procedure.^[15]

The *N*-phenyl carbazole substituted **DPPs 5 – 8** were purified by repeated silica gel column chromatography. The **DPPs 5 – 8** are readily soluble in common organic solvents such as chloroform, toluene, dichloromethane, and were well characterized by ¹H NMR, ¹³C NMR, and HRMS techniques.



Scheme 3.2. Synthesis of *N*-phenyl carbazole substituted TCBD derivatives **7** and **8**.

3.3. Photophysical Properties

The colored photograph of the *N*-phenyl carbazole substituted **DPPs 5 – 8** in dichloromethane solvent in day light is displayed in Figure 1(inset). The

incorporation of TCBD in ethyne bridged **DPPs 5** and **6** exhibit characteristic colour changes from pink and blue to green (**DPPs 7** and **8**).

The electronic absorption spectra of *N*-phenyl carbazole substituted **DPPs 5** – **8** were recorded in dichloromethane at room temperature (Figure 3.1) and data are listed in Table 3.1. The sharp absorption bands in the visible region at 543 nm, 580 nm in **DPP 5** and 571 nm, 616 nm in **DPP 6** were observed due to intramolecular charge transfer (ICT) from *N*-phenyl carbazole to DPP and the $\pi - \pi^*$ transitions respectively. The incorporation of TCBD in mono-*N*-phenyl carbazole substituted **DPP 5** shows the red shift of 115 nm, whereas the incorporation of TCBD in di-substituted **DPP 6** shows red shift of 110 nm. The TCBD substituted **DPPs 7** and **8** show broad absorption bands in visible region at 695 nm and 726 nm respectively.

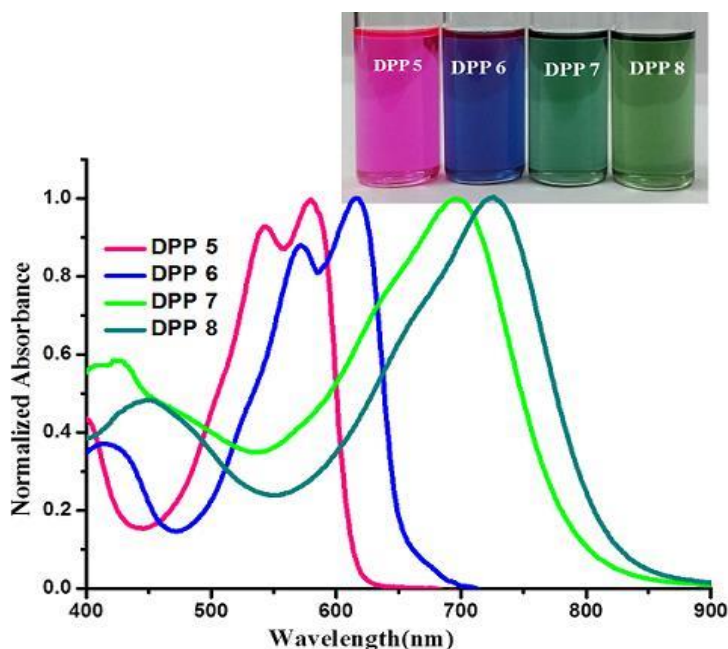


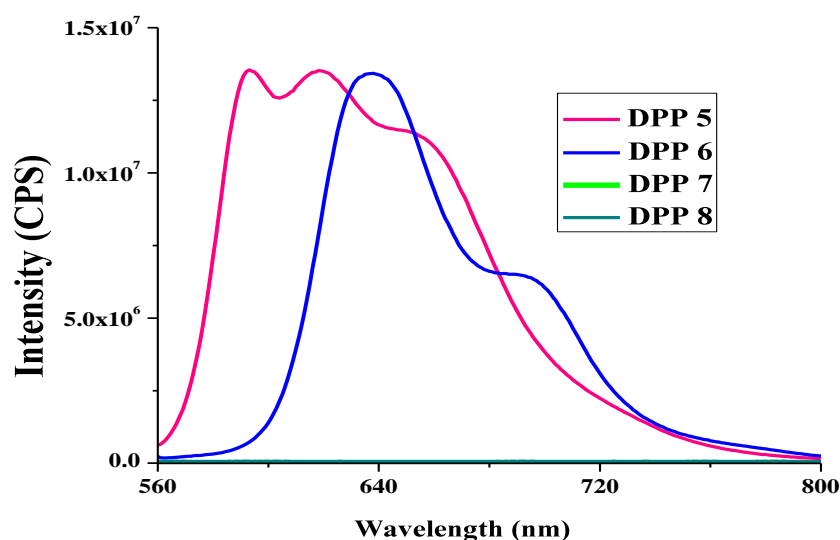
Figure 3.1. Normalized electronic absorption spectra (2×10^{-4} M) and photograph (3×10^{-6} M) of **DPPs 5** – **8** in dichloromethane.

The di-*N*-phenyl carbazole substituted **DPPs 6** and **8** show red shifted absorption compared to their mono-substituted analogues **5** and **7** respectively, due to the increase in conjugation length. The optical band gap calculated for **DPPs 5** – **8** are shown in Table 3.1. The trend in optical band gap follows the order $8 > 7 > 6 > 5$, which indicates that the introduction of TCBD unit in *N*-phenyl carbazole substituted DPP show red shifted absorption with decrease in the HOMO – LUMO gap.

Table 3.1. Photophysical, thermal and computational properties of **DPPs 5 – 8**.

DPP	λ_{abs} (nm)	$\epsilon/10^4$ ($\text{M}^{-1}.\text{cm}^{-1}$) ^a	T_d ($^{\circ}\text{C}$) ^b	Theoretical HOMO–LUMO gap (eV)	Optical Band gap (eV)
DPP 5	580	3.8	333	2.21	1.93
	543	3.5			
DPP 6	616	6.3	398	2.03	1.73
	571	5.5			
DPP 7	695	4.8	266	1.87	1.37
DPP 8	726	7.2	329	1.42	1.32

^aAbsorbance measured in dichloromethane at 2×10^{-4} M concentration, ϵ : Extinction coefficient; ^bDecomposition temperatures for 5% weight loss at a heating rate of $10^{\circ}\text{C min}^{-1}$, under nitrogen atmosphere.

**Figure 3.2.** The fluorescence spectra of **DPPs 5 – 8** in dichloromethane.

The fluorescence spectra of the *N*-phenyl carbazole substituted **DPPs 5 – 8** were recorded in dichloromethane at room temperature (Figure 3.2.). The ethyne bridged **DPPs 5** and **6** are fluorescent whereas their TCBD analogues **7** and **8** are non-fluorescent. The incorporation of TCBD in ethyne bridged *N*-phenyl carbazole

substituted **DPPs 5** and **6** enhances the charge transfer character. The intramolecular charge-transfer and enhanced donor–acceptor interaction in TCBD derivatives **7** and **8** lead to the quenching of fluorescence.^[16]

3.4. Thermal Properties

The thermal properties of the *N*-phenyl carbazole substituted **DPPs 5 – 8** were investigated by the thermogravimetric analysis (TGA) at heating rate of 10 °C min⁻¹ under nitrogen atmosphere and their thermograms are shown in Figure 3.3. The **DPPs 5 – 8** exhibit excellent thermal stability and the decomposition temperatures at 5% weight loss were found to be 333 °C, 398 °C, 266 °C and 329 °C for **DPPs 5, 6, 7** and **8** respectively. The ethyne bridged *N*-phenyl carbazole substituted **DPPs 5** and **6** are thermally more stable compared to their TCBD analogues **7** and **8**. The trend in thermal stability follows the order **6** > **5** > **8** > **7**, which reveals that the incorporation of TCBD in ethyne bridged *N*-phenyl carbazole substituted DPP lowers the thermal stability.

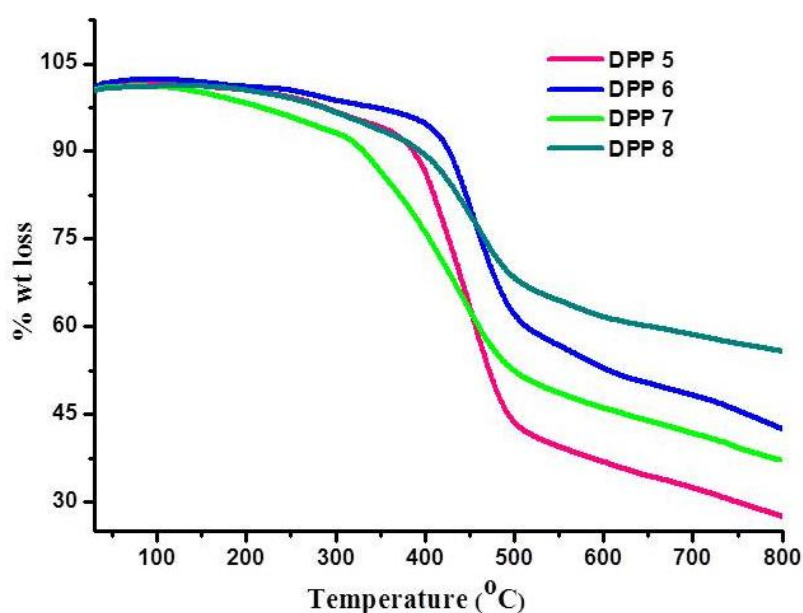


Figure 3.3. Thermogravimetric analysis of **DPPs 5 – 8** measured at a heating rate of 10 °C min⁻¹ under nitrogen atmosphere.

3.5. Electrochemical Properties

The electrochemical properties of *N*-phenyl carbazole substituted **DPPs 5 – 8** were explored by cyclic voltammetry (CV) in dichloromethane solvent using 0.1 M tetrabutylammonium hexafluorophosphate (Bu₄NPF₆) as supporting electrolyte.

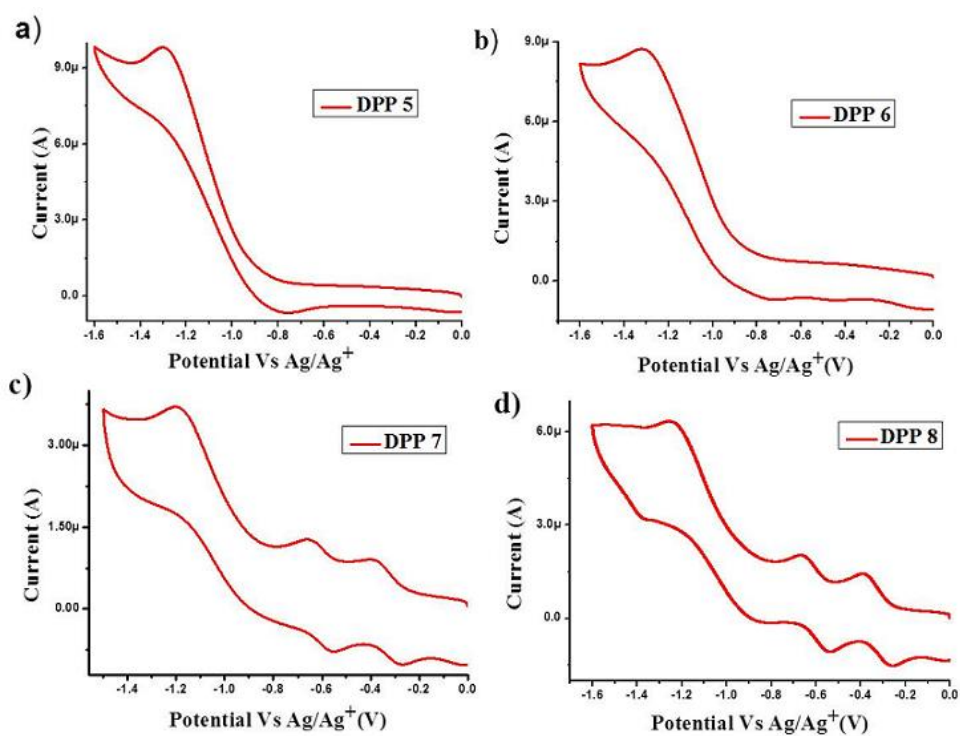


Figure 3.4. CV (red line) oxidation plots of (a) DPP 5, (b) DPP 6, (c) DPP 7, and (d) DPP 8.

The **DPPs 5 – 8** show two oxidation peaks, one corresponding to the oxidation of thiophene and another to oxidation of carbazole moiety. The characteristic changes were observed in the reduction after introduction of TCBD in ethyne bridged DPPs. The CV plots of *N*-phenyl carbazole substituted **DPPs 5 – 8** are shown in Figures (Figure 3.4 and 3.5) and the corresponding data are listed in Table 3.2.

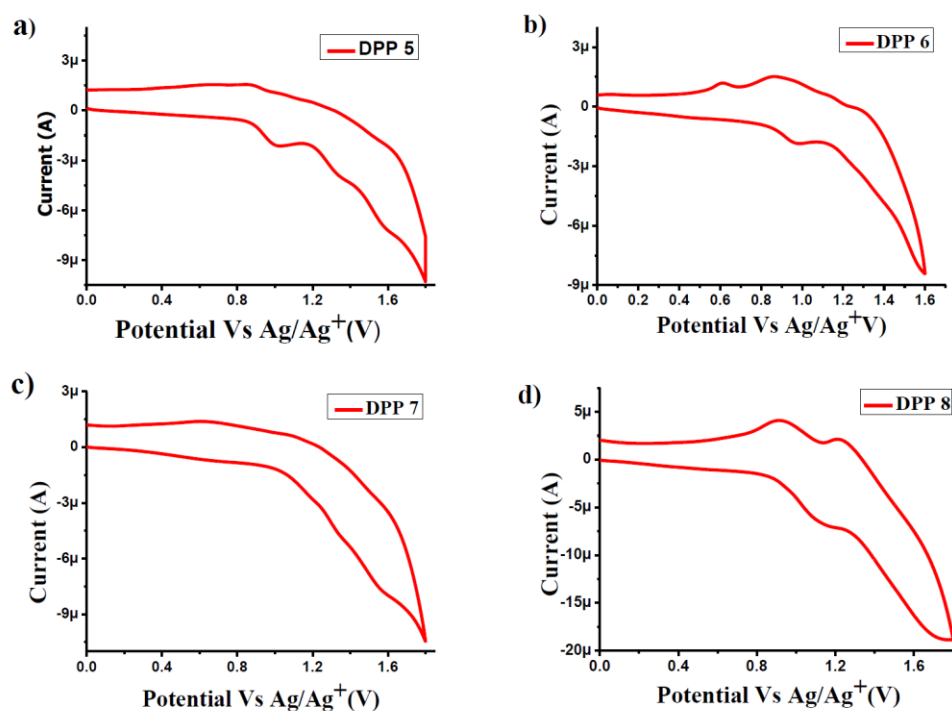


Figure 3.5. CV (red line) oxidation plots of (a) DPP **5**, (b) DPP **6**, (c) DPP **7**, and (d) DPP **8**.

The ethyne bridged *N*-phenyl carbazole substituted **DPPs 5** and **6** show one reduction wave, whereas the TCBD substituted **DPPs 7** and **8** exhibit three reduction waves. The reduction wave corresponding to DPP core was observed at -1.03 V in **DPPs 5** and **6**, and at -1.06 in TCBD derivatives **7** and **8** respectively.

Table 3.2. Electrochemical properties of **DPPs 5 – 8**^a.

	E^1	E^2	E^3	E^1	E^2
	Red	Red	Red	Oxid	Oxid
DPP 5	-1.03	–	–	0.93	1.60
DPP 6	-1.03	–	–	0.92	1.20
DPP 7	-0.33	-0.61	-1.06	0.66	1.58
DPP 8	-0.32	-0.60	-1.06	0.91	1.17

^aThe electrochemical analysis was performed in a 0.1 M solution of Bu_4NPF_6 in dichloromethane at 100 mVs^{-1} scan rate, versus Ag/Ag^+ at 25°C .

The additional reduction waves were observed due to TCBD moiety at -0.33 V, -0.61 V in **DPP 7** and at -0.30 V, -0.60 V in **DPP 8**. The two additional reduction waves observed in TCBD derivatives **7** and **8** are due to generation of dianion at

TCBD unit.^[9] The introduction of TCBD in ethyne bridged DPP makes reduction of DPP unit harder.

3.6. Density Functional Theory Calculations

In order to understand the geometry and electronic structure of *N*-phenyl carbazole substituted **DPPs 5 – 8**, density functional theory (DFT) calculations were carried out by using the Gaussian09W program.^[17]

Table 3.3. The frontier molecular orbitals of **DPPs 5 – 8** estimated from DFT calculations.

	DPP 5	DPP 6	DPP 7	DPP 8
LUMO+2				
LUMO+1				
LUMO				
HOMO				
HOMO-1				
HOMO-2				
HOMO-3				

The geometry optimizations were carried out in the gas phase at the B3LYP/6-31G level. The large alkyl chains were replaced by ethyl group in DPP for reducing the computation time. The frontier molecular orbitals of **DPPs 5 – 8** estimated from DFT calculation are shown in Table 3.3.

The highest occupied molecular orbitals (HOMOs) and lowest unoccupied molecular orbitals (LUMOs) in TCBD derivatives (**7** and **8**) are localized on the

DPP and TCBD unit. The ethyne bridged *N*-phenyl carbazole substituted **DPPs 5** and **6** exhibit planar geometry whereas their TCBD derivatives **7** and **8** show distorted geometry (Table 3.3). The theoretically calculated HOMO levels of *N*-phenyl carbazole substituted **DPPs 5 – 8** are – 4.93, –4.90, –5.55 and –5.38 eV, and the corresponding LUMO levels are –2.72, –2.87, –3.68 and –3.69 eV respectively. The TCBD bridged **DPPs 7** and **8** exhibit lower HOMO and LUMO energy levels than that of ethyne bridged **DPPs 5** and **6**.

Table 3.4. Calculated Electronic Transitions for **DPPs 5 – 8** in the Gas Phase.

DPP	Wavelength (nm)	Composition	f^a
DPP 5	575	HOMO→LUMO (0.71)	0.75
	388	HOMO-3→LUMO (0.37)	0.20
DPP 6	578	HOMO→LUMO (0.71)	1.39
	432	HOMO-1→LUMO (0.64)	0.10
DPP 7	677	HOMO→LUMO (0.69)	0.72
	603	HOMO→LUMO+1	0.08
	456	(0.69) HOMO→LUMO+2	0.13
DPP 8	698	HOMO→LUMO (0.70)	1.04
	612	HOMO→LUMO+1 (0.69)	0.09

f^a = Oscillation Strength

The time dependent density functional theory (TDDFT) calculations were performed at the B3LYP/6-31G level to understand the electronic transitions. The results of TD-DFT calculations indicate that **DPPs 5 – 8** show two main

electronic transitions in visible region. The transitions with composition, oscillator strengths, and assignments are as shown in Table 3.4. The transition occurs from HOMO to LUMO in longer wavelength region is associated to the $\pi - \pi^*$ transitions of DPP and TCBD unit whereas the other transitions in short wavelength region are related to charge transfer transitions as shown in Table 3.4. The main charge transfer transitions in ethyne bridged **DPPs 5** and **6** occur from HOMO-3→LUMO and HOMO-1→LUMO respectively. The charge transfer transitions in TCBD bridged **DPP 7** occurs from HOMO→LUMO+1 and HOMO→LUMO+2 and from HOMO→LUMO+1 in **DPP 8**. The theoretical absorption wavelengths of **DPPs 5 – 8** were found to be lower than that of experimental values may be due to various factors like solvent effect, temperature, dipole moment etc. The theoretical HOMO-LUMO gap values from DFT calculations were found to be in good agreement with the optical band gap values calculated from the UV-vis absorption (Table 3.1).

The previously reported *N*-phenyl carbazole substituted DPPs absorb in 400–700 nm region whereas, the **DPPs 5 – 8** show red shifted absorption in 400–850 nm region, reflecting the lower HOMO – LUMO gap and superior electronic communication.^[11]

3.7. Application in Photovoltaics

We used **DPPs 5** and **6** as donor along with PC₇₁BM as the acceptor for the preparation of solution processed bulk heterojunction organic solar cells (BHJ-OSCs) and after the optimization of the active layers in terms of the weight ratio of donor to acceptor and surface treatment, the OSCs based on **DPP5:PC₇₁BM** and **DPP6:PC₇₁BM** exhibited overall PCEs of 4.65% and 5.73% respectively.^[18]

The incorporation of TCBD improve the accepting ability and we used TCBD bridged derivatives as non-fullerene acceptor for BHJ-OSCs along with donor polymer **P** achieved a respectable PCE upto 7.19%, which is highest efficiency for TCBD bridged non-fullerene acceptor till date.^[19]

3.8. Experimental Section

General methods

The chemicals were used as received unless otherwise indicated. All the moisture sensitive reactions were performed under argon atmosphere using the standard Schlenk method. ¹H NMR (400 MHz) and ¹³C NMR (100 MHz) spectra were recorded by using CDCl₃ as the solvent. The ¹H NMR chemical

shifts are reported in parts per million (ppm) relative to the solvent residual peak (CDCl₃, 7.26 ppm). The multiplicities are given as: s (singlet), d (doublet), t (triplet), m (multiplet), and the coupling constants, *J*, are given in Hz. The ¹³C NMR chemical shifts are reported with relative to the solvent residual peak (CDCl₃, 77.02 ppm). HRMS was recorded on a mass spectrometer (ESI-TOF). The UV-visible absorption spectra of DPPs were recorded on UV-visible Spectrophotometer in dichloromethane. The TGA analyses were performed on the thermal analysis system at the heating rate of 10 °C per minute under nitrogen atmosphere. Cyclic voltammograms (CVs) were recorded on an electrochemical analyzer using glassy carbon as working electrode, Pt wire as the counter electrode, and saturated Ag/Ag⁺ as the reference electrode. The micro-wave irradiation experiments were carried out in a focused microwave CEM discover reactor 300W and the reaction tube with 10 ml capacity and 13 mm internal diameter is used.

Synthesis of DPP 5

In 100 ml round bottom flask monobromodiketopyrrolopyrrole **DPP 3** (0.200 g, 0.30 mmol) and *N*-(4-Ethynylphenyl) carbazole (0.090 g, 0.34 mmol) were dissolved in dry tetrahydrofuran (15 ml) and triethylamine (4 ml). The reaction mixture was degassed with argon for 10 minutes and Pd(PPh₃)₄ (0.018 g, 0.015 mmol), and CuI (0.006 g, 0.030 mmol) were then added. The reaction mixture was stirred overnight at 70 °C. After completion of reaction, the reaction mixture was allowed to cool down to room temperature. The solvents were removed under vacuo and the product was purified by repeated silica-column chromatography with hexane : dichloromethane (3:1) as an eluent in 62% yield.

¹H NMR (400 MHz, CDCl₃, δ in ppm): 8.96 (2H, d, *J* = 8 Hz), 8.15 (2H, d, *J* = 8 Hz), 7.79 (2H, d, *J* = 8 Hz), 7.67 (1H, s), 7.62 (2H, d, *J* = 8 Hz), 7.45 (5H, m), 7.32 (3H, m), 4.17 (4H, m), 1.77 (4H, m), 1.44 (4H, s), 1.26 (24H, s), 0.87 (6H, s); ¹³C NMR (100 MHz, CDCl₃, δ in ppm): 161.3, 161.2, 140.4, 138.3, 135.6, 135.2, 133.3, 133.1, 131.1, 130.8, 129.7, 128.7, 128.0, 126.9, 126.1, 123.6, 121.1, 120.37, 120.40, 109.7, 108.6, 107.8, 42.3, 31.9, 30.1, 29.9, 29.5, 29.27, 29.28, 29.2, 26.9, 22.7, 14.1; HRMS (ESI) *m/z* calcd for C₅₄H₅₉N₃O₂S₂ + H: 846.4083 [M + H]⁺, found 846.4121 [M + H]⁺; UV/vis (Dichloromethane) λ_{max} 580 nm, ε [M⁻¹.cm⁻¹] (3.8×10⁴).

Synthesis of DPP 6

In 100 ml round bottom flask dibromodiketopyrrolopyrrole **DPP 4** (0.200 g, 0.27 mmol) and *N*-(4-Ethynylphenyl) carbazole (0.152 g, 0.57 mmol) were dissolved in dry tetrahydrofuran (15 ml) and triethylamine (4 ml). The reaction mixture was degassed with argon for 10 minutes and Pd(PPh₃)₄ (0.016 g, 0.013 mmol) and CuI (0.005 g, 0.027 mmol) were then added. The reaction mixture was stirred overnight at 70 °C. After completion, the reaction mixture was allowed to cool down to room temperature. The solvents were removed under vacuo and blue colored product was purified by silica-column chromatography with hexane: dichloromethane (3:1) as an eluent in 68% yield.

¹H NMR (400 MHz, CDCl₃, δ in ppm): 8.97 (2H, d, *J* = 4 Hz), 8.15 (4H, d, *J* = 8 Hz), 7.79 (4H, d, *J* = 8 Hz), 7.62 (4H, d, *J* = 8 Hz), 7.44 (10H, m), 7.32 (4H, t), 4.11 (4H, m), 1.79 (4H, m), 1.47 (4H, m), 1.39 (4H, m), 1.27 (18H, s), 0.86 (8H, m); ¹³C NMR (100 MHz, CDCl₃, δ in ppm): 162.2, 140.5, 139.2, 138.4, 135.6, 133.4, 131.1, 130.7, 128.5, 126.9, 126.2, 123.7, 121.1, 120.5, 120.4, 109.8, 108.8, 97.2, 83.2, 53.5, 42.5, 32.0, 30.1, 29.3, 27.0, 22.7, 14.2; HRMS (ESI) *m/z* calcd for C₇₄H₇₀N₄O₂S₂ + H: 1111.4826 [M + H]⁺, found 1111.5013 [M + H]⁺; UV/vis (Dichloromethane) λ_{max} 616 nm, ε [M⁻¹.cm⁻¹] (6.3×10⁴).

Synthesis of DPP 7

In a glass vessel, **DPP 5** (0.100 g, 0.12 mmol) and TCNE (0.017 g, 0.13 mmol) were dissolved in 5 ml of acetonitrile and 1, 2 dichloroethane (1:1) under argon atmosphere. Then, the solution was heated to 135 °C under microwave irradiation for 4 hours. After cooling to room temperature the solvents were removed under vacuo and the product was purified by silica-column chromatography with hexane : dichloromethane (1:1) as an eluent to yield **DPP 7** as a dark green colored solid in 70% yield.

¹H NMR (400 MHz, CDCl₃, δ in ppm): ¹H NMR (400 MHz, CDCl₃, δ in ppm): 9.20 (1H, d, *J* = 4 Hz), 9.11 (1H, d, *J* = 4 Hz), 8.13 (2H, d, *J* = 8 Hz), 8.06 (2H, d, *J* = 8Hz), 7.89 (2H, d, *J* = 8 Hz), 7.84 (1H, d, *J* = 8 Hz), 7.81 (1H, d, *J* = 4Hz), 7.59 (2H, d, *J* = 4 Hz), 7.45 (2H, m), 7.36 (3H, m), 4.10 (m, 4H) 1.76 (4H, s), 1.42 (4H, m), 1.34 (22H, s), 0.87 (8H, s); ¹³C NMR (100 MHz, CDCl₃, δ in ppm): 164.5, 161.6, 160.6, 155.7, 144.6, 144.4, 140.9, 139.6, 138.4, 138.2, 136.1, 135.14, 135.07, 133.8, 131.3, 129.4, 129.2, 128.3, 127.1, 126.6, 124.5, 121.7, 120.7, 120.6, 113.5, 112.8, 111.8, 111.2, 110.0, 108.6, 87.0, 79.8, 42.6,

31.9, 30.5, 29.8, 26.93, 26.87, 22.7, 14.2; HRMS (ESI) m/z calcd for $C_{60}H_{59}N_7O_2S_2 + Na$: 996.4130 $[M + Na]^+$, found 996.4064 $[M + Na]^+$; UV/vis (Dichloromethane) λ_{max} 695 nm, ϵ $[M^{-1}.cm^{-1}]$ (4.8×10^4).

Synthesis of DPP 8

In a glass vessel, **DPP 6** (0.100 g, 0.12 mmol) and TCNE (0.017 g, 0.13 mmol) were dissolved in 5 ml of acetonitrile and 1, 2 dichloroethane (1:1) under argon atmosphere. Then the solution was heated to 135 °C under microwave irradiation for 4 hours. After cooling to room temperature the solvents were removed under vacuo and the product was purified by silica-column chromatography with hexane: dichloromethane (2:1) as an eluent to yield **DPP 8** as a dark green colored solid in 72% yield.

1H NMR (400 MHz, $CDCl_3$, δ in ppm): 9.21 (1H, d, $J = 4$ Hz), 9.14 (1H, d, $J = 4$ Hz), 8.14 (4H, t), 8.06 (2H, d, $J = 8$ Hz), 7.90 (2H, d, $J = 12$ Hz), 7.84 (1H, d, $J = 4$ Hz), 7.80 (2H, d, $J = 8$ Hz), 7.64 (2H, d, $J = 8$ Hz), 7.59 (2H, d, $J = 8$ Hz), 7.51 (1H, d, $J = 4$ Hz), 7.46 (6H, m), 7.35 (4H, m), 4.12 (4H, m), 1.78 (4H, m), 1.46 (2H, m), 1.26 (24 H, brs), 0.87 (8H, m); ^{13}C NMR (100 MHz, $CDCl_3$, δ in ppm): 164.4, 161.4, 160.5, 155.6, 144.4, 140.7, 140.4, 139.5, 138.8, 138.3, 138.2, 136.3, 135.31, 135.27, 133.7, 133.2, 131.5, 131.3, 129.9, 128.2, 126.2, 124.5, 123.8, 121.9, 120.7, 113.6, 111.9, 111.2, 110.0, 109.7, 109.4, 86.9, 83.0, 79.9, 53.5, 42.6, 31.9, 30.5, 30.0, 29.70, 29.20, 26.91, 26.85, 22.7, 14.2; HRMS (ESI) m/z calcd for $C_{80}H_{70}N_8O_2S_2 + Na$: 1261.4900 $[M + Na]^+$, found 1261.4955 $[M + Na]^+$; UV/vis (Dichloromethane) λ_{max} 726 nm, ϵ $[M^{-1}.cm^{-1}]$ (7.2×10^4).

3.9. Conclusions

In summary, we have synthesized *N*-phenyl carbazole substituted unsymmetrical **DPP 5** and symmetrical **DPP 6** by Sonogashira cross-coupling and their TCBD derivatives **7** and **8** by [2+2] cycloaddition-retroelectrocyclization reaction respectively. Dramatic colour change was observed after the incorporation of TCBD in ethyne bridged *N*-phenyl carbazole substituted DPP. The TCBD substituted DPPs show systematic red shift in absorption spectra with decrease in HOMO – LUMO gap. High thermal stability, multiple reduction waves and low HOMO – LUMO gap values make *N*-phenyl carbazole substituted **DPPs 5 – 8** a potential candidate for solar cell applications. The results presented here will be useful in the design and synthesis

of new molecular systems with low HOMO–LUMO gap for optoelectronic applications.

3.10. References

- [1] (a) Wang, H., Xiao, L., Yan, L., Chen, S., Zhu, X., Peng, X., Wang, X., Wong, W.-K., Wong, W.-Y. (2016), Structural engineering of porphyrin-based small molecules as donors for efficient organic solar cells. *Chem. Sci.*, 7, 4301–4307 (DOI: 10.1039/C5SC04783H); (b) Qin, C., Fu, Y., Chui, C.-H., Kan, C.-W., Xie, Z., Wang, L., Wong, W.-Y. (2011), Tuning the Donor–Acceptor Strength of Low-Bandgap Platinum-Acetylide Polymers for Near-Infrared Photovoltaic Applications. *Macromol. Rapid Commun.*, 32, 1472–1477 (DOI: 10.1002/marc.201100247); (c) Wang, X.-Z., Wang, Q., Yan, L., Wong, W.-Y., Cheung, K.-Y., Ng, A., Djurišić, A. B., Chan, W.-K. (2010), Tuning the Donor–Acceptor Strength of Low-Bandgap Platinum-Acetylide Polymers for Near-Infrared Photovoltaic Applications. *Macromol. Rapid Commun.*, 31, 861–867 (DOI: 10.1002/marc.200900885); (d) Qin, C., Wong, W.-Y., Han, L. (2013), Squaraine Dyes for Dye-Sensitized Solar Cells: Recent Advances and Future Challenges. *Chem. Asian J.*, 8, 1706–1711 (DOI: 10.1002/asia.201300185); (e) Gomez-Hens, A. and Aguilar-Caballo, M. P. (2004), Long-wavelength fluorophores: new trends in their analytical use. *Trends Anal. Chem.*, 23, 127–136 (DOI: 10.1016/S0165-9936(04)00305-X); (f) Yuan, L., Lin, W., Zheng, K., He, L., Huang, W. (2013), Far-red to near infrared analyte-responsive fluorescent probes based on organic fluorophore platforms for fluorescence imaging. *Chem. Soc. Rev.*, 42, 622–661 (DOI: 10.1039/C2CS35313J); (g) Hilderbrand, S. A., Weissleder, R. (2010), Near-infrared fluorescence: application to in vivo molecular imaging. *Curr. Opin. Chem. Biol.*, 14, 71–78 (DOI: 10.1016/j.cbpa.2009.09.029).
- [2] Thompson, B. C., Fréchet, Jean M. J. (2008), Polymer–Fullerene Composite Solar Cells, *Angewandte Chemie International Edition*, 47, 58–77 (DOI:10.1002/anie.200702506). (b) Liang, Y., Wu, Y., Feng, D., Tsai, S.-T., Son, H.-J., Li, G., Yu, L. (2009), Development of New Semiconducting Polymers for High Performance Solar Cells, *J. Am. Chem. Soc.*, 131, 56–57 (DOI: 10.1021/ja808373p). (c) Nishizawa, T., Lim, H. K., Tajima, K.,

- Hashimoto, K. (2009) Efficient dyad-based organic solar cells with a highly crystalline donor group, *Chem. Commun.*, 2469–2471 (DOI: 10.1039/B902060H). (d) Yamamoto, T., Morita, A., Miyazaki, Y., Maruyama, T., Wakayama, H., Zhou, Z–H., Nakamura, Y., Kanbara, T., Sasaki, S., Kubota, K. (1992), Preparation of π -conjugated poly(thiophene-2,5-diyl), poly(p-phenylene), and related polymers using zerovalent nickel complexes. Linear structure and properties of the π -conjugated polymers, *Macromolecules*, 25, 1214–1223 (DOI: 10.1021/ma00030a003).
- [3] (a) Gautam, P., Misra, R., Siddiqui, S. A., Sharma, G. D. (2015), Unsymmetrical Donor–Acceptor–Acceptor– π –Donor Type Benzothiadiazole-Based Small Molecule for a Solution Processed Bulk Heterojunction Organic Solar Cell, *ACS Appl. Mater. Interfaces*, 7, 10283–10292 (DOI: 10.1021/acsami.5b02250). (b) Jadhav, T., Misra, R., Biswas, S., Sharma, G. D. (2015), Bulk heterojunction organic solar cells based on carbazole–BODIPY conjugate small molecules as donors with high open circuit voltage, *Phys. Chem. Chem. Phys.*, 17, 26580–26588 (DOI: 10.1039/C5CP04807A). (c) Misra, R., Maragani, R., Patel, K. R., Sharma, G. D. (2014), Synthesis, optical and electrochemical properties of new ferrocenyl substituted triphenylamine based donor–acceptor dyes for dye sensitized solar cells, *RSC Adv.*, 4, 34904–34911 (DOI: 10.1039/C4RA03088E).
- [4] (a) Grzybowski, M., Gryko, D. T. Grzybowski, M., Gryko, D. T. (2015), Diketopyrrolopyrroles: Synthesis, Reactivity, and Optical Properties, *Advanced Optical Materials*, 3, 280–320 (DOI:10.1002/adom.201400559). (b) Ha, J. S., Kim, K. H., Choi, D. H. (2011), 2,5-Bis(2-octyldodecyl)pyrrolo[3,4-c]pyrrole-1,4-(2H,5H)-dione-Based Donor–Acceptor Alternating Copolymer Bearing 5,5'-Di(thiophen-2-yl)-2,2'-biselenophene Exhibiting $1.5 \text{ cm}^2 \cdot \text{V}^{-1} \cdot \text{s}^{-1}$ Hole Mobility in Thin-Film Transistors, *J. Am. Chem. Soc.*, 133, 10364 – 10367 (DOI: 10.1021/ja203189h). (c) Li, Y., Sonar, P., Murphy, L., Hong W. (2013), High mobility diketopyrrolopyrrole (DPP)-based organic semiconductor materials for organic thin film transistors and photovoltaics, *Energy Environ. Sci.*, 6, 1684–1710 (DOI: 10.1039/C3EE00015J). (d) Kobayashi, N., Inagaki, S., Nemykin, V. N., Nonomura, T. (2001), A novel hemiporphyrzine comprising three isoindole-diimine and three thiadiazole units, *Angew. Chem. Int. Ed.*, 40, 2710–2712 (DOI:10.1002/1521-3773(20010716)40:14<2710::AID-

ANIE2710>3.0.CO;2-A).

- [5] (a) Wallquist, O., Lenz, R. (2002), 20 years of DPP pigments – future perspectives. *Macromol. Symp.*, 187, 617–630 (DOI:10.1002/1521-3900(200209)187:1<617::AID-MASY617>3.0.CO;2-5). (b) Hao, Z., Iqbal, A., (1997), Some aspects of organic pigments, *Chem. Soc. Rev.*, 26, 203–213 (DOI: 10.1039/CS9972600203). (c) Iqbal, A., Cassar, L., Rochat, A. C., Pfenninger, J., *J. Coat. Technol.*, 1988, 60, 37. (d) Farnum, D. G., Mehta, G., Moore, G. G., Siegel, F. P. (1974), Attempted reformatskii reaction of benzonitrile, 1,4-diketo-3,6-diphenylpyrrolo[3,4-C]pyrrole. A lactam analogue of pentalene., *Tetrahedron Lett.*, 15, 2549 – 2552 ([https://doi.org/10.1016/S0040-4039\(01\)93202-2](https://doi.org/10.1016/S0040-4039(01)93202-2)). (e) Zambounis, J. S., Hao, Z., Iqbal, A. (1997), Latent pigments activated by heat, *Nature*, 388, 131–132 (DOI:10.1038/40532). (f) Sonar, P., Ng, G.-M., Lin, T. T., Dodabalapur, A., Chen, Z.-K. (2010), Solution processable low bandgap diketopyrrolopyrrole (DPP) based derivatives: novel acceptors for organic solar cells, *J. Mater. Chem.*, 20, 3626 (DOI: 10.1039/B924404B). (g) Walker, B., Tamayo, A. B., Dang, X.-D., Zalar, P., Seo, J. H., Garcia, A., Tantiwivat, M., Nguyen, T.-Q. (2009), Nanoscale Phase Separation and High Photovoltaic Efficiency in Solution-Processed, Small-Molecule Bulk Heterojunction Solar Cells. *Adv. Funct. Mater.*, 19, 3063–3069 (DOI:10.1002/adfm.200900832). (h) Song, B., Wang, Z., Chen, S., Zhang, X., Fu, Y., Smet, M., Dehaen, W. (2005), The Introduction of π - π Stacking Moieties for Fabricating Stable Micellar Structure: Formation and Dynamics of Disklike Micelles. *Angewandte Chemie International Edition*, 44, 4731–4735 (DOI:10.1002/anie.200500980).
- [6] (a) Patil, Y., Jadhav, T., Dhokale, B., Misra, R. (2016), Tuning of the HOMO–LUMO Gap of Symmetrical and Unsymmetrical Ferrocenyl-Substituted Diketopyrrolopyrroles. *Eur. J. Org. Chem.*, 2016, 733–738 (DOI:10.1002/ejoc.201501123). (b) Patil, Y., Misra, R., Keshtov, M. L., Sharma, G. D., (2016) 1,1,4,4-Tetracyanobuta-1,3-diene Substituted Diketopyrrolopyrroles: An Acceptor for Solution Processable Organic Bulk Heterojunction Solar Cells, *J. Phys. Chem. C*, 120, 6324–6335 (DOI: 10.1021/acs.jpcc.5b12307).
- [7] (a) Michinobu, T., May, J. C., Lim, J. H., Boudon, C., Gisselbrecht, J.-P., Seiler, P., Gross, M., Biaggio, I., Diederich, F. (2005), A new class of organic donor–

acceptor molecules with large third-order optical nonlinearities, *Chem. Commun.*, 737–739 (DOI: 10.1039/B417393G). (b) M. Kivala, C. Boudon, J.-P. Gisselbrecht, P. Seiler, M. Gross, F. Diederich, (2007), Charge-Transfer-Chromophore durch Cycloaddition-Retro-Elektrocyclisierung: multivalente Systeme und Kaskadenreaktionen, *Angew. Chem.*, 119, 6473–6477 (DOI: 10.1002/ange.200701733). (c) P. Reutenauer, M. Kivala, P. D. Jarowski, C. Boudon, J. Gisselbrecht, M. Gross, F. Diederich, (2007) New Strong Organic Acceptors by Cycloaddition of TCNE and TCNQ to Donor-substituted Cyanoalkynes, *Chem. Commun.*, 489–4900 (DOI: 10.1039/B714731G). (d) Kivala, M., Stanoeva, T., Michinobu, T., Frank, B., Gescheidt, G., Diederich, F. (2008), One-Electron-Reduced and -Oxidized Stages of Donor-Substituted 1,1,4,4-Tetracyanobuta-1,3-dienes of Different Molecular Architectures. *Chem. Eur. J.*, 14, 7638–7647 (DOI:10.1002/chem.200800716). (e) Frank, B. B., C. Blanco, B., Jakob, S., Ferroni, F., Pieraccini, S., Ferrarini, A., Boudon, C., Gisselbrecht, J.-P., Seiler, P., Spada, G. P., Diederich, F. (2009), N-Arylated 3,5-Dihydro-4H-dinaphtho[2,1-c:1',2'-e]azepines: Axially Chiral Donors with High Helical Twisting Powers for Nonplanar Push–Pull Chromophores, *Chem. Eur. J.*, 15, 9005–9016 (DOI:10.1002/chem.200900913). (f) Yamada, M., Rivera-Fuentes, P., Schweizer, W. B., Diederich, F. (2010), Optische Stabilität axial-chiraler push-pull-substituierter Buta-1,3-diene: Effekt einer einzelnen Methylgruppe auf der Oberfläche von C₆₀, *Angew. Chem.*, 122, 3611–3615 (DOI: 10.1002/ange.200906853). (g) Yamada, M., Schweizer, W. B., Schoenebeck, F., Diederich, F. (2010) Unprecedented thermal rearrangement of push–pull-chromophore–[60]fullerene conjugates: formation of chiral 1,2,9,12-tetrakis-adducts, *Chem. Commun.*, 46, 5334–5336 (DOI: 10.1039/C0CC00881H). (h) Krauß, N., Kielmann, M., Ma, J., Butenschön, H. (2015), Reactions of Alkynyl- and 1,1'-Dialkynylferrocenes with Tetracyanoethylene–Unanticipated Addition at the Less Electron-Rich of Two Triple Bonds, *Eur. J. Org. Chem.*, 2015, 2622–2631 (DOI:10.1002/ejoc.201500105).

- [8] (a) Michinobu, T. (2010), Click synthesis of donor–acceptor-type aromatic polymers, *Pure Appl. Chem.*, 82, 1001–1009 (<http://dx.doi.org/10.1351/PAC-CON-09-09-09>). (b) Shoji, T., Ito, S., Toyota, K., Yasunami, M., Morita, N. (2008), Synthesis, Properties, and Redox Behavior of Mono-, Bis-, and

- Tris[1,1,4,4,-tetracyano-2-(1-azulenyl)-3-butadienyl] Chromophores Binding with Benzene and Thiophene Cores, *Chem. Eur. J.*, 14, 8398–8408 (DOI:10.1002/chem.200701981). (c) Shoji, T., Ito, S., Toyota, K., Iwamoto, T., Yasunami, M., Morita, N. (2009), Reactions between 1-Ethynylazulenes and 7,7,8,8-Tetracyanoquinodimethane (TCNQ): Preparation, Properties, and Redox Behavior of Novel Azulene-Substituted Redox-Active Chromophores. *Eur. J. Org. Chem.*, 2009, 4316–4324. doi:10.1002/ejoc.200900539. (d) T. Shoji, M. Maruyama, S. Ito, N. Morita, *Bull. Chem. Soc. Jpn.* 2012, 85, 773. (e) Shoji, T., Ito, S., Okujima, T., Morita, N. (2012), Synthesis of push–pull chromophores by the sequential [2 + 2] cycloaddition of 1-azulenylbutadiynes with tetracyanoethylene and tetrathiafulvalene, *Org. Biomol. Chem.*, 10, 8308–8313 (DOI: 10.1039/C2OB26028J). (f) Shoji, T., Ito, S., Okujima, T., Morita, N. (2013), Synthesis of 2-Azulenyl-1,1,4,4-tetracyano-3-ferrocenyl-1,3-butadienes by [2+2] Cycloaddition of (Ferrocenylethynyl)azulenes with Tetracyanoethylene, *Chem. Eur. J.*, 19, 5721–5730 (DOI:10.1002/chem.201202257).
- [9] (a) Dhokale, B., Jadhav, T., Shaikh, M. M., Misra, R. (2016), Tetracyanobutadiene functionalized ferrocenyl BODIPY dyes, *Dalton Trans.*, 45, 1476–1483 (DOI: 10.1039/C5DT04037J). (b) Misra, R., Gautam, P. (2014), Tuning of the HOMO–LUMO gap of donor-substituted symmetrical and unsymmetrical benzothiadiazoles, *Org. Biomol. Chem.*, 12, 5448–5457 (DOI: 10.1039/C4OB00629A). (c) Gautam, P., Maragani, R., Misra, R. (2014), Tuning the HOMO–LUMO gap of donor-substituted benzothiazoles, *Tetrahedron Letters*, 55, 6827 – 6830 (<https://doi.org/10.1016/j.tetlet.2014.10.094>).
- [11] (a) Yamagata, T., Kuwabara, J., Kanbara, T. (2012), Yamagata, T., Kuwabara, J., Kanbara, T. (2012), Synthesis and Characterization of Dioxopyrrolopyrrole Derivatives Having Electron-Withdrawing Groups, *Eur. J. Org. Chem.*, 2012: 5282–5290 (DOI:10.1002/ejoc.201200761). (b) Heyer, E., Ziessel, R. (2015) Panchromatic Push–Pull Dyes of Elongated Form from Triphenylamine, Diketopyrrolopyrrole, and Tetracyanobutadiene Modules, *Synlett.*, 26, 2109–2116 (DOI: 10.1055/s-0034-1378818).
- [11] (a) R. B. Aïch, Y. Zou, M. Leclerc, Y. Tao, (2010), Solvent effect and device optimization of diketopyrrolopyrrole and carbazole copolymer based solar cells, *Organic Electronics*, 11, 1053–1058

- (<https://doi.org/10.1016/j.orgel.2010.03.004>). (b) O. Kwon, J. Jo, B. Walker, G. C. Bazana, J. H. Seo, (2013), Pendant group effects on the optical and electrical properties of carbazole-diketopyrrolopyrrole copolymers, *J. Mater. Chem. A*, 1, 7118–7124 (DOI: 10.1039/C3TA11058C). (c) Ji, C., Yin, L., Li, K., Wang, L., Jiang, X., Suna, Y., Li, Y. (2015), D- π -A- π -D-type low band gap diketopyrrolopyrrole based small molecules containing an ethynyl-linkage: synthesis and photovoltaic properties, *RSC Adv.*, 5, 31606–31614 (DOI: DOI: 10.1039/C5RA01946J).
- [12] (a) Jo, M. Y., Park, J. H., Lim, G. E., Cho, J. H., Park, S. S., Hong, S-S., Kim, J. H. (2014), Diketopyrrolopyrrole-based Small Molecule for Application in Solution Processed Organic Solar Cells, *Mol. Cryst. Liq. Cryst.*, 598, 111–119 (DOI: 10.1080/15421406.2014.933382). (b) Palai, A. K., Lee, J., Das, S., Lee, J., Cho, H., Park, S.-U., Pyo, S. (2012), A diketopyrrolopyrrole containing molecular semiconductor: Synthesis, characterization and solution-processed 1D-microwire based electronic devices, *Organic Electronics*, 13, 2553–2560 (<https://doi.org/10.1016/j.orgel.2012.06.027>).
- [13] (a) Misra, R., Jadhav, T., Dhokale, B., Gautam, P., Sharma, R., Maragani, R., Mobin, S. M. (2014), Carbazole-BODIPY conjugates: design, synthesis, structure and properties, *Dalton Trans.*, 43, 13076–13086 (DOI: 10.1039/C4DT00983E). (b) Zhang, L., Zeng, S., Yin, L., Ji, C., Li, K., Li, Y., Wang, Y. (2013), The synthesis and photovoltaic properties of A–D–A-type small molecules containing diketopyrrolopyrrole terminal units, *New J. Chem.*, 37, 632–637 (DOI: 10.1039/C2NJ40963A). (c) Wan, Z., Jia, C., Zhou, L., Huo, W., Yao, X., Shi, Y. (2012), Influence of different arylamine electron donors in organic sensitizers for dye-sensitized solar cells, *Dyes Pigm.*, 95, 41–46 (<https://doi.org/10.1016/j.dyepig.2012.03.028>). (d) Li, J., Grimsdale, A. C. (2010), Carbazole-based polymers for organic photovoltaic devices, *Chem. Soc. Rev.*, 39, 2399–2410 (DOI: 10.1039/B915995A).
- [14] (a) G. Y. Chen, C. M. Chiang, D. Kekuda, S. C. Lan, C. W. Chu, K. H. Wei, (2010), Chen, G.-Y., Chiang, C.-M., Kekuda, D., Lan, S.-C., Chu, C.-W. and Wei, K.-H. (2010), Synthesis and characterization of a narrow-bandgap polymer containing alternating cyclopentadithiophene and diketo-pyrrolo-pyrrole units for solar cell applications, *J. Polym. Sci. A Polym. Chem.*, 48, 1669–1675 (DOI:10.1002/pola.23931). (b) Qu, S., Tian, H., (2012), Diketopyrrolopyrrole

- (DPP)-based materials for organic photovoltaics, *Chem. Commun.*, 48, 3039–3051 (DOI: 10.1039/C2CC17886A). (c) Ha, J. S., Kim, K. H., Choi, D. H. (2011), 2,5-Bis(2-octyldodecyl)pyrrolo[3,4-c]pyrrole-1,4-(2H,5H)-dione-Based Donor–Acceptor Alternating Copolymer Bearing 5,5'-Di(thiophen-2-yl)-2,2'-biselenophene Exhibiting $1.5 \text{ cm}^2 \cdot \text{V}^{-1} \cdot \text{s}^{-1}$ Hole Mobility in Thin-Film Transistors, *J. Am. Chem. Soc.*, 133, 10364–10367 (DOI: 10.1021/ja203189h).
- (d) Huo, L., Hou, J., Chen, H. Y., Zhang, S., Jiang, Y., Chen, T. L., Yang, Y. (2009), Bandgap and Molecular Level Control of the Low-Bandgap Polymers Based on 3,6-Dithiophen-2-yl-2,5-dihydropyrrolo[3,4-c]pyrrole-1,4-dione toward Highly Efficient Polymer Solar Cells, *Macromolecules*, 42, 6564 (DOI: 10.1021/ma9012972).
- (e) Bijleveld, J. C., Zoombelt, A., Mathijssen, S. G. J., Wienk, M. M., Turbiez, M., Leeuw, D. M., Janssen, R. A. J., (2009), Poly(diketopyrrolopyrrole–terthiophene) for Ambipolar Logic and Photovoltaics, *J. Am. Chem. Soc.*, 131, 16616 (DOI: 10.1021/ja907506r).
- [15] Woo, C. H., Beaujuge, P. M., Holcombe, T. W., Lee, O. P., Frechet, J. M. J. (2010), Incorporation of Furan into Low Band-Gap Polymers for Efficient Solar Cells, *J. Am. Chem. Soc.*, 132, 15547–15549 (DOI: 10.1021/ja108115y).
- [16] Dhokale, B., Jadhav, T., Shaikh, M. M., Misra, R. (2015), Synergistic effect of donors on tetracyanobutadine (TCBD) substituted ferrocenyl pyrenes, *RSC Adv.*, 5, 57692–57699 (DOI: 10.1039/C5RA11433K).
- [17] Frisch, M. J., Trucks, G. W., Schlegel, H. B., Scuseria, G. E., Robb, M. A., Cheeseman, J. R., Scalmani, G., Barone, V., Mennucci, B., Petersson, G. A., Nakatsuji, H., Caricato, M., Li, X., Hratchian, H. P., Izmaylov, A. F., Bloino, J., Zheng, G., Sonnenberg, J. L., Hada, M., Ehara, M., Toyota, K., Fukuda, R., Hasegawa, J., Ishida, M., Nakajima, T., Honda, Y., Kitao, O., Nakai, H., Vreven, T., Montgomery Jr, J. A., Peralta, J. E., Ogliaro, F., Bearpark, M., Heyd, J. J., Brothers, E., Kudin, K. N., Staroverov, V. N., Kobayashi, R., Normand, J., Raghavachari, K., Rendell, A., Burant, J. C., Iyengar, S. S., Tomasi, J., Cossi, M., Rega, N., Millam, J. M., Klene, M., Knox, J. E., Cross, J. B., Bakken, V., Adamo, C., Jaramillo, J., Gomperts, R., Stratmann, R. E., Yazyev, O., Austin, A. J., Cammi, R., Pomelli, C., Ochterski, J. W., Martin, R. L., Morokuma, K., Zakrzewski, V. G., Voth, G. A., Salvador, P., Dannenberg, J. J., Dapprich, S., Daniels, A. D., Farkas, Ö., Foresman, J. B., Ortiz, J. V., Cioslowski, J., Fox, D. J. (2009) Gaussian 09, revision D.01 Gaussian, Inc., Wallingford, CT, USA.

- [18] Patil, Y., Misra, R., Chen F.-C., Sharma, G. D. (2016), Small molecules based N-phenyl carbazole Substituted Diketopyrrolopyrroles as donor for solution processed bulk heterojunction organic solar cells. *Phys. Chem. Chem. Phys.*, 18, 22999-23005 (DOI: 10.1039/C6CP03767D).
- [19] Patil, Y., Misra, R., Keshtov, M. L., Sharma, G. D. (2017), Small molecule carbazole based diketopyrrolopyrroles with tetracyanobutadiene acceptor unit as Non-Fullerene Acceptor for Bulk Heterojunction Organic Solar Cells, *J. Mater. Chem. A*, 5, 3311-3319 (DOI: 10.1039/C6TA09607G).

Chapter 4

Triphenylamine functionalized diketopyrrolopyrroles

4.1. Introduction

The donor-acceptor (D–A) molecular systems with π -conjugation attracted attention of scientific community due to their wide variety of applications in organic solar cells (OSCs), organic light emitting diodes (OLEDs), multi-photon absorption and organic field effect transistors (OFETs).^[1]

Diketopyrrolopyrrole (DPP) possesses high thermal stability and used as brilliant colors and pigments.^[2] The DPP derivatives have been explored as potential candidate for aggregation-induced emission and two-photon absorption.^[3] Farnum *et al.* for the first time in 1974 reported synthesis of DPP proceeded *via* an oxidative dimerization.^[4] The diaryl DPP pigments show high insolubility due to the presence of strong intermolecular H-bonding and π – π interactions.^[5] DPP is reported as potential electron acceptor and functionalization with electron donor moiety will result in D–A molecular system. Our group is involved in the design and synthesis of D–A molecular systems with low HOMO–LUMO gap for optoelectronic applications.^[6]

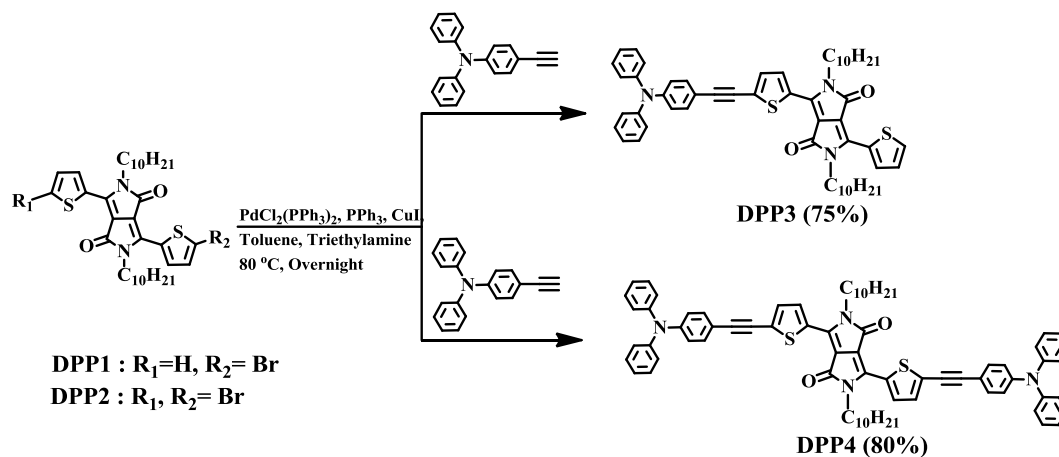
Triphenylamine (TPA) is widely used electron donor with good hole-transporting properties and having variety of applications in optoelectronics.^[7,8] The 1,1,4,4-tetracyanobuta-1,3-diene (TCBD) unit exhibits a strong electron withdrawing character and imparts good solubility in organic solvents because of the nonplanarity of the molecule which leads to efficient solubility and prevents the formation of aggregates.^[9,10,11] Diederich and co-workers have been explored [2+2] cycloaddition–retroelectrocyclization reaction of TCNE with electron rich alkynes resulted in formation of TCBD derivatives.^[12] Kanbara *et al.* have increased the electron accepting ability of DPP by introducing electron withdrawing pentafluorophenyl and TCBD groups.^[13] The materials based on multiple acceptors possess excellent photophysical behaviors such as strong light absorption, coplanar structure, and good photochemical stability.^[14]

By considering the excellent properties of TPA^[15] and DPP we have chosen these two groups for designing symmetrical and unsymmetrical TPA based DPP systems. The main intention of designing these types of DPP systems is to see the effect of donor TPA on the optical, thermal and electrochemical properties of DPP

unit and further the effect of strong electron withdrawing TCBD unit on TPA based DPPs. In this chapter we wish to report the design and synthesis of symmetrical and unsymmetrical TPA based DPP systems, where the TPA and thiophene act as donors, whereas the DPP and TCBD act as acceptor units. The structural, photophysical, thermal and electrochemical properties of these DPP systems were explored.

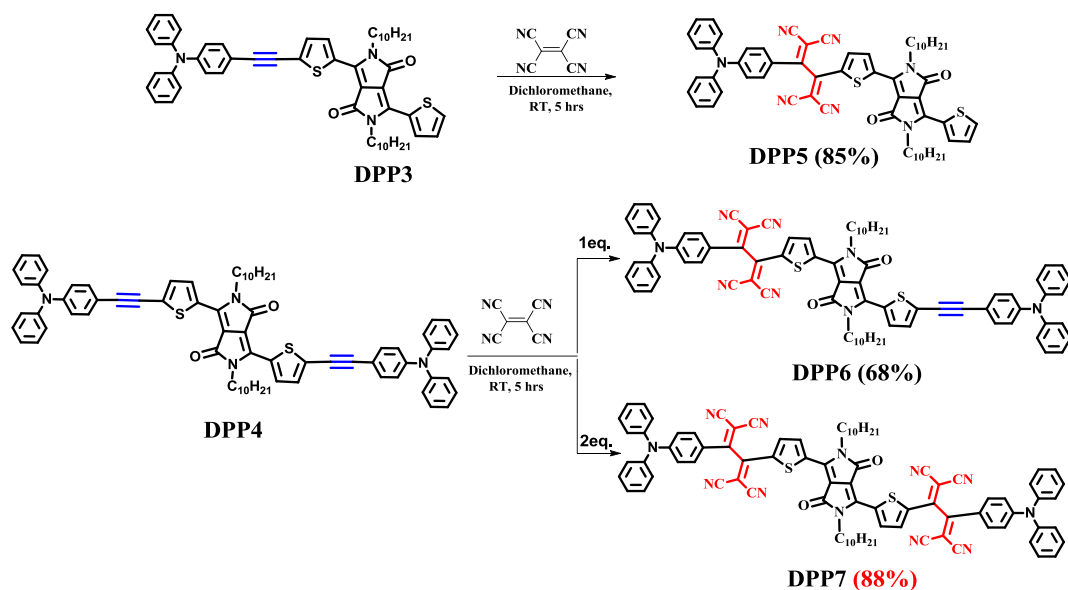
4.2. Results and discussion

The symmetrical and unsymmetrical TPA based DPPs **3** and **4** were synthesized by Pd-catalyzed Sonogashira cross-coupling reaction of (4-ethynylphenyl) diphenylamine with monobromo DPP **1** and dibromo DPP **2** in 75% and 80% yield respectively (Scheme 4.1).



Scheme 4.1: Synthesis of TPA based DPPs **3** and **4**.

Further subsequent [2+2] cycloaddition-retroelectrocyclization reaction of **DPP3** with TCNE resulted in 85% **DPP5** whereas the [2+2] cycloaddition-retroelectrocyclization reaction of **DPP4** with one and two equivalents of TCNE resulted in the formation of **DPP6** in 68% and **DPP7** in 88% yield respectively (Scheme 4.2).



Scheme 4.2. Synthesis of TPA based TCBD bridged **DPPs 5–7**.

The **DPPs 3–7** were purified by repeated silica-gel column chromatography and recrystallization techniques. The **DPPs 3–7** are soluble in common organic solvents like dichloromethane, chloroform toluene, tetrahydrofuran and were well characterized by ^1H NMR, ^{13}C NMR, and HRMS techniques.

4.3. Photophysical Properties

The electronic absorption spectra of TPA based **DPPs 3–7** were recorded in dichloromethane (DCM) at room temperature (Figure 4.1) and the corresponding data are listed in Table 4.1.

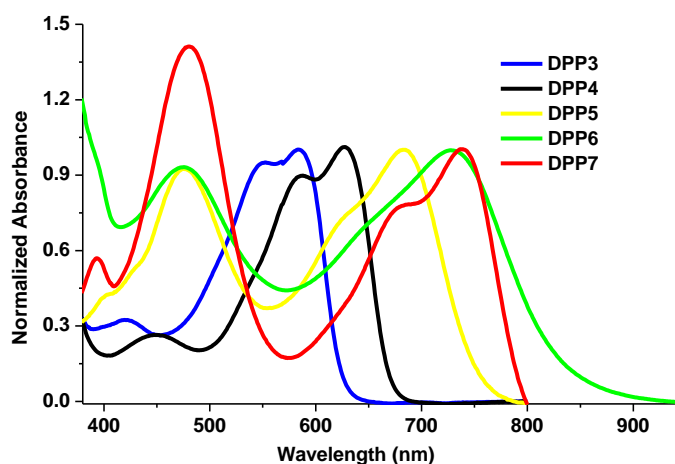


Figure 4.1. Electronic absorption spectra of **DPPs 3 – 7** in DCM solution (10^{-4} M).

The TPA based **DPPs 3 – 7** show absorption bands in UV-Vis-NIR region from 250 nm to 900 nm. The absorption bands at shorter and longer wavelength corresponds to the π - π^* transition and intramolecular charge transfer (ICT) respectively. The absorption maxima at longer wavelength region in TPA based **DPPs 3 – 7** follows the order **7 > 6 > 5 > 4 > 3**, which reveals that the increase in number of TPA or TCNE unit leads to red shift. The red shift is ascribed to systematic extension of π -conjugation by substituting TPA and increased donor-acceptor interaction due to incorporation of TCBD.

The incorporation of TCBD in ethyne bridged **DPP3** exhibited the prominent red shift of 97 nm in **DPP5** whereas incorporation of one and two equivalents of TCBD resulted in red shift of >100 nm (101 nm in **DPP6** and 112 nm in **DPP7**) in long wavelength ICT band respectively. This red shifted CT band in TCBD derivatives **DPPs 5 – 7** indicate the stronger D–A interaction compared to TPA based **DPPs 3** and **4**.

Table 4.1. Photophysical, thermal and computational properties of **DPPs 3 – 7**.

	λ_{max} (nm)	$\epsilon/10^4$ ($\text{M}^{-1} \cdot \text{cm}^{-1}$) ^a	T_d ($^{\circ}\text{C}$) ^b	HOMO–LUMO gap (eV)
DPP3	583	2.3	402	2.24
	551	2.8		
DPP4	627	3.3	398	2.07
	587	2.3		
DPP5	683	1.7	357	1.91
	476	1.5		
DPP6	728	3.1	366	1.66
DPP7	738	1.9	338	1.72
	480	2.6		

^aAbsorbance measured in dichloromethane at 1×10^{-4} M concentration.; ϵ :extinction coefficient;

^bDecomposition temperatures for 10% weight loss at heating rate of $10 \text{ }^{\circ}\text{C min}^{-1}$ under nitrogen atmosphere.

4.4 Thermal Properties

The thermal properties of the TPA based **DPPs 3–7** were investigated by thermogravimetric analysis (TGA) under nitrogen atmosphere and data are shown in

Figure 4.2. The TPA based **DPPs 3 – 7** exhibit good thermal stability and the decomposition temperatures at 10% weight loss in **DPPs 3–7** were 402 °C, 398 °C, 357 °C, 366 °C and 338 °C respectively. The trend observed at 10% weight loss follows the order **3 > 4 > 6 > 5 > 7**, which reveals that the ethyne bridged TPA based **DPPs 3** and **4** show better thermal stability compared to TCBD bridged **DPPs 5 –7**. The incorporation of electron withdrawing TCBD lowers the thermal stability.

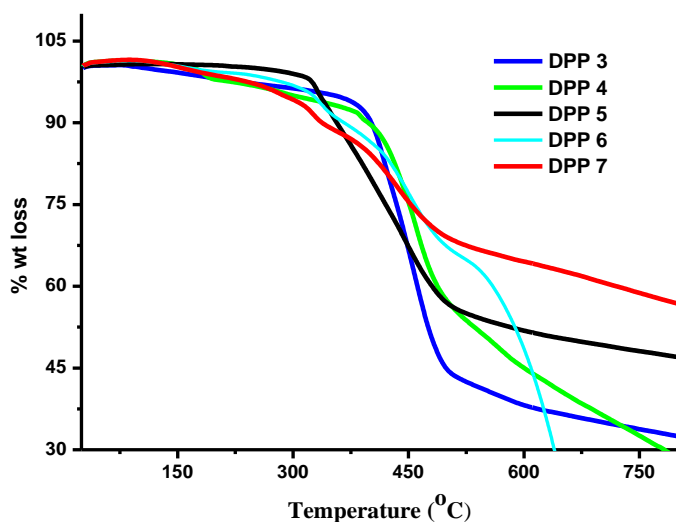


Figure 4.2. Thermogravimetric analysis of **DPPs 3 – 7** measured at heating rate of 10 °C / min under nitrogen atmosphere.

4.5. Electrochemical Properties

The electrochemical properties of TPA based **DPPs 3 – 7** were explored by cyclic voltammetry and differential pulse voltammetry (CV and DPV) techniques in dichloromethane solvent using 0.1 M tetrabutylammonium hexafluorophosphate (Bu_4NPF_6) as supporting electrolyte. The CV and DPV plots of TPA based **DPPs 3 – 7** are shown in Figure 4.3 and the corresponding data are listed in Table 4.2.

The ethyne bridged **DPPs 3** and **4** exhibit four oxidation waves and two reduction waves. The oxidation waves were related to the oxidation of thiophenes and TPA whereas two reductions were corresponds to the formation of mono and dianion at DPP unit. The mono-TCBD bridged **DPPs 5** and **6** show three oxidation waves whereas di-TCBD bridged **DPP7** shows only two oxidation waves. The order of first oxidation potential in TPA based **DPPs 3 – 7**, indicates incorporation of TCBD hardens the oxidation.

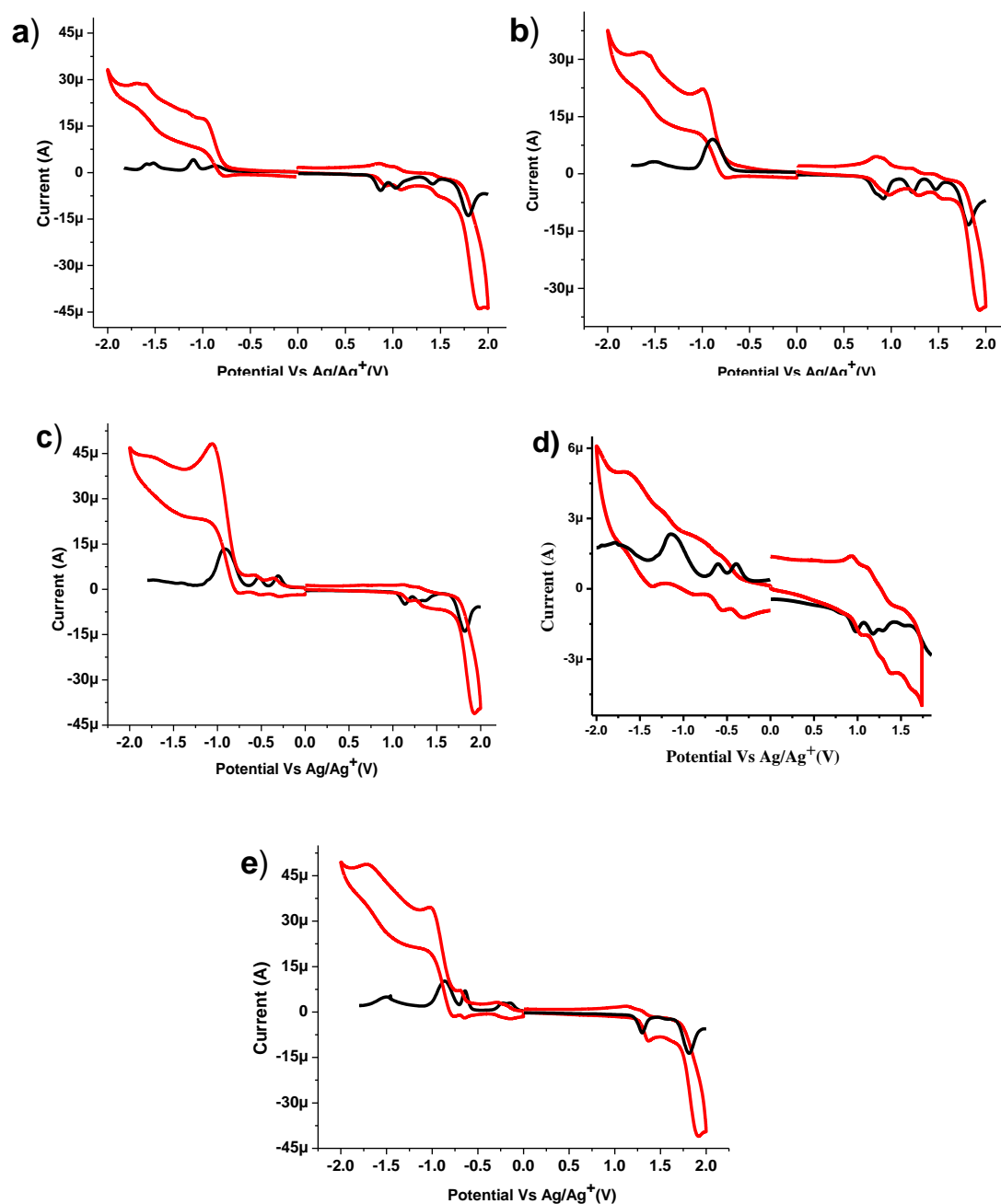


Figure 4.3. CV (red line) and DPV (black line) plots of TPA based **DPP3** (a), **DPP4** (b), **DPP5** (c), **DPP6** (d) and **DPP7** (e).

The TPA functionalized **DPPs 3** and **4** exhibit two reduction waves whereas the TCBD bridged **DPPs 5–7** exhibit four reduction waves. The incorporation of electron withdrawing TCBD in ethyne bridged **DPPs 3** and **4** show two additional reduction waves at low potential in TCBD bridged **DPPs 5 – 7** corresponds to TCBD unit. The reduction of DPP moiety is hardens by incorporation of TCBD. The

two separate waves for the reduction of TCBD indicated independent reduction at TCBD units.

Table 4.2. Electrochemical properties of **DPPs 3 – 7**^a.

	E^4	E^3	E^2	E^1	E^1	E^2	E^3	E^4
	Red	Red	Red	Red	Oxid	Oxid	Oxid	Oxid
DPP3	-	-	-1.51	-1.10	0.86	1.03	1.41	1.79
DPP4	-	-	-1.51	-0.89	0.91	1.22	1.47	1.82
DPP5	-	-0.91	-0.53	-0.30	1.13	1.29	1.82	-
DPP6	-1.78	-1.15	-0.60	-0.39	0.96	1.14	1.28	1.52
DPP7	-1.50	-0.86	-0.64	-0.19	1.30	1.81	-	-

^aThe electrochemical analysis was performed in a 0.1 M solution of Bu₄NPF₆ in dichloromethane at 100 mVs⁻¹ scan rate, versus Ag/Ag⁺ at 25 °C.

4.6. Theoretical calculations

The density functional theory (DFT) calculation was carried to understand the geometry and electronic structure of **DPPs 3 – 7** using the Gaussian09W program at the B3LYP/6-31+G** level.^[16] The geometry optimization was carried out in the gas phase and frontier molecular orbitals (FMOs) are displayed in Figure 4.4.

The HOMO of **DPPs 3–7** is distributed on the whole molecule. The LUMO of ethyne bridged **DPPs 3–4** is localized on DPP unit whereas LUMO in TCBD bridged **DPPs 5–7** is centered on TCBD and DPP units. The localization of LUMO on TCBD and DPP units indicates their acceptor nature. The localization of HOMO on whole molecule and LUMO on acceptor unit shows D–A interaction.

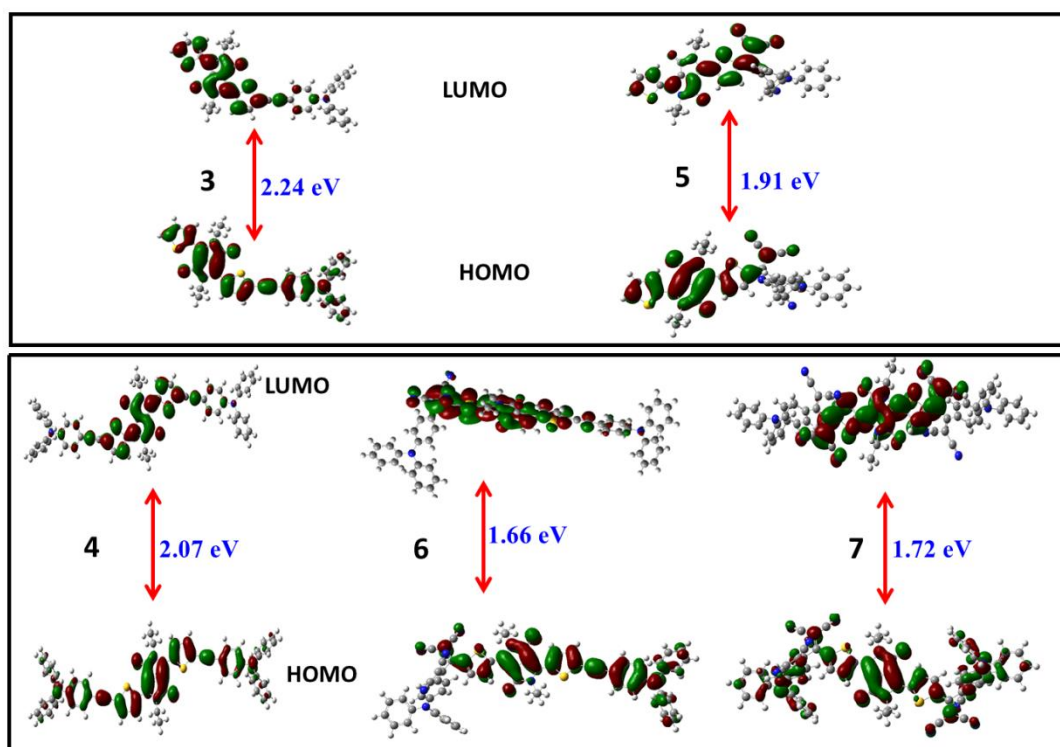


Figure 4.4. The frontier molecular orbitals of **DPPs 3 - 7** estimated by DFT calculation at B3LYP level.

The time dependent density functional theory (TD-DFT) calculation was performed at the B3LYP/6-31G level in order to get the idea of transitions. The main electronic transitions along with composition and oscillator strength for **DPPs 3 - 7** are as shown in Table 4.3. The results of TD-DFT calculation indicates that **DPPs 5-7** show main transitions in the visible region. In unsymmetrical **DPP5** the ICT from TPA to TCBD and DPP units correspond to HOMO-1 to LUMO transition. The HOMO→LUMO transition observed in **DPP6** is related to ICT transition from TPA to DPP and TCBD. The other lower wavelength transitions observed in TPA based **DPP6** were assigned to π - π^* transitions of TPA and TCBD which correspond to HOMO-1→LUMO+1 and HOMO-2→LUMO transitions. In symmetrical **DPP7** HOMO is distributed over whole molecule whereas HOMO-2 is localized on two TPA units. The charge transfer transitions in **DPP7** at long wavelength region from donor TPA to TCBD and DPP acceptors units corresponds to HOMO-2→LUMO and HOMO→LUMO transition.

Table 4.3. The main electronic transitions with composition and oscillator strengths for **DPPs 3 – 7**.

	Wavelength (nm)	Composition	f^a
DPP3	479	HOMO→LUMO (0.71)	0.56
DPP4	521	HOMO→LUMO (0.70)	0.77
DPP5	664	HOMO-1→LUMO (-0.21)	0.72
DPP6	794	HOMO→LUMO (0.70)	1.58
	467	HOMO-2→LUMO+1 (0.70)	0.45
DPP7	732	HOMO-2→LUMO (0.50)	1.23
		HOMO→LUMO (0.49)	

f^a = Oscillator Strength

4.7. Application in Photovoltaics

We used **DPPs 3** and **4** as donor along with PC₇₁BM as the acceptor for the preparation of solution processed bulk heterojunction organic solar cells (BHJ-OSCs). The solution processed BHJ small molecule processed with CF solution showed PCE of 2.23% and 3.05% for **DPP3:PC₇₁BM** and **DPP4:PC₇₁BM** active layers, respectively.^[17] The incorporation of TCBD improves the accepting ability and we used TCBD bridged derivatives as non-fullerene acceptor for BHJ-OSCs along with donor polymer **P** achieved a respectable PCE upto 4.95%.^[18] Herein for the first time we used TCBD based molecule as non-fullerene acceptor in OSCs.

4.8. Experimental Section

General methods

The chemicals were used as received unless otherwise indicated. All the moisture sensitive reactions were performed under argon atmosphere using the standard Schlenk method. ¹H NMR (400 MHz) and ¹³C NMR (100 MHz) spectra were recorded by using CDCl₃ as the solvent. The ¹H NMR chemical shifts are reported in parts per million (ppm) relative to the solvent residual peak (CDCl₃, 7.26 ppm). The multiplicities are given as: s (singlet), d (doublet), t (triplet), m (multiplet), and the coupling constants, *J*, are given in Hz. The ¹³C NMR chemical shifts are reported with relative to the solvent residual peak (CDCl₃, 77.02 ppm). HRMS was recorded on a mass spectrometer (ESI-TOF). The UV-visible absorption spectra of

DPPs were recorded on UV-visible Spectrophotometer in dichloromethane. The TGA analyses were performed on the thermal analysis system at the heating rate of 10 °C per minute under nitrogen atmosphere. Cyclic voltammograms (CVs) were recorded on an electrochemical analyzer using glassy carbon as working electrode, Pt wire as the counter electrode, and saturated Ag/Ag⁺ as the reference electrode.

Synthesis of DPP3

In 100 ml round bottom flask monobromo-diketopyrrolopyrrole **1** (0.100 g, 0.15 mmol) and (4-ethynylphenyl) diphenylamine (0.041 g, 0.15 mmol) were dissolved in dry THF (10 ml) and triethylamine (6 ml). The reaction mixture was degassed with argon for 10 minutes and Pd(PPh₃)₄ (0.0018 g, 0.015 mmol) and CuI (0.0028 g, 0.015 mmol) were added. The reaction mixture was stirred at 70 °C for 24 hours. After completion of reaction, the reaction mixture was allowed to cool down to room temperature. The solvent were removed under vacuo and the product was purified by silica-column chromatography with hexane: dichloromethane (3:1) as an eluent in 75% yield.

¹H NMR (400 MHz, CDCl₃, δ in ppm): 8.93 (2H, s), 7.64 (1H, s), 7.36 (3H, m), 7.28 (4H, m), 7.12 (7H, m), 7.00 (2H, d, *J* = 8 Hz), 4.05 (4H, s), 2.35 (1H, s), 1.74 (4H, s), 1.41 (4H, s), 1.25 (23 H, s), 0.86 (6H, s); ¹³C NMR (100 MHz, CDCl₃, δ in ppm): 161.3, 161.2, 148.7, 146.9, 139.9, 139.1, 135.5, 135.4, 132.6, 132.5, 130.8, 129.9, 129.8, 129.5, 129.2, 128.7, 125.3, 124.0, 121.6, 114.5, 108.3, 107.9, 98.5, 81.7, 42.3, 31.9, 30.1, 30.0, 29.5, 29.31, 29.26, 26.9, 22.7, 14.1; HRMS (ESI) *m/z* calcd for C₅₄H₆₁N₃O₂S₂ + Na: 870.4097 [M + Na]⁺, found 870.4094 [M + Na]⁺.

Synthesis of DPP4

In 100 ml round bottom flask dibromodiketopyrrolopyrrole **2** (0.100 g, 0.14 mmol) and (4-ethynylphenyl) diphenylamine (0.073 g, 0.28 mmol) were dissolved in dry THF (10 ml) and triethylamine (6 ml). The reaction mixture was degassed with argon for 10 minutes and Pd(PPh₃)₄ (0.015 g, 0.014 mmol) and CuI (0.0025 g, 0.014 mmol) were then added. The reaction mixture was stirred at 70 °C for 24 hours. After completion, the reaction mixture was allowed to cool down to room temperature. The solvents were removed under vacuo and colored product was purified by silica-column chromatography with hexane: dichloromethane (3:1) as an eluent in 80% yield.

¹H NMR (400 MHz, CDCl₃, δ in ppm): 8.93 (2H, s), 7.36 (6H, m), 7.29 (9H, m), 7.10 (11H, m), 7.00 (4H, d, *J* = 8 Hz), 4.07 (4H, m), 3.13 (2H, m), 1.75 (4H, m),

1.45 (6H, m), 1.25 (21H, s), 0.85 (6H, m); ^{13}C NMR (100 MHz, CDCl_3 , δ in ppm): 161.2, 148.7, 147.0, 139.0, 135.7, 132.6, 130.0, 129.7, 129.5, 129.4, 125.4, 124.0, 121.7, 114.5, 108.5, 98.7, 81.8, 46.1, 42.4, 31.9, 30.1, 29.7, 29.6, 29.31, 29.26, 26.9, 22.7, 14.2, 8.7; HRMS (ESI) m/z calcd for $\text{C}_{74}\text{H}_{74}\text{N}_4\text{O}_2\text{S}_2 + \text{Na}$: 1137.5145 [$\text{M} + \text{Na}$] $^+$, found 1137.5127 [$\text{M} + \text{Na}$] $^+$.

Synthesis of DPP5:

In 50 ml round bottom flask **DPP3** (0.100 g, 0.13 mmol) and TCNE (0.018 g, 0.14 mmol) were dissolved in dichloromethane (15 ml) under argon atmosphere. The reaction mixture was stirred at room temperature for 5 hours. The solvent was removed under vacuo and the product was purified by silica-column chromatography with Hexane: Dichloromethane (1:1) afforded the desired product **DPP5**, as dark colored solid in 85% yield.

^1H NMR (400 MHz, CDCl_3 , δ in ppm): 9.18 (1H, s), 9.04 (1H, s), 7.78 (1H, s), 7.72 (1H, s), 7.68 (2H, m), 7.40 (5H, m), 7.35 (1H, s), 7.25 (5H, m), 6.92 (2H, d, $J = 8\text{Hz}$), 4.08 (4H, s), 1.74 (4H, s), 1.42 (4H, s), 1.28 (24 H, s), 0.86 (6H, s); ^{13}C NMR (100 MHz, CDCl_3 , δ in ppm): 162.4, 161.5, 160.6, 157.3, 154.0, 144.4, 144.1, 140.1, 138.2, 138.0, 136.9, 135.5, 135.1, 133.5, 131.8, 130.2, 129.3, 129.2, 127.0, 126.9, 120.9, 118.1, 113.5, 112.92, 112.89, 112.7, 111.9, 108.5, 79.9, 78.1, 42.7, 42.5, 31.9, 30.4, 29.9, 29.5, 29.3, 29.2, 26.8, 22.7, 14.2; HRMS (ESI) m/z calcd for $\text{C}_{60}\text{H}_{61}\text{N}_7\text{O}_2\text{S}_2 + \text{H}$: 976.4401 [$\text{M} + \text{H}$] $^+$, found 976.4511 [$\text{M} + \text{H}$] $^+$.

Synthesis of DPP6:

In 50 ml round bottom flask **DPP4** (0.100g, 0.10 mmol) and TCNE (0.013 g, 0.10 mmol) were dissolved in dichloromethane (15 ml) under argon atmosphere. The reaction mixture was stirred at room temperature for 5 hours. The solvent was removed under vacuo and the product was purified by silica-column chromatography with hexane: dichloromethane (2:1) as a eluent to yield 68% **DPP6**.

^1H NMR (400 MHz, CDCl_3 , δ in ppm): 9.19 (1H, d, $J = 4\text{Hz}$), 9.05 (1H, d, $J = 4\text{Hz}$), 7.67-7.73 (3H, m), 7.37-7.42 (7H, m), 7.29-7.33 (5H, m), 7.22 (4H, m), 7.11-7.15 (7H, m), 7.00 (2H, d, $J = 8\text{ Hz}$), 6.92 (2H, d, $J = 8\text{Hz}$), 4.08, (4H, m), 1.74 (4H, m), 1.43 (4H, brs), 1.17–1.37 (24H, m), 0.86 (6H, m); ^{13}C NMR (100 MHz, CDCl_3 , δ in ppm): 161.4, 160.5, 154.0, 146.8, 144.4, 143.0, 140.1, 138.4, 136.8, 135.2, 135.1, 132.9, 132.7, 131.8, 130.1, 129.6, 127.0, 126.8, 125.5, 124.2, 121.0, 118.1, 113.8, 113.4, 113.2, 112.9, 109.1, 79.7, 78.2, 53.4, 31.9, 30.4, 30.0, 29.3, 26.8, 22.7, 14.1;

HRMS (ESI) m/z calcd for $C_{80}H_{74}N_8O_2S_2 + H$: 1243.5449 $[M + H]^+$, found 1243.5584 $[M + H]^+$.

Synthesis of DPP7:

In 50 ml round bottom flask **DPP4** (0.100g, 0.10 mmol) and TCNE (0.026 g, 0.20 mmol) were dissolved in dichloromethane (15 ml) under argon atmosphere. The reaction mixture was stirred at room temperature for 5 hours. The solvent was removed under vacuo and the product was purified by silica-column chromatography with hexane : dichloromethane (2:1) as a eluent to yield 88% **DPP7** as a dark colored solid.

1H NMR (400 MHz, $CDCl_3$, δ in ppm): 9.15 (2H, s), 7.75 (2H, s), 7.67 (4H, d, $J = 8$ Hz), 7.40 (8H, m), 7.28 (4H, m), 7.23 (8H, m), 6.92 (4H, d, $J = 8$ Hz), 4.07 (4H, s), 1.73 (4H, s), 1.42 (4H, s), 1.25 (24 H, s), 0.86 (6H, m); ^{13}C NMR (100 MHz, $CDCl_3$, δ in ppm): 162.0, 160.8, 157.5, 154.2, 144.4, 139.6, 138.8, 138.7, 138.2, 136.9, 134.8, 131.9, 130.3, 127.12, 127.08, 120.8, 118.2, 113.5, 112.9, 112.8, 112.7, 111.6, 81.8, 78.1, 43.0, 32.0, 30.4, 29.62, 29.59, 29.40, 29.36, 26.9, 22.8, 14.3; HRMS (ESI) m/z calcd for $C_{86}H_{74}N_{12}O_2S_2 + Na$: 1393.5391 $[M + H]^+$, found 1393.5390 $[M + H]^+$.

4.9. Conclusions

In conclusions, we have synthesized symmetrical and unsymmetrical TPA functionalized **DPPs 3 – 7** by Sonogashira cross-coupling and by [2+2] cycloaddition-retroelectrocyclization reaction respectively. The incorporation of TCBD in TPA substituted DPPs exhibited red shifted absorption with lowering HOMO – LUMO gap values. The incorporation of TCBD shifts the absorption from visible to NIR region with around 100 nm red shift. High thermal stability and low HOMO – LUMO gap of **DPPs 3 – 7** makes them potential candidate for organic photovoltaics. The results presented here will useful in the design and synthesis of new molecular systems with low HOMO –LUMO gap for optoelectronic applications.

4.10. References

[1] (a) Kobayashi, N., Inagaki, S., Nemykin, V. N., Nonomura, T. (2001), A novel hemiporphyrine comprising three isoindoleimine and three thiadiazole units, *Angew. Chem. Int. Ed.*, 40, 2710–2712 (DOI:10.1002/1521-3773(20010716)40:14<2710::AID-ANIE2710>3.0.CO;2-A). (b) Ji, C., Yin, L., Li, K., Wang, L., Jiang, X., Suna, Y., Li, Y. (2015), D– π –A– π –D-type low band

- gap diketopyrrolopyrrole based small molecules containing an ethynyl-linkage: synthesis and photovoltaic properties, *RSC Adv.*, 5, 31606–31614 (DOI: DOI: 10.1039/C5RA01946J). (c) Wong, W. Y., Wong, W. K., Raithby, P. R. (1998), Synthesis, characterisation and properties of platinum(II) acetylide complexes of ferrocenylfluorene: novel soluble donor–acceptor heterometallic materials, *J. Chem. Soc. Dalton Trans.*, 2761–2766 (DOI: 10.1039/A803168A). (d) Liu, H., Jia, H., Wang, L., Wu, Y., Zhan, C., Fu, H., Yao, J. (2012), Intermolecular electron transfer promoted by directional donor–acceptor attractions in self-assembled diketopyrrolopyrrole-thiophene films, *Phys. Chem. Chem. Phys.*, 14, 14262–14269 (DOI: 10.1039/C2CP41288H).
- [2] (a) Hao, Z., Iqbal, A., (1997), Some aspects of organic pigments, *Chem. Soc. Rev.*, 26, 203–213 (DOI: 10.1039/CS9972600203). (b) O. Wallquist in *High Performance Pigments* (Ed.: H. M. Smith), Wiley-VCH Verlag-GmbH, Weinheim, 2002, pp. 159–184. (c) Zambounis, J. S., Hao, Z., Iqbal, A. (1997), Latent pigments activated by heat, *Nature*, 388, 131–132 (DOI:10.1038/40532).
- [3] Wang, B.; He, N.; Li, B.; Jiang, S.; Qu, Y.; Qu, S.; Hua, J. (2012), Aggregation-Induced Emission and Large Two-Photon Absorption Cross-Sections of Diketopyrrolopyrrole (DPP) Derivatives, *Aust. J. Chem.*, 65, 387–394 (<https://doi.org/10.1071/CH11410>).
- [4] Farnum, D. G., Mehta, G., Moore, G. G., Siegel, F. P. (1974), Attempted reformatskii reaction of benzonitrile, 1,4-diketo-3,6-diphenylpyrrolo[3,4-C]pyrrole. A lactam analogue of pentalene, *Tetrahedron Lett.*, 15, 2549–2552 ([https://doi.org/10.1016/S0040-4039\(01\)93202-2](https://doi.org/10.1016/S0040-4039(01)93202-2)).
- [5] Grzybowski, M., Gryko, D. T. Grzybowski, M., Gryko, D. T. (2015), Diketopyrrolopyrroles: Synthesis, Reactivity, and Optical Properties, *Advanced Optical Materials*, 3, 280–320 (DOI:10.1002/adom.201400559).
- [6] (a) Dhokale, B., Jadhav, T., Shaikh, M. M., Misra, R. (2015), Synergistic effect of donors on tetracyanobutadiene (TCBD) substituted ferrocenyl pyrenes, *RSC Adv.*, 5, 57692–57699 (DOI: 10.1039/C5RA11433K). (b) Jadhav, T., Maragani, R., Misra, R., Sreeramulu, V., Rao, D. N., Mobin, S. M. (2013), Design and synthesis of donor–acceptor pyrazabole derivatives for multiphoton absorption, *Dalton Trans.*, 42, 4340–4342 (DOI: 10.1039/C3DT33065F). (c) Misra, R., Gautam, P., Jadhav, T., Mobin, M. (2013), Donor–Acceptor Ferrocenyl-

Substituted Benzothiadiazoles: Synthesis, Structure, and Properties, *J. Org. Chem.*, 78, 4940–4948 (DOI: 10.1021/jo4005734).

- [7] (a) Grolleau, J., Gohier, F., Allain, M., Legoupy, S., Cabanetos, C., Frère, P. (2017), Rapid and green synthesis of complementary D-A small molecules for organic photovoltaics, *Organic Electronics*, 42, 322–328 (<https://doi.org/10.1016/j.orgel.2016.12.046>). (b) Gu, Y., Zhou, X., Li, Y., Wu, K., Wang, F., Huang, M., Guo, F., Wang, Y., Gong, S., Ma, D., Yang, C. (2015), Tetrasubstituted adamantane derivatives with arylamine groups: Solution-processable hole-transporting and host materials with high triplet energy and good thermal stability for organic light-emitting devices, *Organic Electronics*, 25, 193-199 (<https://doi.org/10.1016/j.orgel.2015.06.036>).
- [8] (a) Can, M., Yigit, M. Z., Seintis, K., Karageorgopoulos, D., Demic, S., Icli, S., Giannetas, V., Fakis, M., Stathatos, E. (2014), Synthesis of two tri-arylamine derivatives as sensitizers in dye-sensitized solar cells: Electron injection studies and photovoltaic characterization, *Synthetic Metals*, 188, 77–85 (<https://doi.org/10.1016/j.synthmet.2013.11.015>). (b) Madec, M.-B., Morrison, J. J., Rabjohns, M., Turner, M. L., Yeates, S. G. (2010), Effect of poly(triarylamine) molar mass distribution on organic field effect transistor behavior, *Organic Electronics*, 11, 686-691 (<https://doi.org/10.1016/j.orgel.2009.12.015>).
- [9] (a) Shoji, T., Ito, S., Okujima, T., Morita, N. (2013), Synthesis of 2-Azulenyl-1,1,4,4-tetracyano-3-ferrocenyl-1,3-butadienes by [2+2] Cycloaddition of (Ferrocenylethynyl)azulenes with Tetracyanoethylene, *Chem. Eur. J.*, 19, 5721–5730 (DOI:10.1002/chem.201202257). (b) Krauß, N., Kielmann, M., Ma, J., Butenschön, H. (2015), Reactions of Alkynyl- and 1,1'-Dialkynylferrocenes with Tetracyanoethylene—Unanticipated Addition at the Less Electron-Rich of Two Triple Bonds, *Eur. J. Org. Chem.*, 2015, 2622–2631 (DOI:10.1002/ejoc.201500105). (c) Shoji, T., Maruyama, A., Yaku, C., Kamata, N., Ito, S., Okujima, T., Toyota, K. (2015), Synthesis, Properties, and Redox Behavior of 1,1,4,4-Tetracyano-2-ferrocenyl-1,3-butadienes Connected by Aryl, Biaryl, and Teraryl Spacers. *Chem. Eur. J.*, 21, 402–409 (DOI:10.1002/chem.201405004). (d) Yuan, Y., Michinobu, T., Satoh, N., Ashizawa, M., Han, L., J. (2015), Efficient Synthesis and Photosensitizer Performance of Nonplanar Organic Donor–Acceptor Molecules, *Nanosci.*

- Nanotechnol.*, 15, 5856–5866 (<https://doi.org/10.1166/jnn.2015.10032>). (e) Leliège, A., Blanchard, P., Rousseau, T., Roncali, J. (2011), Triphenylamine/Tetracyanobutadiene-Based D-A-D π -Conjugated Systems as Molecular Donors for Organic Solar Cells, *Org. Lett.*, 13, 3098–3101 (DOI: 10.1021/ol201002j).
- [10] (a) Bruce, M. I., Low, P. J., Hartl, F., Humphrey, P. A., de Montigny, F., Jevric, M., Lapinte, C., Perkins, G. J., Roberts, R. L., Skelton, B. W., White, A. H. (2005), Syntheses, Structures, Some Reactions, and Electrochemical Oxidation of Ferrocenylethynyl Complexes of Iron, Ruthenium, and Osmium, *Organometallics*, 24, 5241–5255 (DOI: 10.1021/om0504831). (b) Michinobu, T., Kumazawa, H., Noguchi, K., Shigehara, K. (2009), One-Step Synthesis of Donor–Acceptor type Conjugated Polymers from Ferrocene-Containing Poly(aryleneethynylene)s, *Macromolecules*, 42, 5903–5905 (DOI: 10.1021/ma9013324).
- [11] (a) Tang, X., Liu, W., Wu, J., Lee, C.-S., You, J., Wang, P. (2010), Synthesis, Crystal Structures, and Photophysical Properties of Triphenylamine-Based Multicyano Derivatives, *J. Org. Chem.*, 75, 7273–7278 (DOI: 10.1021/jo101456v). (b) Betou, M., Kerisit, N., Meledje, E., Leroux, Y. R., Katan, C., Halet, J.-F., Guillemin, J.-C., Trolez, Y. (2014), High-Yield Formation of Substituted Tetracyanobutadienes from Reaction of Ynamides with Tetracyanoethylene. *Chem. Eur. J.*, 20, 9553–9557 (DOI:10.1002/chem.201402653).
- [12] (a) Michinobu, T., May, J. C., Lim, J. H., Boudon, C., Gisselbrecht, J., Seiler, P., Gross, M., Biaggio, I., Diederich, F. (2005), A new class of organic donor–acceptor molecules with large third-order optical nonlinearities, *Chem. Commun.*, 2005, 737–739 (DOI: 10.1039/B417393G). (b) Michinobu, T., Boudon, C., Gisselbrecht, J.-P., Seiler, P., Frank, B., Moonen, N. N. P., Gross, M., Diederich, F. (2006), Donor-Substituted 1,1,4,4-Tetracyanobutadienes (TCBDs): New Chromophores with Efficient Intramolecular Charge-Transfer Interactions by Atom-Economic Synthesis, *Chem. Eur. J.*, 12, 1889–1905 (DOI:10.1002/chem.200501113).
- [13] Yamagata, T., Kuwabara, J., Kanbara, T. (2012), Synthesis and Characterization of Dioxopyrrolopyrrole Derivatives Having Electron-

- Withdrawing Groups, *Eur. J. Org. Chem.*, 2012: 5282–5290 (DOI:10.1002/ejoc.201200761).
- [14] Jo, J. W., Bae, S., Liu, F., Russell, T. P., Jo, W. H. (2015), Comparison of Two D–A Type Polymers with Each Being Fluorinated on D and A Unit for High Performance Solar Cells, *Adv. Funct. Mater.*, 25, 120–125 (DOI:10.1002/adfm.201402210).
- [15] Ning, Z., Tian, H. (2009), Triarylamine: a promising core unit for efficient photovoltaic materials, *Chem. Commun.*, 5483–5495 (DOI: 10.1039/B908802D).
- [16] Frisch, M. J., Trucks, G. W., Schlegel, H. B., Scuseria, G. E., Robb, M. A., Cheeseman, J. R., Scalmani, G., Barone, V., Mennucci, B., Petersson, G. A., Nakatsuji, H., Caricato, M., Li, X., Hratchian, H. P., Izmaylov, A. F., Bloino, J., Zheng, G., Sonnenberg, J. L., Hada, M., Ehara, M., Toyota, K., Fukuda, R., Hasegawa, J., Ishida, M., Nakajima, T., Honda, Y., Kitao, O., Nakai, H., Vreven, T., Montgomery Jr, J. A., Peralta, J. E., Ogliaro, F., Bearpark, M., Heyd, J. J., Brothers, E., Kudin, K. N., Staroverov, V. N., Kobayashi, R., Normand, J., Raghavachari, K., Rendell, A., Burant, J. C., Iyengar, S. S., Tomasi, J., Cossi, M., Rega, N., Millam, J. M., Klene, M., Knox, J. E., Cross, J. B., Bakken, V., Adamo, C., Jaramillo, J., Gomperts, R., Stratmann, R. E., Yazyev, O., Austin, A. J., Cammi, R., Pomelli, C., Ochterski, J. W., Martin, R. L., Morokuma, K., Zakrzewski, V. G., Voth, G. A., Salvador, P., Dannenberg, J. J., Dapprich, S., Daniels, A. D., Farkas, Ö., Foresman, J. B., Ortiz, J. V., Cioslowski, J., Fox, D. J. (2009) Gaussian 09, revision D.01 Gaussian, Inc., Wallingford, CT, USA.
- [17] Patil, Y., Misra, R., Chen, F. C., Keshtov, M. L., Sharma, G. D. (2016), Symmetrical and Unsymmetrical Triphenylamine based Diketopyrrolopyrroles and their use as Donor for Solution Processed Bulk Heterojunction Organic Solar Cells. *RSC Adv.*, 6, 99685–99694 (DOI: 10.1039/C6RA10442H).
- [18] Patil, Y., Misra, R., Keshtov, M. L., Sharma, G. D. (2016), 1,1,4,4-Tetracyanobuta-1,3-diene Substituted Diketopyrrolopyrroles: An Acceptor for Solution Processable Organic Bulk Heterojunction Solar Cells. *J. Phys. Chem. C*, 120, 6324–6335 (DOI: 10.1021/acs.jpcc.5b12307).

Chapter 5

Ferrocenyl functionalized diketopyrrolopyrroles

5.1. Introduction

The π -conjugated donor-acceptor (D–A) molecular systems are of great interest because of their variety of applications in the field of organic light emitting diodes (OLEDs), organic solar cells (OSCs), multi-photon absorption, and organic field effect transistors (OFETs).^[1] The conjugated small organic molecules with D- π -A framework are potentially used for optoelectronics.^[2]

The diketopyrrolopyrrole (DPP) is well known electron acceptor made up of two lactam rings and has strong electron withdrawing character.^[3] Farnum *et al.* in 1974 first reported the synthesis of DPP^[4] and later on Iqbal, Cassar, and Rochat during 1982-1983 improved the synthetic pathway.^[5] Recently DPP derivatives have been explored as promising materials in organic electronics and photovoltaics.^[6,7] The functionalization of the DPP with strong donor like ferrocene will result in D–A molecular architecture and the nature of donor will influence the strength of D-A interaction. The ferrocene is one of the most widely studied donor,^[8] with redox active centre and its derivatives are useful in the field of non-linear optics (NLO) and dye sensitized solar cells (DSSC). Ferrocenyl derivatives possess excellent thermal and photochemical stability.^[9] Diederich *et al.* have explored [2+2] cycloaddition–retroelectrocyclization reaction of tetracyanoethylene (TCNE) with different donor moieties.^[10] We have recently reported variety of symmetrical and unsymmetrical D–A molecular systems for optoelectronic applications.^[11] There are no reports found in literature on ferrocenyl functionalized DPP. Therefore we were interested to functionalize ferrocene unit on the DPP. Further their tetracyanobutadiene (TCBD) derivatives were synthesized to evaluate the effect of TCBD incorporation in terms of photonic and electrochemical properties of ferrocenyl DPPs.

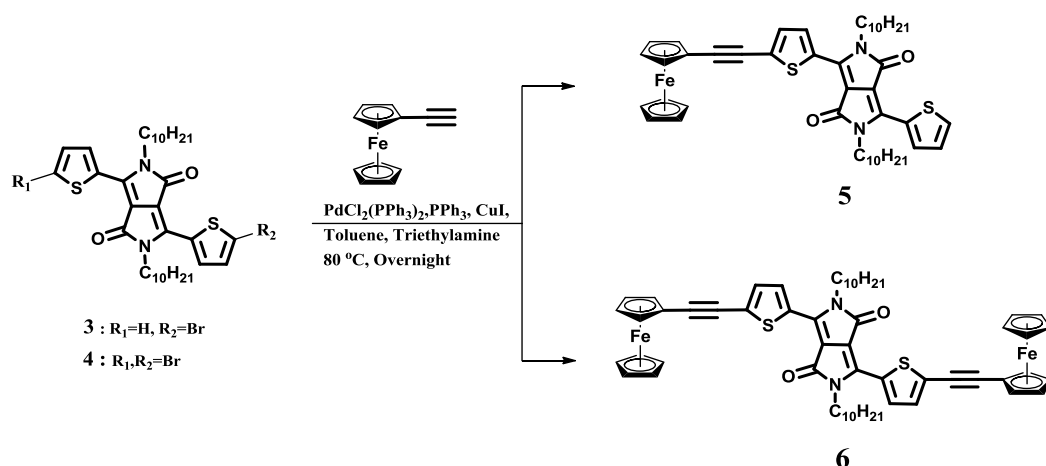
Ziessel and co-workers in 2015 investigated the BODIPY and DPP based molecular designs for the energy transfer cassettes and photoinduced electron transfer processes.^[12] Recently we have shown that the incorporation of TCNE or tetracyanoquinodimethane (TCNQ) acceptor in a D–A system extends the absorption to longer wavelength region with lowering of HOMO-LUMO gap.^[13] We

were interested to investigate photonic properties of donor substituted symmetrical and unsymmetrical DPPs to tune the HOMO-LUMO gap.

In this chapter we wish to report the design and synthesis of symmetrical and unsymmetrical ferrocene based DPP systems, where the ferrocene and thiophene act as donors, whereas the DPP and TCBD act as acceptor units. The alkyl chains were attached on nitrogen of lactam ring of DPP to improve the solubility in common organic solvents.^[14] Here our aim was to investigate the effect of ferrocene as donor and TCBD as a secondary acceptor on photophysical, thermal and electrochemical properties of DPP.

5.2. Results and discussion

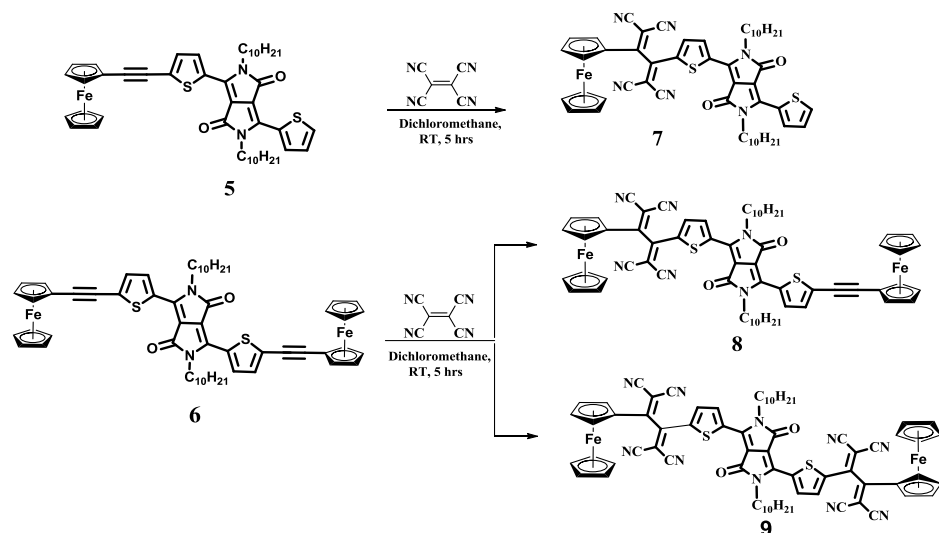
The ethyne bridged ferrocenyl **DPPs 5** and **6** were synthesized by the Pd-catalyzed Sonogashira cross-coupling reaction of **3** and **4** with excess equivalents of ethynyl ferrocene in 91% and 95% yield respectively.



Scheme 5.1. Synthesis of ethyne bridged ferrocenyl **DPPs 5** and **6**.

Further subsequent [2+2] cycloaddition-retroelectrocyclization reaction of **DPP 5** with TCNE resulted in **DPP 7** whereas the [2+2] cycloaddition-retroelectrocyclization reaction of **DPP 6** with one and two equivalents of TCNE resulted in the formation of **DPPs 8** and **9** respectively (Scheme 5.2). The starting precursors monobromo **DPP 3** and dibromo **DPP 4** were synthesized by reported procedure.¹⁵ The Sonogashira cross-coupling reaction of monobromo **DPP 3** and dibromo **DPP 4** with one and two equivalents of ethynyl ferrocene resulted the unsymmetrical ferrocenyl **DPP 5** and symmetrical ferrocenyl **DPP 6** in 80% and 85% yield respectively. The [2 + 2] cycloaddition–retroelectrocyclization reactions were carried out at room temperature for five hours. The ferrocenyl **DPPs 5 – 9** were

purified by silica gel column chromatography and having good solubility in common organic solvents. The ferrocenyl **DPPs 5 – 9** were well characterized by ^1H NMR, ^{13}C NMR and HRMS techniques.



Scheme 5.2. Synthesis of TCBD bridged ferrocenyl **DPPs 7 – 9**.

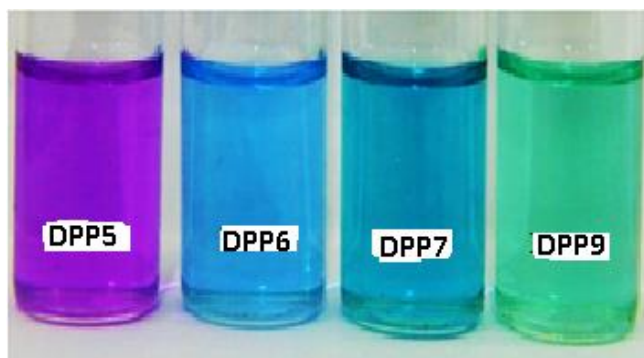


Figure 5.1. Photograph of **DPPs (5–7 and 9)** in dichloromethane (10^{-6}M).

5.3. Photophysical Properties

The photograph of the ferrocenyl **DPPs 5–7 and 9** in dichloromethane solvent in day light is displayed in Figure 5.1. The electronic absorption spectra of ferrocenyl **DPPs 5** and **6** and their TCBD derivatives **DPPs 7–9** were recorded in dichloromethane at room temperature (Figure 5.2) and data are listed in Table 5.1.

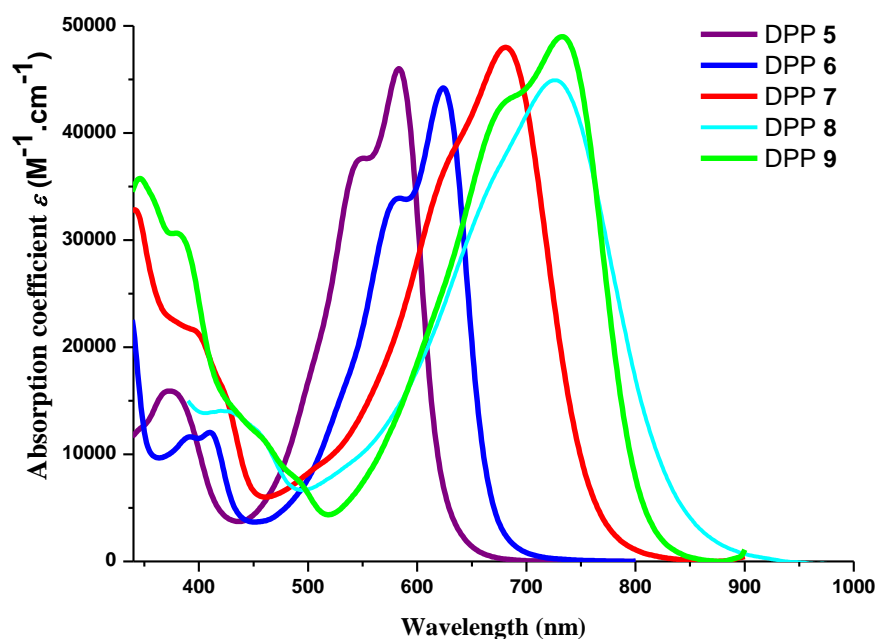


Figure 5.2. Electronic absorption spectra of **DPPs 5 – 9** in dichloromethane solution (10^{-4}M).

The electronic absorption spectra of **DPPs 5 – 9** in dichloromethane exhibit broad absorption bands covering whole UV-Vis-NIR region. The weak absorption bands at shorter wavelength region and strong absorption bands at longer wavelength correspond to the $\pi \rightarrow \pi^*$ transition of DPP and TCBD moiety. The symmetrical **DPPs 6** and **8** show red shifted absorption compared to unsymmetrical **DPPs 5, 7** and **8**. The incorporation of TCBD in unsymmetrical ferrocenyl **DPP 5** shows the red shift of 97 nm whereas incorporation of one TCBD shows red shift of 101 nm and incorporation of two TCBD units in **DPP 6** show red shift of 108 nm in longer wavelength absorption band respectively. The red shift in longer wavelength absorption band of TCBD derivatives leads to decrease in the HOMO – LUMO gap.

The solvent dependent UV-vis spectra of **DPPs 5 – 7** and **DPP 9** were recorded which shows negative solvatochromism effect, as polarity increases from toluene to methanol blue shift occurs (Table 5.4) and absorption curves are shown in Figure 5.6).

Table 5.1. Photophysical properties of **DPPs 5–9**.

	λ_{abs} (nm)	$\epsilon/10^4$ ($\text{M}^{-1}\cdot\text{cm}^{-1}$) ^a	T_d ($^{\circ}\text{C}$) ^b
DPP 5	584	4.6	377
	548	3.7	
	373	1.6	
	305	2.5	
DPP 6	624	4.4	387
	580	3.4	
	410	1.2	
	335	2.4	
DPP 7	681	4.8	379
	622	3.6	
	398	2.1	
	341	3.3	
DPP 8	725	4.0	373
DPP 9	732	4.9	410
	682	4.3	
	385	3.0	
	347	3.6	

^aAbsorbance measured in dichloromethane at 1×10^{-4} M concentration, ϵ : extinction coefficient;

^bDecomposition temperatures for 10% weight loss at heating rate of $10 \text{ }^{\circ}\text{C min}^{-1}$ under nitrogen atmosphere.

5.4. Thermal Properties

The thermal properties of the ferrocenyl **DPPs 5–9** were investigated by the thermogravimetric analysis (TGA) under nitrogen atmosphere and their thermograms are shown in Figure 5.3. The ethyne bridged **DPPs (5 and 6)** and their TCBD derivatives **DPPs 7, 8 and 9** exhibit good thermal stability. The decomposition of symmetrical **DPP 6** and **DPP 8** occurs slowly with increase in temperature may be due to greater degree of π -electron conjugation than unsymmetrical **DPPs 5, 7 and 8**. With extension of the π -conjugation thermal

stability of the compounds increased. The trend in thermal stability reveals that symmetrical ferrocenyl **DPPs** (**6** and **8**) are thermally more stable as compared to unsymmetrical ferrocenyl **DPPs** (**5**, **7** and **8**).

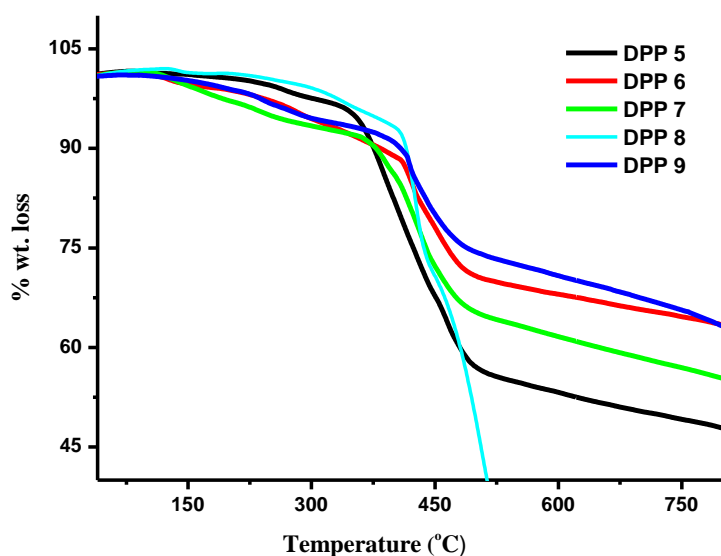


Figure 5.3. Thermogravimetric analysis of **DPPs** **5** – **8** measured at a heating rate of 10 °C / min under nitrogen atmosphere.

5.5. Electrochemical Properties

The electrochemical properties of ferrocenyl **DPPs** **5** and **6** and their TCBD derivatives **DPPs** **7–9** were explored by cyclic voltammetry and differential pulse voltammetry (CV and DPV) techniques in dichloromethane solvent using 0.1 M tetrabutylammonium hexafluorophosphate (Bu_4NPF_6) as supporting electrolyte. The CV and DPV plots of ferrocenyl **DPPs** and their TCBD derivatives are shown in Figure 5.4 and the corresponding data are listed in Table 5.2.

The unsymmetrical **DPPs** **5** and **7**, show three oxidation waves, one for ferrocenyl moiety and other two for two different thiophenes (terminal thiophene and thiophene adjacent to ferrocene). The ethyne and TCBD bridged **DPP** **8** shows four oxidation waves related to different electronic environment of thiophene and ferrocene. The symmetrical **DPP** **6** and its di-TCBD derivative **9** show only two oxidation waves, one attributed to thiophene and another to ferrocene.

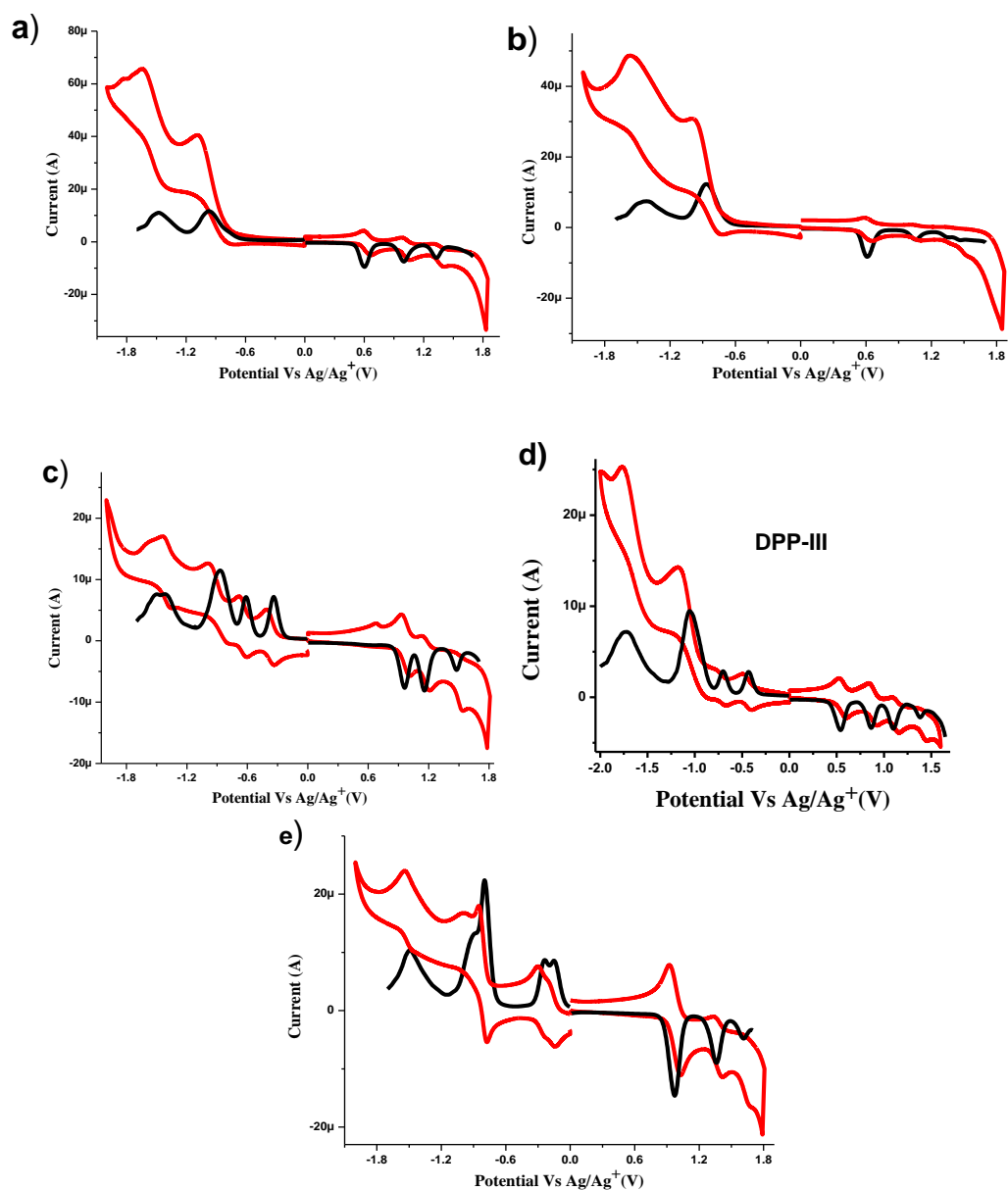


Figure 5.4. CV (red line) and DPV (black line) plots of (a) **DPP 5**, (b) **DPP 6**, (c) **DPP 7** (d) **DPP 8** and **DPP 9**.

The incorporation of TCNE shifts the oxidation potential of ferrocene from 0.60 eV to 0.96 eV in **7** and 0.61 eV to 0.97 eV in **9** compared to their precursors. This shows that the oxidation of ferrocene and thiophene becomes harder due to introduction of TCBD unit.

Table 5.2. Electrochemical properties of **DPPs 5 – 9**^a.

	E^4	E^3	E^2	E^1	E^1	E^2	E^3	E^4
	Oxid	Oxid	Oxid	Oxid	Red	Red	Red	Red
DPP 5	-	1.33	1.00	0.60	-0.97	-1.49	-	-
DPP 6	-	-	1.06	0.61	-0.87	-1.43	-	-
DPP 7	-	1.47	1.15	0.96	-0.34	-0.61	-1.15	-1.45
DPP 8	1.38	1.10	0.86	0.53	-0.39	-0.60	-1.10	-1.38
DPP 9	-	-	1.36	0.97	-0.15	-0.24	-0.80	-1.50

^aThe electrochemical analysis was performed in a 0.1 M solution of Bu₄NPF₆ in dichloromethane at 100 mVs⁻¹ scan rate, versus Ag/Ag⁺ at 25 °C.

The DPP moiety show two reduction waves in ferrocenyl DPPs corresponding to mono and dianion formation. The **DPPs 7–9** exhibit four reduction waves, two corresponding to TCBD and two for DPP unit. Incorporation of electron withdrawing TCBD in ferrocenyl **DPPs** show additional reduction waves corresponds to TCBD unit in CV and DPV. The trend of first reduction potential follows the order **5** > **6** > **8** > **7** > **9**, which indicates incorporation of TCBD in ethyne bridged **DPPs** (**5** and **6**) make easier reduction of TCBD derivatives **7–9**.

5.6. Density Functional Theory (DFT) calculation

The density functional theory (DFT) calculations were carried out to understand the geometry, and the electronic structure of **DPPs 5 – 9** using the Gaussian09W program.^[15] The geometry optimizations were carried out in the gas phase. The DFT calculations were performed at the B3LYP/6-31+G** for C, H, N, S, O, and Lanl2DZ for Fe level of theory.

The geometry optimized structures of **DPPs 5** and **6** exhibit planar geometry, whereas TCBD substituted **DPPs 7–9** exhibit distorted geometry. The Figure 5.5 depicts the frontier molecular orbitals (FMO) of the **DPPs 5–9**. The HOMO in **DPPs 5** and **6** is distributed on the whole molecule whereas LUMO is localized on the DPP and thiophene units. In case of TCBD bridged **DPPs 7–9**, the HOMO and LUMO orbitals are located on the DPP and TCBD unit.

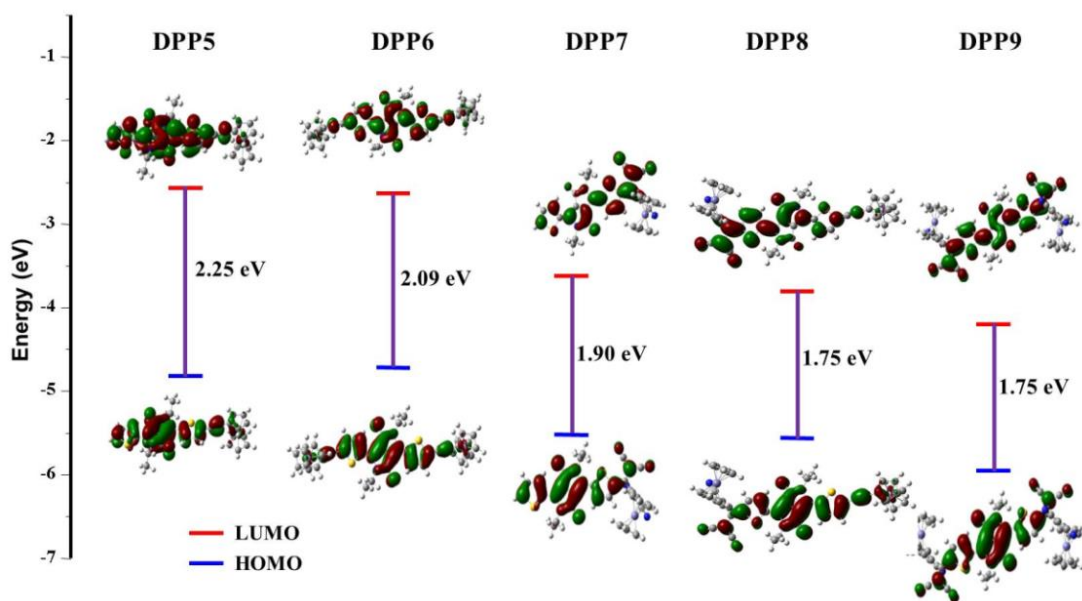


Figure 5.5. The frontier molecular orbitals of **DPPs 5–9** estimated by DFT calculations.

The theoretical HOMO-LUMO gap values obtained from DFT calculations were found to be in good agreement with the optical gap values calculated from the UV-vis absorption. The trend in the theoretical HOMO-LUMO value follows the order **5 > 6 > 7 > 8~9** which shows that the HOMO-LUMO value decreases with increase in the number of ferrocene and TCBD units. The incorporation of TCBD stabilizes both HOMOs and LUMOs in ferrocenyl **DPPs 7–9**. The LUMOs are comparatively more stabilized which resulted in lowering of HOMO – LUMO gap values.

Table 5.3. Calculated major electronic transitions for **DPPs 5 – 9** in the gas phase.

DPP	Wavelength (nm)	Composition	Assignment	f^a
DPP5	562	HOMO→LUMO (0.66)	π - π^* transition	0.83
DPP6	636	HOMO→LUMO (0.59)	π - π^* transition	1.23
DPP7	672	HOMO→LUMO (0.60)	π - π^* transition	0.51
DPP8	737	HOMO→LUMO (0.69)	π - π^* transition	1.25
DPP9	735	HOMO→LUMO (0.70)	π - π^* transition	1.07

f^a = Oscillation Strength

The time dependent density functional theory (TD-DFT) calculation was performed to understand the exact idea about transitions. The major transitions with composition, oscillator strengths, and assignments are shown in Table 5.3. The ferrocenyl **DPPs 5 – 9** show one major transition in the longer wavelength region which is assigned to HOMO→LUMO transition which is related to the $\pi - \pi^*$ transition of the DPP moiety in **DPPs 5** and **6** whereas the long wavelength transitions in **DPPs 7–9** are related to the $\pi - \pi^*$ transition of the DPP and TCBD moieties.

Table 5.3. Comparison of band gaps in **DPPs 5 – 9**.

	Theoretical Band gap (eV)	Optical Band gap (eV)	Electrochemical Band gap (eV)
DPP 5	2.25	1.91	1.17
DPP 6	2.09	1.77	1.12
DPP 7	1.90	1.55	0.98
DPP 8	1.75	1.34	0.88
DPP 9	1.75	1.47	0.71

Table 5.4. Absorption maxima of **DPPs 5 – 7** and **9** in different solvents.

	λ_{\max} (nm)			
	TOLUENE	DCM	THF	METHANOL
DPP 5	588	583	582	573
DPP 6	627	623	620	611
DPP 7	693	680	670	628
DPP 9	742	732	720	677

Kanbara *et al* reported *N, N*-dimethylaniline based D – A system, where they have shown that the charge transfer transition occurs from HOMO-1, and HOMO-2 to the LUMO from *N, N*-dimethylanilino groups to the TCBD and the DPP core.^[4c] The literature reveals ethyne bridged *N, N*-dimethyl phenyl, carbazole substituted

DPP systems show absorption in the region of 300 nm – 700 nm with charge transfer band in 500 – 850 nm and theoretical HOMO-LUMO gap in 2.10 – 2.70 eV region. Here our results show red shifted absorption with low HOMO-LUMO gap in between 1.75 – 2.25eV.

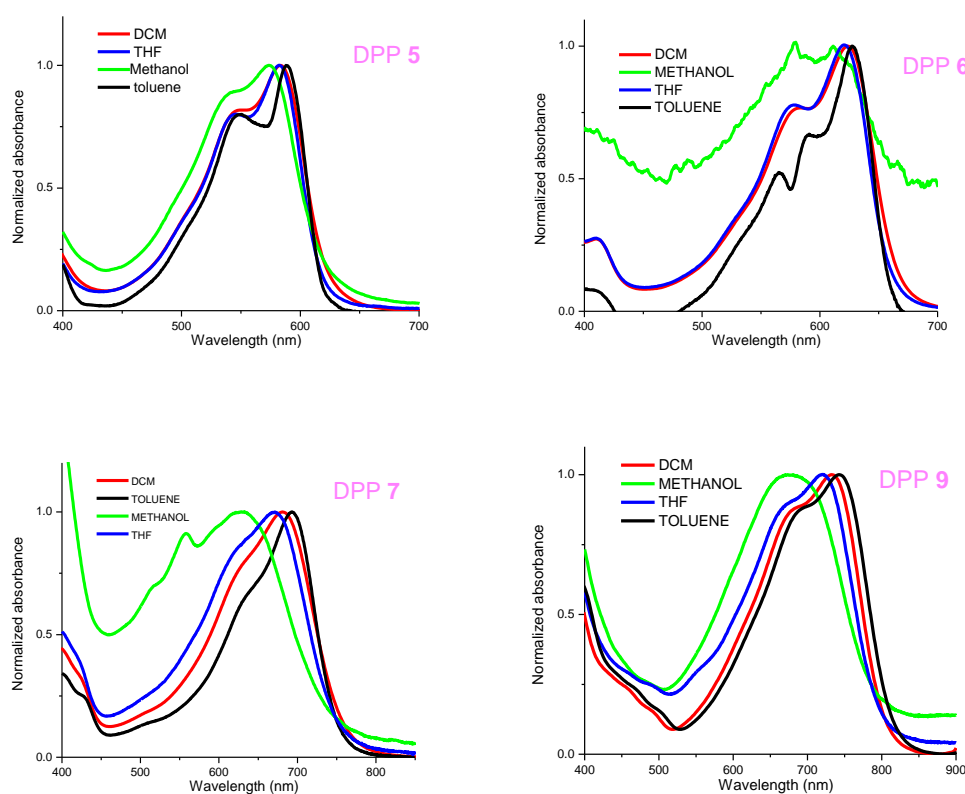


Figure 5.6. Absorption curves of **DPPs 5 – 7** and **DPP9** in different solvents.

5.7. Application in Photovoltaics

We used **DPP6** as donor along with PC₇₁BM as the acceptor for the preparation of solution processed bulk heterojunction organic solar cells (BHJ-OSCs) an achieved power conversion efficiency upto 6.44%.^[16]

The incorporation of TCBD improves the accepting ability of molecule and we used TCBD bridged derivatives as non-fullerene acceptor for BHJ-OSCs along with donor polymer **P** achieved a respectable PCE upto 6.89%.^[17] Herein for the first time we have used organometallic derivatives as non-fullerene acceptor in OSCs.

5.8. Experimental Section:

General methods

The chemicals were used as received unless otherwise indicated. All the moisture sensitive reactions were performed under argon atmosphere using the standard Schlenk method. ^1H NMR (400 MHz) and ^{13}C NMR (100 MHz) spectra were recorded by using CDCl_3 as the solvent. The ^1H NMR chemical shifts are reported in parts per million (ppm) relative to the solvent residual peak (CDCl_3 , 7.26 ppm). The multiplicities are given as: s (singlet), d (doublet), t (triplet), q (quartet), m (multiplet), and the coupling constants, J , are given in Hz. The ^{13}C NMR chemical shifts are reported with relative to the solvent residual peak (CDCl_3 , 77.02 ppm). HRMS was recorded on a mass spectrometer (ESI-TOF). The UV-visible absorption spectra of DPPs were recorded on UV-visible Spectrophotometer in dichloromethane. The TGA analyses were performed on the thermal analysis system at the heating rate of 10 °C per minute under a nitrogen atmosphere. Cyclic voltammograms (CVs) and differential voltammograms (DPVs) were recorded on an electrochemical analyzer using glassy carbon as working electrode, Pt wire as the counter electrode, and saturated Ag/Ag^+ as the reference electrode.

Synthesis of DPP 5:

In 100 ml round bottom flask monobromo-diketopyrrolopyrrole **3** (0.200 g, 0.30 mmol) and ethynyl ferrocene (0.064 g, 0.30 mmol) were dissolved in dry toluene (10 ml) and triethylamine (6 ml). The reaction mixture was degassed with argon for 10 minutes and $\text{PdCl}_2(\text{PPh}_3)_2$ (0.028 g, 0.030 mmol), PPh_3 (0.014 g, 0.060 mmol) and CuI (0.006 g, 0.030 mmol) were added. The reaction mixture was stirred overnight at 80 °C. After completion of reaction, the reaction mixture was allowed to cool down to room temperature. The solvents were removed under vacuo and the product was purified by repeated silica-column chromatography with hexane: dichloromethane (3:1) as an eluent to get 0.191 gm product in 80% yield.

^1H NMR (400 MHz, CDCl_3 , δ in ppm): 8.94 (1H, d, $J = 4$ Hz), 8.89 (1H, d, $J = 4$), 7.65 (1H, d), 7.32 (1H, d), 7.29 (1H, m), 4.56 (2H, s), 4.33 (2H, s), 4.28 (4H, s), 4.07 (4H, m), 1.75 (4H, s), 1.42 (4H, s), 1.26 (24H, s), 0.87 (6H, m); ^{13}C NMR (100 MHz, CDCl_3 , δ in ppm): 161.4, 161.3, 139.9, 139.3, 135.5, 135.4, 132.3, 130.8, 129.9, 129.7, 129.5, 128.7, 108.2, 107.9, 98.2, 78.8, 71.7, 70.2, 69.6, 63.9, 53.5, 42.3, 31.9, 30.1, 30.0, 29.8, 29.6, 29.4, 29.3, 22.7, 14.2; HRMS (ESI) m/z calcd for

$C_{46}H_{56}N_2FeO_2S_2 + H$: 788.3128 $[M + H]^+$, found 788.3122 $[M + H]^+$; UV/vis (Dichloromethane) λ_{max} 584 nm, $\epsilon[M^{-1}.cm^{-1}](4.6 \times 10^4)$; M. P. = 92 °C.

Synthesis of DPP 6:

In 100 ml round bottom flask dibromodiketopyrrolopyrrole **4** (0.200 g, 0.28 mmol) and ethynyl ferrocene (0.116 g, 0.56 mmol) were dissolved in dry toluene (10 ml) and triethylamine (6 ml). The reaction mixture was degassed with argon for 10 minute and $PdCl_2(PPh_3)_2$ (0.020 g, 0.028 mmol), PPh_3 (0.014 g, 0.056 mmol) and CuI (0.006 g, 0.028 mmol) were then added. The reaction mixture was stirred overnight at 80 °C. After completion, the reaction mixture was allowed to cool down to room temperature. The solvents were removed under vacuo and blue colored product was purified by silica-column chromatography with hexane: dichloromethane (3:1) as an eluent to get 0.230 gm product in 85% yield.

1H NMR (400 MHz, $CDCl_3$, δ in ppm): 8.90 (2H, d), 7.32 (2H, d), 4.55 (4H, s), 4.32 (4H, d), 4.28 (4H, d), 4.07 (4H, m), 1.75 (4H, s), 1.42 (6H, s), 1.25 (22 H, s), 0.86 (6H, m); ^{13}C NMR (100 MHz, $CDCl_3$, δ in ppm): 163.1, 139.0, 135.5, 132.3, 129.8, 129.6, 108.5, 78.8, 71.7, 70.2, 69.6, 63.9, 53.5, 42.4, 31.9, 30.1, 29.8, 29.6, 29.3, 27.0, 22.7, 14.2; HRMS (ESI) m/z calcd for $C_{58}H_{64}N_2Fe_2O_2S_2 + H$: 996.3106 $[M + H]^+$, found 996.3019 $[M + H]^+$; UV/vis (Dichloromethane) λ_{max} 624 nm, $\epsilon[M^{-1}.cm^{-1}](2.6 \times 10^4)$; M. P. = 130 °C.

Synthesis of DPP 7:

In 50 ml round bottom flask **DPP 5** (0.100 g, 0.13 mmol) and TCNE (0.018 g, 0.14 mmol) were dissolved in dichloromethane (15 ml) under argon atmosphere. The reaction mixture was stirred at room temperature for 5 hours. The solvent was removed under vacuo and the product was purified by silica-column chromatography with hexane : dichloromethane (1:1) as an eluent to yield 0.105 gm of **DPP 7** as a dark blue colored solid in 91% yield.

1H NMR (400 MHz, $CDCl_3$, δ in ppm): 9.16 (1H, d), 8.96 (1H, d), 7.78 (1H, d), 7.63 (1H, s), 7.34 (1H, t), 5.57 (1H, s), 5.07 (1H, s), 4.87 (1H, s), 4.52 (4H, d), 4.49 (1H, d), 4.04 (4H, m), 1.70 (4H, m), 1.41 (4H, m), 1.27 (24H, s), 0.87 (6H, m); ^{13}C NMR (100 MHz, $CDCl_3$, δ in ppm): 171.9, 161.5, 160.6, 155.0, 144.1, 139.8, 138.0, 137.7, 136.2, 135.4, 134.8, 133.4, 134.8, 133.5, 129.3, 112.9, 112.8, 112.7, 108.5, 79.5, 78.6, 75.9, 75.1, 72.9, 72.5, 71.7, 42.7, 42.6, 31.9, 31.8, 30.4, 29.9, 29.6, 29.5, 29.4, 29.3, 29.2, 26.9, 26.8, 22.8, 22.7, 14.2, 14.2; HRMS (ESI) m/z calcd for

$C_{52}H_{56}N_6FeO_2S_2 + H$: 939.3149 $[M + Na]^+$, found 939.3090 $[M + Na]^+$; UV/vis (Dichloromethane) λ_{max} 681 nm, $\epsilon[M^{-1}.cm^{-1}](4.8 \times 10^4)$; M. P. = 178 °C.

Synthesis of DPP 8:

In 50 ml round bottom flask **DPP6** (0.100 g, 0.10 mmol) and TCNE (0.013 g, 0.10 mmol) were dissolved in dichloromethane (15 ml) under argon atmosphere. The reaction mixture was stirred at room temperature for 5 hours. The solvent was removed under vacuo and the product was purified by silica-column chromatography with hexane : dichloromethane (2:1) as an eluent to yield 65% **DPP8**. 1H NMR (400 MHz, $CDCl_3$, δ in ppm): 9.14 (1H, s), 8.98 (1H, s), 7.64 (1H, s), 7.36 (1H, s), 5.56 (2H, s), 5.06 (1H, s), 4.87 (2H, s), 4.55 (6H, m), 4.32 (5H, m), 4.08, (4H, m), 1.72 (4H, s), 1.26–1.42 (26H, m), 0.88 (8H, s); ^{13}C NMR (100 MHz, $CDCl_3$, δ in ppm): 172.0, 161.4, 160.5, 154.9, 143.1, 139.8, 139.3, 138.4, 137.8, 136.0, 134.9, 134.8, 132.9, 132.6, 128.7, 114.1, 113.6, 113.1, 112.6, 108.9, 100.8, 79.4, 78.9, 78.3, 75.9, 75.1, 72.9, 72.6, 71.8, 71.7, 70.3, 69.9, 63.4, 58.5, 53.5, 33.1, 32.0, 31.9, 30.4, 30.3, 29.7, 29.6, 29.5, 29.2, 28.9, 26.8, 22.7, 18.4, 14.1; HRMS (ESI) m/z calcd for $C_{64}H_{64}Fe_2N_6O_2S_2 + Na$: 1147.3127 $[M + Na]^+$, found 1147.3127 $[M + Na]^+$.

Synthesis of DPP 9:

In 50 ml round bottom flask **DPP 6** (0.100 g, 0.10 mmol) and TCNE (0.026 g, 0.20 mmol) were dissolved in dichloromethane (15 ml) under argon atmosphere. The reaction mixture was stirred at room temperature for 5 hours. The solvent was removed under vacuo and the product was purified by silica-column chromatography with hexane : dichloromethane (2:1) as an eluent to yield 0.118 gm of **DPP 8** as a dark green colored solid in 95% yield.

1H NMR (400 MHz, $CDCl_3$, δ in ppm): 9.07 (2H, s), 7.63 (2H, m), 5.61 (2H, s), 5.61 (2H, s), 5.30 (1H, s), 5.09 (2H, s), 4.88 (2H, s), 4.52 (8H, s), 4.44 (2H, s), 4.08, (4H, m), 1.66 (4H, m), 1.26 (28H, s), 0.87 (6H, s); ^{13}C NMR (100 MHz, $CDCl_3$, δ in ppm): 171.5, 160.6, 154.9, 139.3, 138.3, 137.9, 137.6, 137.5, 136.5, 113.5, 112.7, 112.6, 112.5, 112.1, 80.2, 80.1, 77.4, 75.7, 75.2, 73.0, 72.6, 71.5, 53.5, 42.9, 31.9, 30.3, 29.6, 29.5, 29.3, 29.2, 26.8, 22.7, 14.2; HRMS (ESI) m/z calcd for $C_{70}H_{64}N_{10}Fe_2O_2S_2 + H$: 1275.3251 $[M + Na]^+$, found 1275.3281 $[M + Na]^+$; UV/vis(Dichloromethane) λ_{max} 732 nm, $\epsilon[M^{-1}.cm^{-1}](4.9 \times 10^4)$; M. P. = 202 °C.

The data containing ^{13}C -NMR spectrum of compounds it seems some of signals are missing is mainly due to overlap of signals.

5.9. Conclusions

In conclusions, we have synthesized symmetrical and unsymmetrical ferrocenyl **DPPs 5** and **6** by Sonogashira cross-coupling and their TCBD derivatives (**7–9**) by [2+2] cycloaddition-retroelectrocyclization reaction respectively. The incorporation of TCBD in ferrocenyl DPPs improves the absorption with lowering of HOMO – LUMO gap values. The TCBD substituted DPPs show systematic red shift in absorption with enhanced thermal stability. High thermal stability and low HOMO – LUMO gap of **DPPs 5 – 9** makes them potential candidate for organic photovoltaics. Currently we are synthesizing new donor substituted DPPs and their TCBD analogues for optoelectronic applications.

5.10. References

- [1] (a) Kobayashi, N., Inagaki, S., Nemykin, V. N., Nonomura, T. (2001), A novel hemiporphyrazine comprising three isoindoleimine and three thiadiazole units, *Angew. Chem. Int. Ed.*, 40, 2710–2712 (DOI:10.1002/1521-3773(20010716)40:14<2710::AID-ANIE2710>3.0.CO;2-A). (b) Ji, C., Yin, L., Li, K., Wang, L., Jiang, X., Sun, Y., Li, Y. (2015), D- π -A- π -D-type low band gap diketopyrrolopyrrole based small molecules containing an ethynyl-linkage: synthesis and photovoltaic properties, *RSC Adv.*, 5, 31606–31614 (DOI: 10.1039/C5RA01946J). (c) Wong, W. Y., Wong, W. K., Raithby, P. R. (1998), Synthesis, characterisation and properties of platinum(II) acetylide complexes of ferrocenylfluorene: novel soluble donor–acceptor heterometallic materials, *J. Chem. Soc. Dalton Trans.*, 2761–2766 (DOI: 10.1039/A803168A).
- [2] Liu, H., Jia, H., Wang, L., Wu, Y., Zhan, C., Fu, H., Yao, J. (2012), Intermolecular electron transfer promoted by directional donor–acceptor attractions in self-assembled diketopyrrolopyrrole-thiophene films, *Phys. Chem. Chem. Phys.*, 14, 14262–14269 (DOI: 10.1039/C2CP41288H).
- [3] (a) Zhang, H., Wan, X., Xue, X., Li, Y., Yu, A., Chen, Y. (2010), Selective Tuning of the HOMO–LUMO Gap of Carbazole-Based Donor–Acceptor–Donor Compounds toward Different Emission Colors, *Eur. J. Org. Chem.*, 2010: 1681–1687 (DOI:10.1002/ejoc.200901167). (b) Yamagata, T., Kuwabara, J., Kanbara, T. (2012), Yamagata, T., Kuwabara, J., Kanbara, T. (2012), Synthesis and

- Characterization of Dioxopyrrolopyrrole Derivatives Having Electron-Withdrawing Groups, *Eur. J. Org. Chem.*, 2012: 5282–5290 (DOI:10.1002/ejoc.201200761). (c) Heyer, E., Ziessel, R. (2015) Panchromatic Push–Pull Dyes of Elongated Form from Triphenylamine, Diketopyrrolopyrrole, and Tetracyanobutadiene Modules, *Synlett.*, 26, 2109–2116 (DOI: 10.1055/s-0034-1378818).
- [4] Farnum, D. G., Mehta, G., Moore, G. G., Siegel, F. P. (1974), Attempted reformatzkii reaction of benzonitrile, 1,4-diketo-3,6-diphenylpyrrolo[3,4-C]pyrrole. A lactam analogue of pentalene, *Tetrahedron Lett.*, 15, 2549 – 2552 ([https://doi.org/10.1016/S0040-4039\(01\)93202-2](https://doi.org/10.1016/S0040-4039(01)93202-2)).
- [5] (a) Rochat, A. C., Cassar, L., Iqbal, A. (CIBA-GEIGY AG). EP94911, 1983; (b) Iqbal, A., Cassar, L. (CIBA-GEIGY AG). EP61426, 1982.
- [6] (a) Wienk, M. M., Turbiez, M., Gilot, J., Janssen, R. A. J. (2008), *Adv. Mater.*, 20, 2556–2560 (doi.org/10.1002/adma.200800456); (b) Walker, B., Tamayo, A. B., Dang, X.-D., Zalar, P., Seo, J. H., Garcia, A., Tantiwivat, M., Nguyen, T.-Q. (2009), Nanoscale Phase Separation and High Photovoltaic Efficiency in Solution-Processed, Small-Molecule Bulk Heterojunction Solar Cells. *Adv. Funct. Mater.*, 19, 3063–3069 (DOI:10.1002/adfm.200900832).
- [7] (a) Huo, L., Hou, J., Chen, H. Y., Zhang, S., Jiang, Y., Chen, T. L., Yang, Y. (2009), Bandgap and Molecular Level Control of the Low-Bandgap Polymers Based on 3,6-Dithiophen-2-yl-2,5-dihydropyrrolo[3,4-c]pyrrole-1,4-dione toward Highly Efficient Polymer Solar Cells, *Macromolecules*, 42, 6564 (DOI: 10.1021/ma9012972). (b) Sharma, G. D., Mikroyannidis, J. A., Sharma, S. S., Roy, M. S., Thomas, K. R. J. (2012), Efficient bulk heterojunction photovoltaic devices based on diketopyrrolopyrrole containing small molecule as donor and modified PCBM derivatives as electron acceptors, *Organic Electronics*, 13, 652–666 (<https://doi.org/10.1016/j.orgel.2011.11.021>).
- [8] Krauß, N., Kielmann, M., Ma, J., Butenschön, H. (2015), Reactions of Alkynyl- and 1,1'-Dialkynylferrocenes with Tetracyanoethylene—Unanticipated Addition at the Less Electron-Rich of Two Triple Bonds, *Eur. J. Org. Chem.*, 2015, 2622–2631 (DOI:10.1002/ejoc.201500105).

- [9] Kato, S.-I., Kivala, M., Schweizer, W. Bernd., Boudon, C., Gisselbrecht, J.-P., Diederich, F. (2009), Origin of Intense Intramolecular Charge-Transfer Interactions in Nonplanar Push–Pull Chromophores, *Chem. Eur. J.*, 15: 8687–8691 (DOI:10.1002/chem.200901630).
- [10] (a) Michinobu, T., May, J. C., Lim, J. H., Boudon, C., Gisselbrecht, J., Seiler, P., Gross, M., Biaggio, I., Diederich, F. (2005), A new class of organic donor–acceptor molecules with large third-order optical nonlinearities, *Chem. Commun.*, 2005, 737–739 (DOI: 10.1039/B417393G). (b) Kivala, M., Boudon, C., Gisselbrecht, J., Seiler, P., Gross, M., Diederich, F. (2007), A novel reaction of 7,7,8,8-tetracyanoquinodimethane (TCNQ): charge-transfer chromophores by [2 + 2] cycloaddition with alkynes, *Chem. Commun.*, 4731–4733 (DOI: 10.1039/B713683H). (c) Štefko, M., Tzirakis, M. D., Breiten, B., Ebert, M.-O., Dumele, O., Schweizer, W. B., Gisselbrecht, J.-P., Boudon, C., Beels, M. T., Biaggio, I., Diederich, F. (2013), Donor–Acceptor (D–A)-Substituted Polyene Chromophores: Modulation of Their Optoelectronic Properties by Varying the Length of the Acetylene Spacer, *Chem. Eur. J.*, 19, 12693–12704 (DOI:10.1002/chem.201301642). (d) Wu, Y., Stuparu, M. C., Boudon, C., Gisselbrecht, J., Schweizer, W. B., Baldrige, K. K., Siegel, J. S., Diederich, F. (2012), Structural, Optical, and Electrochemical Properties of Three-Dimensional Push–Pull Corannulenes, *J. Org. Chem.*, 77, 11014–11026 (DOI: 10.1021/jo302217n). (e) Michinobu, T., Boudon, C., Gisselbrecht, J.-P., Seiler, P., Frank, B., Moonen, N. N. P., Gross, M., Diederich, F. (2006), Donor-Substituted 1,1,4,4-Tetracyanobutadienes (TCBDs): New Chromophores with Efficient Intramolecular Charge-Transfer Interactions by Atom-Economic Synthesis, *Chem. Eur. J.*, 12, 1889–1905 (DOI:10.1002/chem.200501113). (f) Kivala, M., Diederich, F. (2009), Acetylene-Derived Strong Organic Acceptors for Planar and Nonplanar Push–Pull Chromophores, *Acc. Chem. Res.*, 42, 235–248 (DOI: 10.1021/ar8001238). (g) Kato, S. I., Diederich, F. (2010), Non-planar push–pull chromophores, *Chem. Commun.*, 1994–2006 (DOI: 10.1039/B926601A). (h) Jayamurugan, G., Gisselbrecht, J.-P., Boudon, C., Schoenebeck, F., Schweizer, W. B., Bernet, B., Diederich, F. (2011), Expanding the chemical space for push-pull chromophores by non-concerted [2+2] and [4+2] cycloadditions: access to a highly functionalised 6,6-dicyanopentafulvene

- with an intense, low-energy charge-transfer band *Chem. Commun.*, 47, 4520–4522 (DOI: 10.1039/C1CC10247H).
- [11] (a) Dhokale, B., Gautam, P., Misra, R. (2012), Donor–acceptor perylenediimide–ferrocene conjugates: synthesis, photophysical, and electrochemical properties. *Tetrahedron Lett.*, 53, 2352–2354 (<https://doi.org/10.1016/j.tetlet.2012.02.107>). (b) Jadhav, T., Maragani, R., Misra, R., Sreeramulu, V., Rao, D. N., Mobin, S. M. (2013), Design and synthesis of donor–acceptor pyrazabole derivatives for multiphoton absorption, *Dalton Trans.*, 42, 4340–4342 (DOI: 10.1039/C3DT33065F). (c) Misra, R., Gautam, P., Jadhav, T., Mobin, M. (2013), Donor–Acceptor Ferrocenyl-Substituted Benzothiadiazoles: Synthesis, Structure, and Properties, *J. Org. Chem.*, 78, 4940–4948 (DOI: 10.1021/jo4005734).
- [12] Heyer, E., Ziessel, R. (2015) Step-by-Step Synthesis of Multimodule Assemblies Engineered from BODIPY, DPP, and Triphenylamine Moieties, *J. Org. Chem.*, 80, 6737–6753 (DOI: 10.1021/acs.joc.5b00917).
- [13] (a) Gautam, P., Misra, R., Siddiqui, S. A., Sharma, G. D. (2015), Unsymmetrical Donor–Acceptor–Acceptor– π –Donor Type Benzothiadiazole-Based Small Molecule for a Solution Processed Bulk Heterojunction Organic Solar Cell, *ACS Appl. Mater. Interfaces*, 7, 10283–10292 (DOI: 10.1021/acsami.5b02250). (b) Misra, R., Gautam, P., Mobin, S. M. (2013), Aryl-Substituted Unsymmetrical Benzothiadiazoles: Synthesis, Structure, and Properties, *J. Org. Chem.*, 2013, 78, 12440–12452 (DOI: 10.1021/jo402111q). (c) Misra, R., Gautam, P. (2014), Tuning of the HOMO–LUMO gap of donor-substituted symmetrical and unsymmetrical benzothiadiazoles, *Org. Biomol. Chem.*, 12, 5448–5457 (DOI: 10.1039/C4OB00629A).
- [14] (a) Woo, C. H., Beaujuge, P. M., Holcombe, T. W., Lee, O. P., Frechet, J. M. J. (2010), Incorporation of Furan into Low Band-Gap Polymers for Efficient Solar Cells, *J. Am. Chem. Soc.*, 132, 15547–15549 (DOI: 10.1021/ja108115y). (b) Wu, X.-F., Fu, W.-F., Xu, Z., Shi, M., Liu, F., Chen, H.-Z., Wan, J.-H., Russell, T. P. (2015), Spiro Linkage as an Alternative Strategy for Promising Nonfullerene

Acceptors in Organic Solar Cells, *Adv. Funct. Mater.*, 25, 5954–5966. (DOI:10.1002/adfm.201502413).

- [15] Frisch, M. J., Trucks, G. W., Schlegel, H. B., Scuseria, G. E., Robb, M. A., Cheeseman, J. R., Scalmani, G., Barone, V., Mennucci, B., Petersson, G. A., Nakatsuji, H., Caricato, M., Li, X., Hratchian, H. P., Izmaylov, A. F., Bloino, J., Zheng, G., Sonnenberg, J. L., Hada, M., Ehara, M., Toyota, K., Fukuda, R., Hasegawa, J., Ishida, M., Nakajima, T., Honda, Y., Kitao, O., Nakai, H., Vreven, T., Montgomery Jr, J. A., Peralta, J. E., Ogliaro, F., Bearpark, M., Heyd, J. J., Brothers, E., Kudin, K. N., Staroverov, V. N., Kobayashi, R., Normand, J., Raghavachari, K., Rendell, A., Burant, J. C., Iyengar, S. S., Tomasi, J., Cossi, M., Rega, N., Millam, J. M., Klene, M., Knox, J. E., Cross, J. B., Bakken, V., Adamo, C., Jaramillo, J., Gomperts, R., Stratmann, R. E., Yazyev, O., Austin, A. J., Cammi, R., Pomelli, C., Ochterski, J. W., Martin, R. L., Morokuma, K., Zakrzewski, V. G., Voth, G. A., Salvador, P., Dannenberg, J. J., Dapprich, S., Daniels, A. D., Farkas, Ö., Foresman, J. B., Ortiz, J. V., Cioslowski, J., Fox, D. J. (2009) Gaussian 09, revision D.01 Gaussian, Inc., Wallingford, CT, USA.
- [16] Patil, Y., Misra, R., Singh, M. K., Sharma, G. D. (2017), Ferrocene-diketopyrrolopyrrole based small molecule donors for bulk heterojunction solar cells. *Phys. Chem. Chem. Phys.*, 19, 7262–7269 (DOI: 10.1039/C7CP00231A).
- [17] Patil, Y., Misra, R., Keshtov, M. L., Singhal, R., Sharma, G. D. (2017), Ferrocene-diketopyrrolopyrrole based non-fullerene acceptors for bulk heterojunction polymer solar cells. (2017), *J. Mater. Chem. A*, 5, 13625-13633 (DOI: 10.1039/C7TA03322B).

Chapter 6

Metal functionalized diketopyrrolopyrroles

6.1. Introduction

The synthesis of organic chromophores with strong absorption in the near infrared (NIR) region has gained considerable attention of the scientific community due to their applications in optoelectronics and biomedical imaging.^[1] The NIR absorbing small molecules possess low HOMO-LUMO gap, larger dielectric constant, high dipole moment, and lower exciton binding energy which are promising features for generating efficient materials for optoelectronic applications.^[2]

Diketopyrrolopyrrole (DPP) and its derivatives have received great deal of attention because of their applications in wide variety of fields like aggregation induced emission (AIE), organic field effect transistor (OFET), dye sensitized solar cell (DSSC), bulk heterojunction (BHJ) solar cell.^[3,6] The first synthesis of DPP chromophore was reported by Farnum et al. in 1974.^[4] DPPs are generally synthesized by the reaction of aromatic nitrile with dialkyl succinate *via* cyclization.^[5] A variety of donor based unsymmetrical and symmetrical molecular DPPs were reported in literature for BHJ organic solar cells.^[6]

The metal-dithiolene based systems are of interest because of their interesting redox chemistry and formation of electron transfer complexes.^[7] Metalladithiolene ring is a π -conjugated metallacycle containing one metal, two sulfurs and two unsaturated carbons and is of particular interest because both substitution and addition reactions occur with ring due to the coexistence of aromaticity and unsaturation.^[8] Champness et al. have reported ferrocene and cobalt-dithiolene based multistate redox-active architectures of perylenebisimides (PBI).^[9] Castellano et al. have reported the photophysical properties of iridium metal coordinated DPP (**Ir-DPP-Ir**).^[10] The photophysical properties of platinum (II) derivative (**Pt-DPP-Pt**) of the DPP was reported by Schanze *et.al* (Figure 6.1).^[11]

The photophysical properties of ferrocenyl flanked DPP (**Fc-DPP-Fc**) showed absorption in visible region and showed promising power conversion efficiency (PCE) of 6.44% when used as donor for bulk heterojunction organic solar cells.^[12b, 12c] Herein in order to extend the absorption to near infrared region and to

investigate the effect of cobalt metal on photonic, thermal and electronic properties of DPP we have designed and synthesized cobalt-dithiolene based symmetrical DPP, **Co-DPP-Co** (Figure 6.1).

6.2. Results and discussion

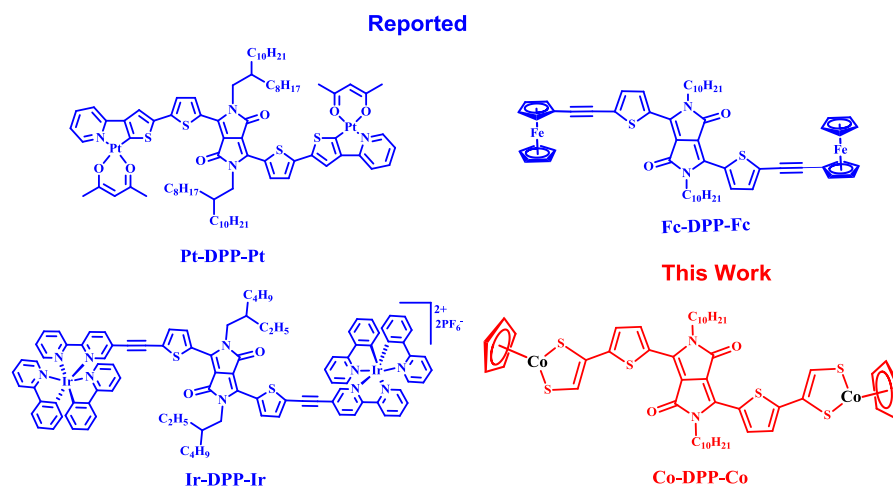
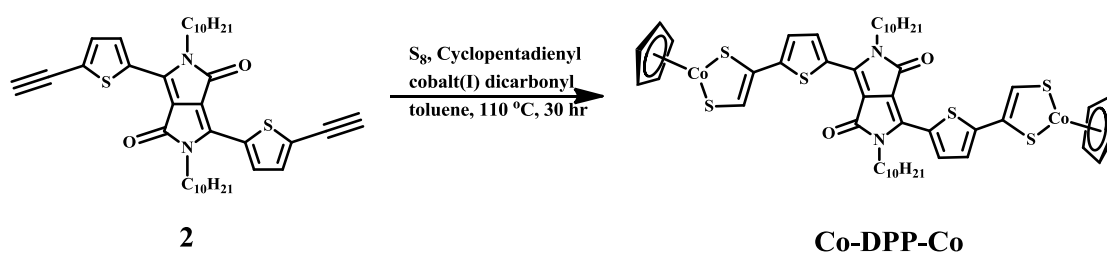


Figure 6.1. Chemical structures of metal coordinated DPPs.

The cobalt-dithiolene functionalized **Co-DPP-Co** was synthesized by the reaction of di-ethynyl diketopyrrolopyrrole **DPP2** with cyclopentadienyl cobalt (I) dicarbonyl and sulfur in degassed toluene for 30 hours in 63% yield (Scheme 6.1). We have synthesized **Fc-DPP-Fc** and **DPP2** as per reported procedure.¹² The cobalt-dithiolene functionalized **Co-DPP-Co** was purified by column chromatography. The **Co-DPP-Co** possesses good solubility in organic solvents such as dichloromethane, toluene, chloroform, and was characterized by ¹H, ¹³C NMR, and HRMS techniques.



Scheme 6.1. Synthesis of **Co-DPP-Co**.

6.3. Photophysical Properties

The electronic absorption spectra of **Co-DPP-Co** and **Fc-DPP-Fc** were recorded in dichloromethane (Figure 6.2) and corresponding absorption data are

listed in Table 6.1. The **Co-DPP-Co** and **Fc-DPP-Fc** showed absorption in Vis-NIR region. The **Co-DPP-Co** exhibit two absorption bands, one broad less intense shoulder band in NIR region at 820 nm due to transition from HOMO to LUMO+2 and another intense band in visible region at 620 nm related to transition from HOMO to LUMO. The broad shoulder band in 750–1050 nm wavelength region is observed for **Co-DPP-Co**. The **Fc-DPP-Fc** shows two absorption bands in visible region one at 624 nm and another shoulder band at 582 nm.

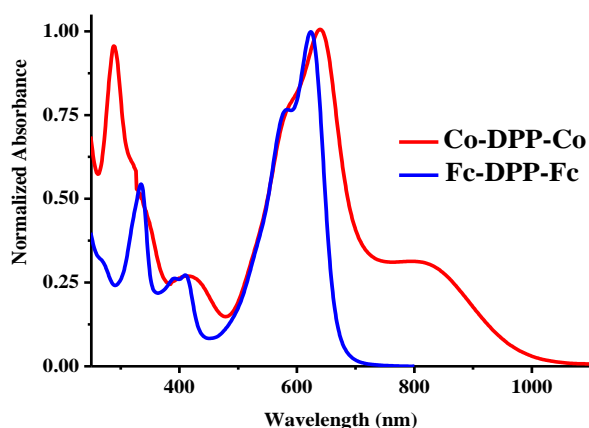


Figure 6.2. Normalized electronic absorption spectra of **Co-DPP-Co** and **Fc-DPP-Fc** in dichloromethane solution (10^{-4} M).

The cobalt-dithiolene functionalized **Co-DPP-Co** shows 16 nm red shift compared to ferrocenyl substituted **Fc-DPP-Fc** (Table 6.1). The results show functionalization of cobalt to DPP results in red shifted absorption compared to ferrocene functionalization to DPP. The optical gap values calculated from onset absorption for **Co-DPP-Co** and **Fc-DPP-Fc** are 1.22 eV and 1.78 eV respectively.

Table 6.1. Photophysical, thermal and electrochemical^c properties of **Co-DPP-Co** and **Fc-DPP-Fc**.

DPP	λ_{abs} (nm)	$\epsilon/10^4$ ($\text{M}^{-1} \cdot \text{cm}^{-1}$) ^a	T_d ($^{\circ}\text{C}$) ^b	E^2 Oxid	E^1 Oxid	E^1 Red	E^2 Red	E_g^d (eV)
Co-DPP-Co	640	3.2	275	0.78	0.61	-0.71	-1.05	1.22
Fc-DPP-Fc	624	2.6	290	1.06	0.61	-0.87	-1.43	1.78

^aAbsorbance measured in dichloromethane at 1×10^{-4} M concentration, ϵ :extinction coefficient;

^bDecomposition temperatures for 5% weight loss at a heating rate of $10 \text{ }^{\circ}\text{C min}^{-1}$, under a nitrogen atmosphere; ^cThe electrochemical analysis was performed in a 0.1 M solution of Bu_4NPF_6 in

dichloromethane at 100 mVs^{-1} scan rate, versus Ag/Ag^+ at $25 \text{ }^\circ\text{C}$; ^dOptical gap obtained from onset absorption.

The fluorescence spectra of the **Co-DPP-Co** and **Fc-DPP-Fc** were recorded in dichloromethane at room temperature and both the **Co-DPP-Co** and **Fc-DPP-Fc** are non-fluorescent.

6.4. Thermal Properties

The thermogravimetric analysis (TGA) of the **Co-DPP-Co** and **Fc-DPP-Fc** were investigated in order to understand the stability under nitrogen atmosphere. The thermograms of **Co-DPP-Co** and **Fc-DPP-Fc** are shown in Figure 6.3 and data are listed in Table 6.1. The **Co-DPP-Co** and **Fc-DPP-Fc** exhibit good thermal stability and the decomposition temperatures for 5% weight loss were found to be $275 \text{ }^\circ\text{C}$ and $290 \text{ }^\circ\text{C}$ respectively. The result shows **Co-DPP-Co** is less stable compared to **Fc-DPP-Fc**.

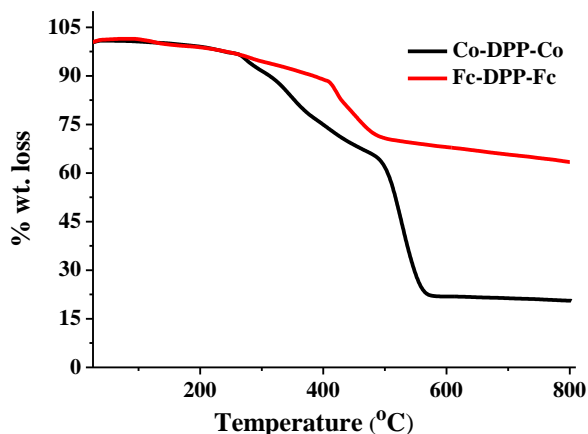


Figure 6.3 TGA of **Co-DPP-Co** and **Fc-DPP-Fc**.

6.5. Electrochemical Properties

The cyclic voltammetry (CV) and differential pulse voltammetry (DPV) of **Co-DPP-Co** and **Fc-DPP-Fc** in dichloromethane solvent using supporting electrolyte of 0.1 M tetrabutylammonium hexafluorophosphate (Bu_4NPF_6) were recorded to investigate electrochemical properties.

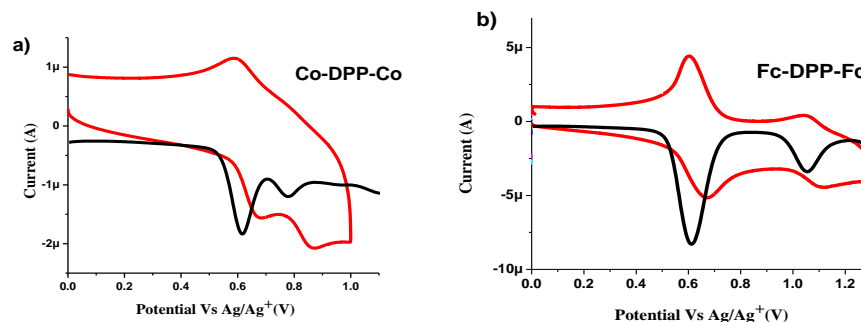


Figure 6.4. CV (red line) and DPV (black line) oxidation plots of a) **Co-DPP-Co** and b) **Fc-DPP-Fc**.

The CV and DPV curves of **Co-DPP-Co** and **Fc-DPP-Fc** show two oxidation waves, first wave at 0.61V is due to the oxidation of cobalt/ferrocenyl moiety and second at 0.78V and 1.06V for the oxidation of thiophene moiety respectively (Figure 6.4).

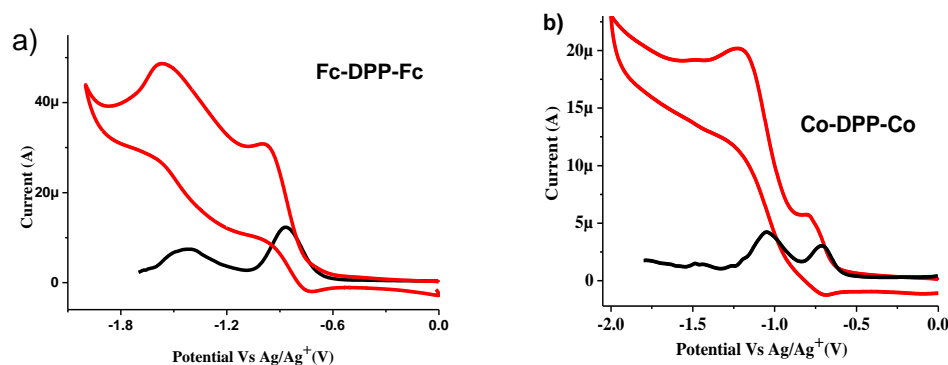


Figure 6.5. CV (red line) and DPV (black line) reduction plots of (a) **Fc-DPP-Fc** and (b) **Co-DPP-Co**.

The **Co-DPP-Co** and **Fc-DPP-Fc** exhibit two reduction waves due to the formation of monoanion and dianion of DPP (Figure 6.5). The energy levels of **Co-DPP-Co** and **Fc-DPP-Fc** were estimated from the first oxidation and reduction potentials. The estimated HOMO/LUMO energy levels are as -4.4/-5.01eV and -3.69/-5.01 eV for **Co-DPP-Co** and **Fc-DPP-Fc** respectively.

6.6. Theoretical Calculations

In order to understand the geometry and electronic structure of the **Co-DPP-Co** and **Fc-DPP-Fc**, the density functional theory (DFT) calculation was carried out using Gaussian 09W program. The DFT calculation was performed at the B3LYP/6-

31+G** for C, H, O, N, B and Lan12DZ for Fe and Co level of theory^[13] and geometry optimization was carried out in the gas phase.

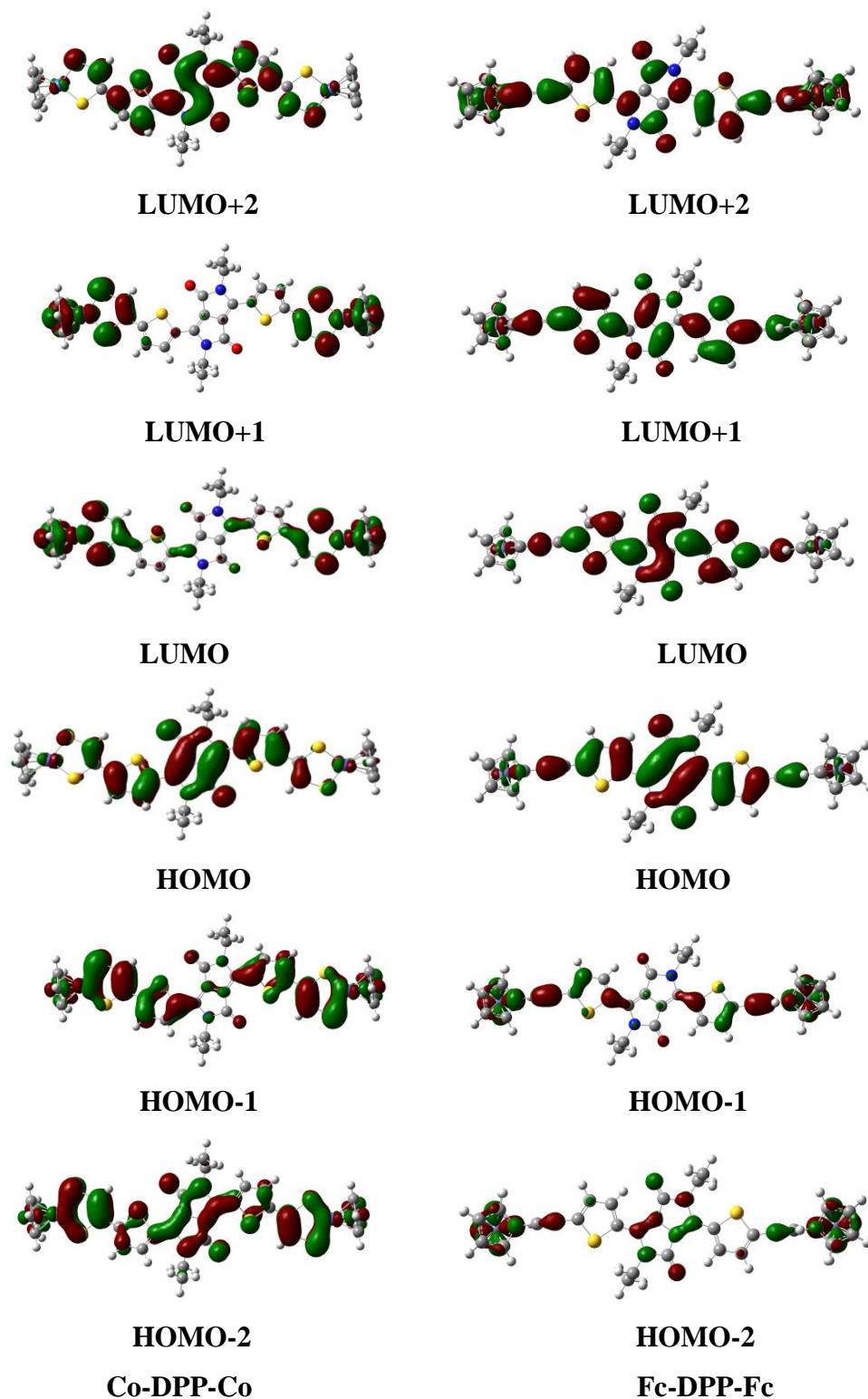


Figure 6.5. The frontier molecular orbitals of Co-DPP-Co and Fc-DPP-Fc.

The long alkyl chains of DPP chromophore were replaced by ethyl group in order to reduce the computation time. The frontier molecular orbitals of **Co-DPP-Co** and **Fc-DPP-Fc** are shown in Figure 6.5 and Figure 6.6.

The geometry optimized structure of **Co-DPP-Co** exhibits cis geometry of cobalt-di-thiophene ring whereas in **Fc-DPP-Fc** planar geometry of ferrocenyl unit has been observed (Figure 6.6). The optimized structure of **Co-DPP-Co** shows that both the methyl groups are one below another whereas **Fc-DPP-Fc** shows the methyl groups in alkyl chain are opposite side to one another (Figure 6.6). The HOMO/LUMO levels of **Co-DPP-Co** and **Fc-DPP-Fc** estimated as -2.63/-4.72 eV and -3.06/4.70eV and the HOMO-LUMO gap values are 1.64 eV and 2.09 eV respectively which are in agreement with the experimental values estimated from the absorption spectra and electrochemical study.

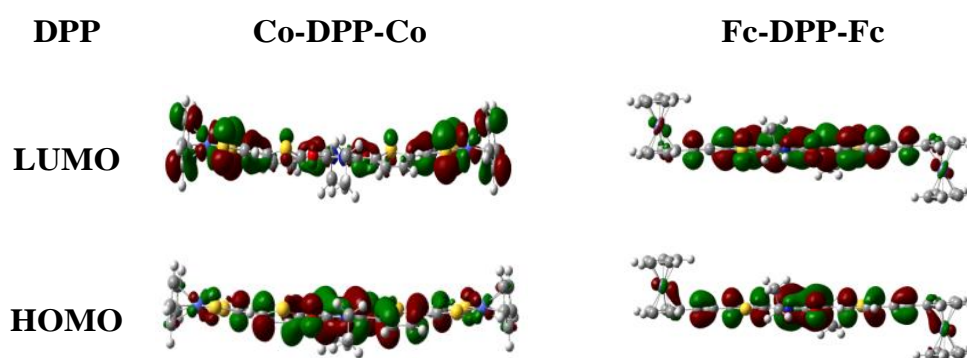


Figure 6.6. The frontier molecular orbitals of **Co-DPP-Co** and **Fc-DPP-Fc** at B3LYP/6-31G(d) level.

The time dependent density functional theory (TDDFT) calculation was performed to understand the electronic transitions in **Co-DPP-Co** and **Fc-DPP-Fc**. The electronic transitions in **Co-DPP-Co** and **Fc-DPP-Fc** from TDDFT calculation with composition, assignment and oscillator strength are shown in Table 6.2.

The **Co-DPP-Co** shows two absorption bands in visible-NIR region at 587 nm and 842 nm. The broad less intense shoulder band was observed at 842 nm is due to the transition from HOMO to LUMO+2 and intense band observed at 587 nm is related to HOMO to LUMO transition along with other minor transitions. The **Fc-DPP-Fc** show two absorption bands in visible region at 636 nm and 590 nm and for both bands the major transition was observed from HOMO to LUMO related to

$\pi \rightarrow \pi^*$ transition (Table 6.2). The various other transitions were observed which are given in Table 6.2.

Table 6.2. Calculated electronic transitions for **Co-DPP-Co** and **Fc-DPP-Fc** in the gas phase.

DPP	Wavelength (nm)	Composition	f^a
Co-DPP-Co	842	HOMO-19→LUMO+1 (0.11)	0.30
		HOMO-18→LUMO (0.11)	
		HOMO-4→LUMO (0.24)	
		HOMO-3→LUMO+1 (0.22)	
		HOMO→LUMO (0.56)	
	587	HOMO-2 → LUMO (0.24)	0.98
		HOMO-1 →LUMO+1 (0.27)	
		HOMO→ LUMO+2 (0.58)	
Fc-DPP-Fc	636	HOMO-4→LUMO+5 (0.14)	1.23
		HOMO-3→LUMO+4 (0.14)	
		HOMO-2→LUMO (0.14)	
		HOMO-2→LUMO+2 (0.14)	
		HOMO-2→LUMO+6 (0.13)	
		HOMO-1→LUMO+1 (0.12)	
		HOMO-1→LUMO+3 (0.16)	
		HOMO→LUMO (0.59)	
	590	HOMO-5→LUMO+3 (0.13)	0.40
		HOMO-4→LUMO+5 (0.25)	
		HOMO-3→LUMO+4 (0.25)	
		HOMO-2→LUMO (0.17)	
		HOMO-2→LUMO+2 (0.19)	
		HOMO-2→LUMO+6 (0.19)	
		HOMO-1→LUMO+1 (0.12)	
		HOMO-1→LUMO+3 (0.22)	
		HOMO→LUMO (0.39)	

f^a = Oscillation Strength

6.7. Experimental Section

General Methods

The chemicals were used as received unless otherwise indicated. ^1H NMR (400 MHz) and ^{13}C NMR (100 MHz) spectra were recorded by using CDCl_3 as the solvent. The ^1H NMR chemical shifts are reported in parts per million (ppm) relative to the solvent residual peak (CDCl_3 , 7.26 ppm). The multiplicities are given as: s (singlet), d (doublet), and m (multiplet). The ^{13}C NMR chemical shifts are reported with relative to the solvent residual peak (CDCl_3 , 77.02 ppm). HRMS was recorded on a mass spectrometer (ESI-TOF). The UV-visible absorption spectra were recorded on UV-visible Spectrophotometer in dichloromethane. The TGA analyses were performed on the thermal analysis system at the heating rate of 10 °C per minute under a nitrogen atmosphere. Cyclic voltammograms (CVs) and differential voltammograms (DPVs) were recorded on an electrochemical analyzer using glassy carbon as working electrode, Pt wire as the counter electrode, and saturated Ag/Ag^+ as the reference electrode.

Synthesis of Co-DPP-Co

A mixture of **DPP 2** (200 mg, 0.1 mmol), cyclopentadienyl cobalt (I) dicarbonyl (39 mg, 0.216 mmol) and sulfur (13 mg, 0.41 mmol) in degassed toluene (30 mL) was stirred under reflux at 110 °C for 30 h. The solvent was removed under reduced pressure and the residue was purified by silica-gel column chromatography by using hexane:dichloromethane (1:1) to yield dark blue colored **Co-DPP-Co** in 63% yield. ^1H NMR (400 MHz, CDCl_3 , δ in ppm): 8.76-9.32 (4H, m), 7.51 (2H, s), 5.10-5.77 (8H, m), 4.10 (4H, s), 1.76 (4H, m), 1.00-1.54 (28H, m), 0.86 (6H, m); ^{13}C NMR (100 MHz, CDCl_3 , δ in ppm): 162.5, 161.4, 156.89, 156.87, 149.6, 129.32, 129.30, 124.8, 108.4, 108.3, 79.7, 53.5, 53.4, 42.4, 42.37, 32.0, 30.1, 29.8, 27.0, 22.8; HRMS (ESI) m/z calcd for $\text{C}_{48}\text{H}_{58}\text{Co}_2\text{N}_2\text{O}_2\text{S}_6$: 1004.1481 [M] $^+$, found 1004.1597 [M] $^+$.

6.8. Conclusions

In conclusion, the synthesis, structural characterization, optical, thermal, electrochemical and computational properties of symmetrical cobalt-dithiolene functionalized DPP **Co-DPP-Co** was investigated and compared with ferrocenyl based symmetrical **Fc-DPP-Fc**. The absorption spectra of **Co-DPP-Co** exhibited red shifted absorption in Vis-NIR region with shoulder band in longer wavelength region. The cobalt based **Co-DPP-Co** shows good thermal stability. The DFT investigation exhibited cis geometry of cobalt-dithiolene ring in **Co-DPP-Co**

whereas the trans geometry of ferrocenyl unit has been observed in **Fc-DPP-Fc**. The broad absorption in NIR region, high thermal stability and low HOMO – LUMO gap values makes **Co-DPP-Co** as a potential candidate for photovoltaic applications.

6.9. References

- [1] (a) Wang, H., Xiao, L., Yan, L., Chen, S., Zhu, X., Peng, X., Wang, X., Wong, W.-K., Wong, W.-Y. (2016), Structural engineering of porphyrin-based small molecules as donors for efficient organic solar cells. *Chem. Sci.*, 7, 4301-4307 (DOI: 10.1039/C5SC04783H); (b) Qin, C., Fu, Y., Chui, C.-H., Kan, C.-W., Xie, Z., Wang, L., Wong, W.-Y. (2011), Tuning the Donor–Acceptor Strength of Low-Bandgap Platinum-Acetylide Polymers for Near-Infrared Photovoltaic Applications. *Macromol. Rapid Commun.*, 32, 1472–1477 (DOI: 10.1002/marc.201100247); (c) Wang, X.-Z., Wang, Q., Yan, L., Wong, W.-Y., Cheung, K.-Y., Ng, A., Djurišić, A. B., Chan, W.-K. (2010), Tuning the Donor–Acceptor Strength of Low-Bandgap Platinum-Acetylide Polymers for Near-Infrared Photovoltaic Applications. *Macromol. Rapid Commun.*, 31, 861–867 (DOI: 10.1002/marc.200900885); (d) Qin, C., Wong, W.-Y., Han, L. (2013), Squaraine Dyes for Dye-Sensitized Solar Cells: Recent Advances and Future Challenges. *Chem. Asian J.*, 8, 1706–1711 (DOI: 10.1002/asia.201300185); (e) Gomez-Hens, A. and Aguilar-Caballos, M. P. (2004), Long-wavelength fluorophores: new trends in their analytical use. *Trends Anal. Chem.*, 23, 127–136 (DOI: 10.1016/S0165-9936(04)00305-X); (f) Yuan, L., Lin, W., Zheng, K., He, L., Huang, W. (2013), Far-red to near infrared analyte-responsive fluorescent probes based on organic fluorophore platforms for fluorescence imaging. *Chem. Soc. Rev.*, 42, 622–661 (DOI: 10.1039/C2CS35313J); (g) Hilderbrand, S. A., Weissleder, R. (2010), Near-infrared fluorescence: application to in vivo molecular imaging. *Curr. Opin. Chem. Biol.*, 14, 71–78 (DOI: 10.1016/j.cbpa.2009.09.029).
- [2] (a) Li, G., Zhu, R., Yang, Y. (2012), Polymer solar cells. *Nat. Photonics*, 6, 153–161 (DOI: 10.1038/nphoton.2012.11); (b) Janssen, R. A. J., Nelson, J. (2013), Factors Limiting Device Efficiency in Organic Photovoltaics. *Adv. Mater.*, 25, 1847–1858 (DOI: 10.1002/adma.201202873); (c) Zhao, Y., Guo, Y., Liu, Y. (2013), Recent Advances in n-Type and Ambipolar Organic Field-

- Effect Transistors. *Adv. Mater.*, 25, 5372–5391 (DOI: 10.1002/adma.201302315); (d) You, J., Dou, L., Yoshimura, K., Kato, T., Ohya, K., Moriarty, T., Emery, K., Chen, C.-C., Gao, J., Li, G., Yang, Y. (2013), A polymer tandem solar cell with 10.6% power conversion efficiency. *Nat. Commun.*, 4, 1446 (DOI: 10.1038/ncomms2411); (e) Dou, L., Liu, Y., Hong, Z., Li, G., Yang, Y. (2015), Low-Bandgap Near-IR Conjugated Polymers/Molecules for Organic Electronics. *Chem. Rev.*, 115, 12633–12665 (DOI: 10.1021/acs.chemrev.5b00165); (f) Chen, S., Xiao, L., Zhu, X., Peng, X., Wong, W.-K., Wong, W.-Y. (2015), Solution-processed new porphyrin-based small molecules as electron donors for highly efficient organic photovoltaics. *Chem. Commun.*, 51, 14439-14442 (DOI: 10.1039/c5cc05807d); (g) Xiao, L., Chen, S., Gao, K., Peng, X., Liu, F., Cao, Y., Wong, W.-Y., Wong, W.-K., Zhu, X. (2016), New Terthiophene-Conjugated Porphyrin Donors for Highly Efficient Organic Solar Cells. *ACS Appl. Mater. Interfaces*, 8, 30176–30183 (DOI: 10.1021/acsami.6b09790); (h) Liu, Q., Zhu, N., Ho, C.-L., Fu, Y., Lau, W.-S., Xie, Z., Wang, L., Wong, W.-Y. (2016), Synthesis, characterization, photophysical and photovoltaic properties of new donor–acceptor platinum(II) acetylide complexes. *J. Organomet. Chem.*, 812, 2-12 (DOI: <https://doi.org.10.1016/j.jorganchem.2015.06.017>).
- [3] (a) Zhu, Y., Rabindranath, A. R., Beyerlein, T., Tieke, B. (2007), Highly Luminescent 1,4-Diketo-3,6-diphenylpyrrolo[3,4-c] pyrrole- (DPP-) Based Conjugated Polymers Prepared Upon Suzuki Coupling. *Macromolecules.*, 40, 6981 (DOI: 10.1021/ma0710941); (b) Fischer, G. M., Ehlers, A. P., Zumbusch, A., Daltrozzo, E. (2007), Near-Infrared Dyes and Fluorophores Based on Diketopyrrolopyrroles. *Angew. Chem. Int. Ed.*, 46, 3750–3753 (DOI: 10.1002/anie200604763); (c) Yang, J., Tan, H., Li, D., Jiang, T., Gao, Y., Li, B., Qu, X., Hua, J. (2016), Synthesis, two-photon absorption and aggregation-induced emission properties of multi-branched triphenylamine derivatives based on diketopyrrolopyrrole for bioimaging. *RSC Adv.*, 6, 58434–58442 (DOI: 10.1039/C6RA11269B). (d) Lim, B., Sun, H., Lee, J., Noh, Y.-Y. (2017), High Performance Solution Processed Organic Field Effect Transistors with Novel Diketopyrrolopyrrole-Containing Small Molecules, *Scientific Reports*, 7, 164 (DOI:10.1038/s41598-017-00277-7). (e) Favereau, L., Warnan, J., Pellegrin,

- Y., Blart, E., Boujtita, M., Jacquemin, D., Odobel, F. (2013), Diketopyrrolopyrrole derivatives for efficient NiO-based dye-sensitized solar cells. *Chem. Commun.*, 49, 8018–8020 (DOI: 10.1039/C3CC44232B)
- [4] Farnum, D. G., Mehta, Moore, G. G. G. I., Siegal, F. P. (1974), Attempted reformatskii reaction of benzonitrile, 1,4-diketo-3,6-diphenylpyrrolo[3,4-C] pyrrole. A lactam analogue of pentalene. *Tetrahedron Lett.*, 29, 2549–2552 (DOI: [https://doi.org/10.1016/S0040-4039\(01\)93202-2](https://doi.org/10.1016/S0040-4039(01)93202-2))
- [5] A. Iqbal, L. Cassar, U.S. Patent 4 415 (1983) 685.
- [6] (a) Tang, A., Zhan, C., Yao, J., Zhou, E. (2017), Design of Diketopyrrolopyrrole (DPP)-Based Small Molecules for Organic-Solar-Cell Applications. *Adv. Mater.*, 29, 1600013 (DOI: 10.1002/adma.201600013). (b) Patil, Y., Misra, R., Keshtov, M. L., Sharma, G. D. (2016), 1,1,4,4-Tetracyanobuta-1,3-diene Substituted Diketopyrrolopyrroles: An Acceptor for Solution Processable Organic Bulk Heterojunction Solar Cells. *J. Phys. Chem. C*, 120, 6324–6335 (DOI: 10.1021/acs.jpcc.5b12307); (c) Patil, Y., Jadhav, T., Dhokale, B., Misra, R. (2016), Design and Synthesis of Low HOMO–LUMO Gap N-Phenylcarbazole-Substituted Diketopyrrolopyrroles. *Asian J. Org. Chem.* 5, 1008–1014 (DOI: 10.1002/ajoc.201600194); (d) Patil, Y., Misra, R., Keshtov, M. L., Sharma, G. D. (2017), Small molecule carbazole-based diketopyrrolopyrroles with tetracyanobutadiene acceptor unit as a non-fullerene acceptor for bulk heterojunction organic solar cells. *J. Mater. Chem. A*, 5, 3311–3319 (DOI: 10.1039/C6TA09607G); (e) Li, S., Zhang, Z., Shi, M., Li, C.-Z., Chen, H. (2017), Molecular electron acceptors for efficient fullerene-free organic solar cells. *Phys. Chem. Chem. Phys.*, 19, 3440–3458 (DOI: 10.1039/C6CP07465K); (f) Liu, Q., Ho, C.-L., Lo, Y. H., Li, H., Wong, W.-Y. (2015), Narrow Bandgap Platinum(II)-Containing Polyynes with Diketopyrrolopyrrole and Isoindigo Spacers. *J Inorg Organomet Polym.*, 25, 159 (DOI: 10.1007/s10904-014-0120-2).
- [7] (a) Selby-Karneya, T., Grossieb, D. A., Arumugamb, K., Wrightb, E., Chandrasekaran, P. (2017), Structural and spectroscopic characterization of five coordinate iron and cobalt bis(dithiolene)-trimethylphosphine complexes. *Journal of Molecular Structure*, 1141, 477–483 (DOI: <https://doi.org/10.1016/j.molstruc.2017.03.119>); (b) Eisenberg, R., Gray, H. B. (2011), Noninnocence in Metal Complexes: A Dithiolene Dawn. *Inorg. Chem.*,

- 50, 9741–9751 (DOI: 10.1021/ic2011748); (c) Lim, B. S., Fomitchev, D. V., Holm, R. H. (2001), Nickel Dithiolenes Revisited: Structures and Electron Distribution from Density Functional Theory for the Three-Member Electron-Transfer Series $[\text{Ni}(\text{S}_2\text{C}_2\text{Me}_2)_2]^{0,1-,2-}$. *Inorg. Chem.*, 40, 4257-4262 (DOI: 10.1021/ic010138y); (d) Sproules, S., Benedito, F. L., Bill, E., Weyhermüller, T., DeBeer, S. G., Wieghardt, K. (2009), Characterization and Electronic Structures of Five Members of the Electron Transfer Series $[\text{Re}(\text{benzene-1,2-dithiolato})_3]^z$ ($z = 1+, 0, 1-, 2-, 3-$): A Spectroscopic and Density Functional Theoretical Study. *Inorg. Chem.*, 48, 10926-10941 (DOI: 10.1021/ic9010532); (e) Sproules, S., Weyhermüller, T., DeBeer, S., Wieghardt, K. (2010), Six-Membered Electron Transfer Series $[\text{V}(\text{dithiolene})_3]^z$ ($z = 1+, 0, 1-, 2-, 3-, 4-$). An X-ray Absorption Spectroscopic and Density Functional Theoretical Study. *Inorg. Chem.*, 49, 5241-5261 (DOI: 10.1021/ic100344f).
- [8] (a) Sugimori, A., Akiyama, T., Kajitani, M., Sugiyama, T. (1999), Synthesis and Chemical Properties of Metalladithiolene and Metalladithiazole Rings. Unique Reactions Due to Coexistence of Aromaticity and Unsaturation, *Bull. Chem. Soc. Jpn.* 72, 879 (DOI: <http://doi.org/10.1246/bcsj.72.879>); (b) Nomura, M., Sasao, T., Hashimoto, T., Sugiyama, T., Kajitani, M. (2010), Structures and electrochemistry of monomeric and dimeric CpCo(dithiolene) complexes with substituted benzene-1,2-dithiolate ligand. *Inorganica Chimica Acta*, 363, 3647–3653 (DOI: 10.1016/j.ica.2010.05.005).
- [9] Goretzki, G., Davies, E. S., Argent, S. P., Warren, J. E., Blake, A. J., Champness, N. R. (2009), Building Multistate Redox-Active Architectures Using Metal-Complex Functionalized Perylene Bis-imides. *Inorg. Chem.*, 48, 10264–10274 (DOI: 10.1021/ic901379d).
- [10] McCusker, C. E., Hablot, D., Ziessel, R., Castellano, F. N. (2012), Metal Coordination Induced π -Extension and Triplet State Production in Diketopyrrolopyrrole Chromophores. *Inorg. Chem.*, 51, 7957–7959 (DOI: 10.1021/ic301238e).
- [11] Goswami, S., Winkel, R.W., Alarousu, E., Ghiviriga, I., Mohammed, O. F., Schanze, K. S. (2014), Photophysics of Organometallic Platinum(II) Derivatives of the Diketopyrrolopyrrole Chromophore, *J. Phys. Chem. A*, 118, 11735–11743 (DOI: 10.1021/jp509987p).

- [12] (a) Yu, C., Liu, Z., Yang, Y., Yao, J., Cai, Z., Luo, H., Zhang, G., Zhang, D. (2014), New dithienyl-diketopyrrolopyrrole-based conjugated molecules entailing electron withdrawing moieties for organic ambipolar semiconductors and photovoltaic materials. *J. Mater. Chem. C*, 2, 10101–10109 (DOI: 10.1039/C4TC01872A); (b) Patil, Y., Jadhav, T., Dhokale, B., Misra, R. (2016), Tuning of the HOMO–LUMO Gap of Symmetrical and Unsymmetrical Ferrocenyl-Substituted Diketopyrrolopyrroles. *Eur. J. Org. Chem.*, 4, 733–738 (DOI: 10.1002/ejoc.201501123); (c) Patil, Y., Misra, R., Singh, M. K. and Sharma, G. D. (2017), Ferrocene-diketopyrrolopyrrole based small molecule donors for bulk heterojunction solar cells. *Phys. Chem. Chem. Phys.*, 19, 7262–7269 (DOI : 10.1039/C7CP00231A).
- [13] Frisch, M. J., Trucks, G. W., Schlegel, H. B., Scuseria, G. E., Robb, M. A., Cheeseman, J. R., Scalmani, G., Barone, V., Mennucci, B., Petersson, G. A., Nakatsuji, H., Caricato, M., Li, X., Hratchian, H. P., Izmaylov, A. F., Bloino, J., Zheng, G., Sonnenberg, J. L., Hada, M., Ehara, M., Toyota, K., Fukuda, R., Hasegawa, J., Ishida, M., Nakajima, T., Honda, Y., Kitao, O., Nakai, H., Vreven, T., Montgomery Jr, J. A., Peralta, J. E., Ogliaro, F., Bearpark, M., Heyd, J. J., Brothers, E., Kudin, K. N., Staroverov, V. N., Kobayashi, R., Normand, J., Raghavachari, K., Rendell, A., Burant, J. C., Iyengar, S. S., Tomasi, J., Cossi, M., Rega, N., Millam, J. M., Klene, M., Knox, J. E., Cross, J. B., Bakken, V., Adamo, C., Jaramillo, J., Gomperts, R., Stratmann, R. E., Yazyev, O., Austin, A. J., Cammi, R., Pomelli, C., Ochterski, J. W., Martin, R. L., Morokuma, K., Zakrzewski, V. G., Voth, G. A., Salvador, P., Dannenberg, J. J., Dapprich, S., Daniels, A. D., Farkas, Ö., Foresman, J. B., Ortiz, J. V., Cioslowski, J., Fox, D. J. (2009) Gaussian 09, revision D.01 Gaussian, Inc., Wallingford, CT, USA.

Chapter 7

Diketopyrrolopyrrole based monomer, dimers and trimer: A comparative study

7.1. Introduction

The diketopyrrolopyrrole (DPP) and its derivatives are chemically and thermally stable. DPP derivatives have showed potential applications in various fields such as organic field effect transistor (OFET), solar cell, in paints, inks, plastics, aggregation induced emission (AIE), and as high performance pigments in several industrial products.^[1,2] DPP derivatives are poorly soluble in common organic solvents due to hydrogen bonding and strong π - π interactions, in order to improve their solubility alkyl chains were attached at nitrogen atoms of the DPP.^[3] Recently DPP derivatives have been reported for various applications such as in two-photon absorption, sensors, fluorescing near-infrared (NIR) probes and photothermal agent in cancer therapy.^[4]

The photophysical and electronic properties of vinylene bridged DPP copolymers and polymers are reported in literature.^[5] DPP-based π -conjugated small molecules and polymers are reported as efficient materials for organic photovoltaics (OPVs).^[1,6] In recent time DPP is widely for designing non-fullerene acceptors due to the strong electron withdrawing nature with planar fused ring which enhances the intermolecular interactions.^[4a] There are number of DPP based dimers and trimers are reported for bulk heterojunction organic solar cells (BHJ OSCs).^[7,8,9] Jo *et al.* reported thienyl and phenyl bridged DPP dimers as small molecule donors in OSCs along with PC₇₁BM acceptor.^[10] Choi and Balandier *et al.* reported that as the number of thiophenes between two DPP units increases, the blue shift in absorption has been observed due to the increased flexibility of π -conjugated system.^[11]

Herein we have designed and synthesized DPP based monomer (**1**), dimers (**2** and **3**) and trimer (**4**), their photophysical and electrochemical properties were explored. We were interested to see the effect of connecting bridge between DPP unit and number of DPP units on photophysical and electrochemical properties of DPP. The chemical structures of DPP based monomer (**1**), dimers (**2** and **3**) and trimer (**4**) are shown in Figure 7.1.

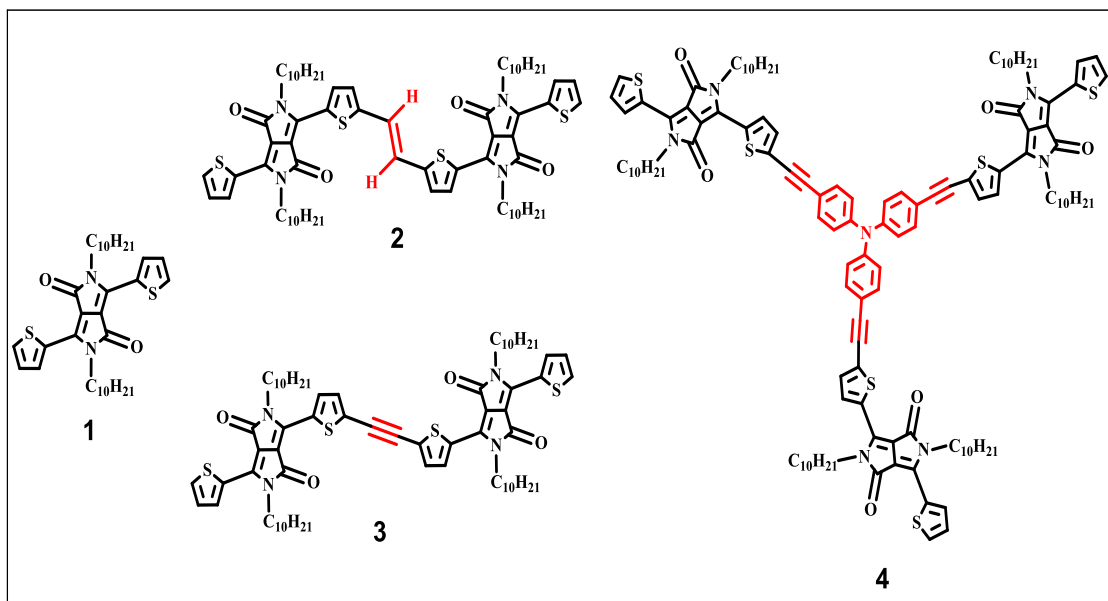
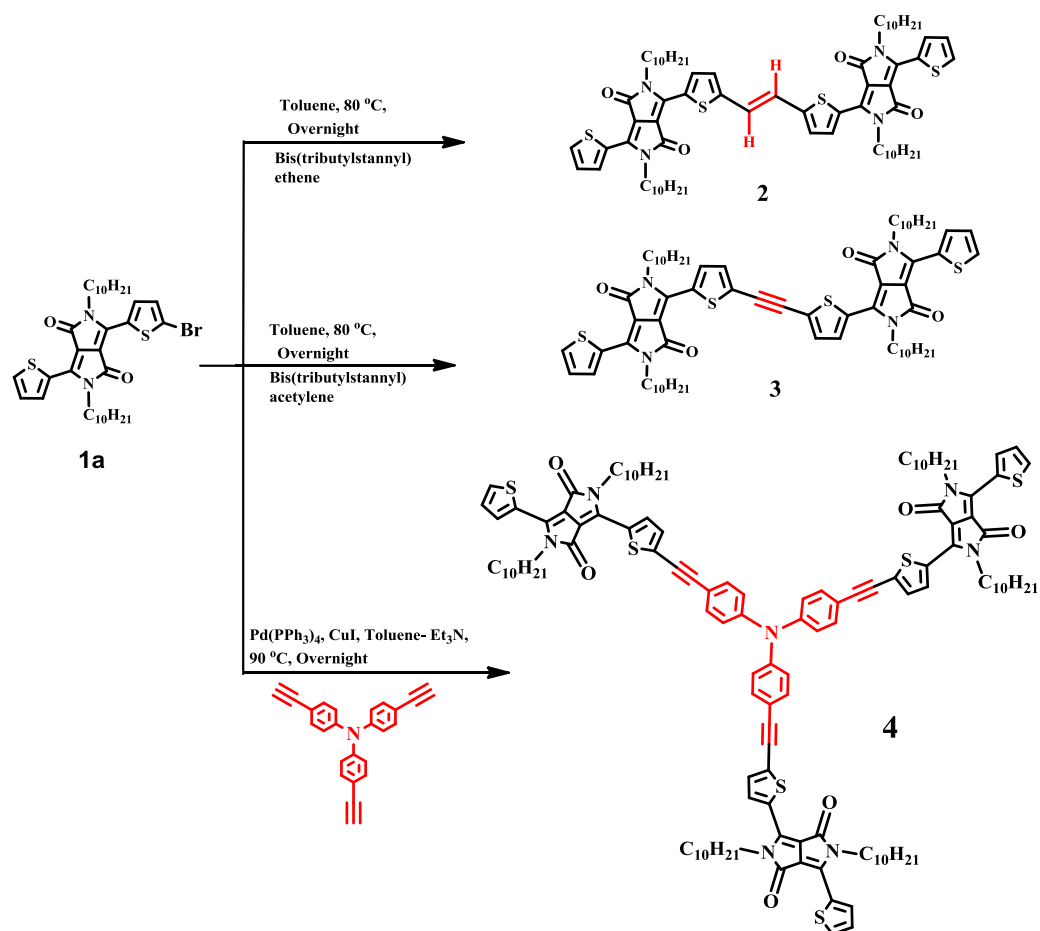


Figure 7.1. Chemical structures of DPP based monomer (**1**), dimers (**2** and **3**) and trimer (**4**).

7.2. Results and discussion

The monomer of DPP **1** was synthesized as per literature procedure which involves the reaction of 2-thiophenecarbonitrile with half equivalent of dimethyl succinate^[7a] in presence of strong base sodium *tert*-butoxide in *tert*-butanol at 120 °C for 12 hours under argon atmosphere followed by alkylation with 1-bromodecane in 23% yield. The DPP dimers **2** and **3** were synthesized by the Pd-catalyzed Stille coupling reaction of monobromo DPP **1a** with half equivalent of bis(tributylstannyl)ethene and bis(tributylstannyl)acetylene in 65% and 58% yield respectively (Scheme 7.1). The Sonogashira cross-coupling reaction of tri-ethynyl triphenylamine with three equivalents of mono-bromo DPP led to the formation of trimer **4** in 65% yield (Scheme 7.1). The bromination of triphenylamine with three equivalents of *N*-bromosuccinimide at room temperature resulted in tribromo-triphenylamine. The tri-ethynyl triphenylamine was synthesized by Sonogashira cross coupling of tribromo-triphenylamine with three equivalents of trimethylsilylacetylene (TMS) followed by deprotection in THF-methanol (1:1) at room temperature for four hours.



Scheme 7.1. Synthesis of DPP based dimers (**2** and **3**) and trimer (**4**).

The DPP based monomer (**1**), dimers (**2** and **3**) and trimer (**4**) were purified by silica-gel column chromatography and are readily soluble in common organic solvents such as dichloromethane, toluene and chloroform. The DPP based monomer (**1**), dimers (**2** and **3**) and trimer (**4**) were well characterized by ¹H NMR, ¹³C NMR, and HRMS techniques.

7.3. Photophysical Properties

The electronic absorption spectra of DPP based monomer (**1**), dimers (**2** and **3**) and trimer (**4**) were recorded in dichloromethane at room temperature (Figure 7.2) and the corresponding data are listed in Table 7.1.

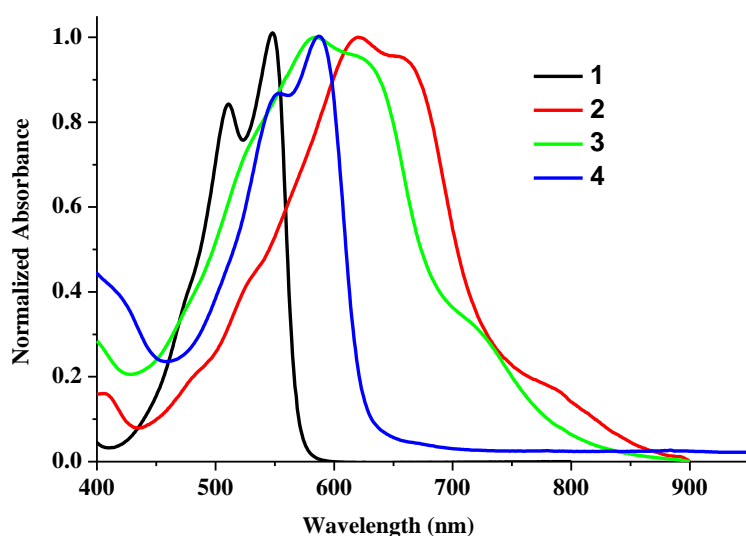


Figure 7.2. Normalized electronic absorption spectra of DPP based monomer (**1**), dimers (**2** and **3**) and trimer (**4**) in dichloromethane solution (10^{-4} M).

The absorption spectra of DPP based monomer (**1**), dimers (**2** and **3**) and trimer (**4**) in dichloromethane exhibit broad absorption bands covering whole visible region. DPP based monomer (**1**), dimers (**2** and **3**) and trimer (**4**) exhibit absorption peaks at 551 nm, 619 nm, 584 nm and 587 nm respectively. This shows that the dimerization of DPP results in the red shift of 68 nm in ethene bridged dimer **2** and 33 nm in ethyne bridged dimer **3**, whereas red shift of 36 nm was observed after the trimerization of DPP in **4** with tri-ethynyl triphenylamine.

Table 7.1. Photophysical, thermal and electrochemical properties of DPP based monomer (**1**), dimers (**2** and **3**) and trimer (**4**).

DPP	λ_{abs} (nm)	$\epsilon/10^4$ ($\text{M}^{-1} \cdot \text{cm}^{-1}$) ^a	T_d ($^{\circ}\text{C}$) ^b	E^2 Red ^c	E^1 Red ^c	E^1 Oxid ^c	E^2 Oxid ^c	E^3 Oxid ^c	E_d DFT
1	551	4.6	286	-1.26	-1.04	0.87	1.26	-	2.54
2	619	5.1	355	-	-0.99	0.89	1.34	-	1.94
3	584	4.9	304	-	-1.01	0.99	1.29	-	2.02
4	587	3.7	326	-	-1.02	0.93	1.15	1.40	2.08

^aAbsorbance measured in dichloromethane at 1×10^{-4} M concentration, ϵ : extinction coefficient;

^bDecomposition temperatures for 5% weight loss at a heating rate of $10 \text{ }^{\circ}\text{C min}^{-1}$, under a nitrogen

atmosphere; ^cThe electrochemical analysis was performed in a 0.1 M solution of Bu₄NPF₆ in dichloromethane at 100 mVs⁻¹ scan rate, versus Ag/Ag⁺ at 25 °C;

^dHOMO–LUMO gap calculated from DFT calculation.

The ethene bridged dimer **2** shows more red shifted absorption compared to ethyne bridged **3** by 35 nm indicates superior electronic communication in ethene bridged dimer compared to ethyne bridged analogue. The absorption values in Table 7.1 indicate that the dimerization and trimerization of DPP red shifts the absorption and broadening of absorption has been observed in dimer analogues (**2** and **3**).

7.4. Thermal Properties

The thermal properties of the DPP based monomer (**1**), dimers (**2** and **3**) and trimer (**4**) were investigated by the thermogravimetric analysis (TGA) at a heating rate of 10 °C / min under nitrogen atmosphere and their plots are shown in Figure 7.3.

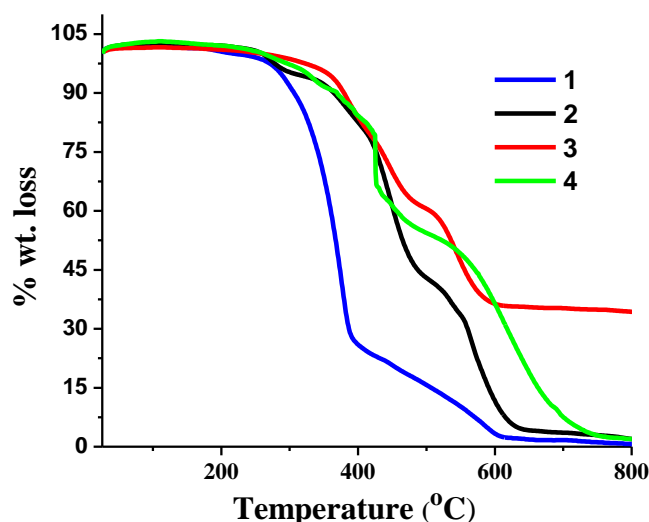


Figure 7.3. TGA of DPP based monomer (**1**), dimers (**2** and **3**) and trimer (**4**).

The DPP based monomer (**1**), dimers (**2** and **3**) and trimer (**4**) exhibit excellent thermal stability. The decomposition temperatures at 5% weight loss were found to be 286 °C, 355 °C, 304 °C and 325 °C for DPP based monomer (**1**), dimers (**2** and **3**) and trimer (**4**) respectively. DPP based dimers (**2** and **3**) and trimer (**4**) exhibit higher thermal stability compared to monomer (**1**) which indicates that the dimerization and trimerization of DPP improves the thermal stability.

7.5. Electrochemical Properties

The electrochemical properties of the DPP based monomer (**1**), dimers (**2** and **3**) and trimer (**4**) were explored by cyclic voltammetry and differential pulse voltammetry (CV and DPV) techniques in dichloromethane solvent using 0.1 M tetrabutylammonium hexafluorophosphate (Bu_4NPF_6) as a supporting electrolyte.

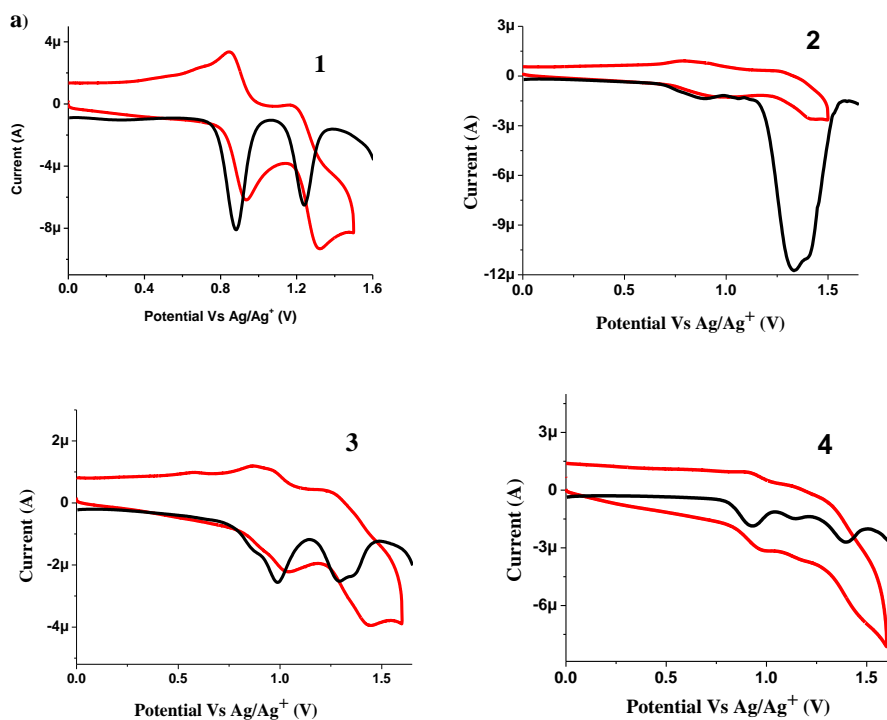


Figure 7.4. CV (red line) and DPV (black line) oxidation plots of DPP based monomer (**1**), dimers (**2** and **3**) and trimer (**4**).

The CV and DPV plots of DPP based monomer (**1**), dimers (**2** and **3**) and trimer (**4**) are shown in Figure 7.4 and Figure 7.5. The DPP monomer **1** shows two oxidation waves corresponding to the oxidation of two thiophene units whereas DPP dimers **2** and **3** show two oxidation waves along with shoulder waves in each oxidation indicating merging of two waves. The DPP and triphenylamine based trimer **4** exhibits three oxidation waves and the additional oxidation wave observed at 1.15 V is related to the oxidation of triphenylamine unit. The dimerization and trimerization of DPP hardens the oxidation of thienyl moiety. The monomer **1** exhibits two reduction waves corresponding to the reduction of DPP moiety whereas only one reduction wave was observed in dimers (**2** and **3**) and trimer (**4**).

The reduction peaks for DPP based monomer (**1**), dimers (**2** and **3**) and trimer (**4**) were observed at 1.04V, 1.26V, 0.99V, 1.01V, 1.02V respectively which

indicate that dimerization or trimerization of DPP makes easier reduction of DPP unit.

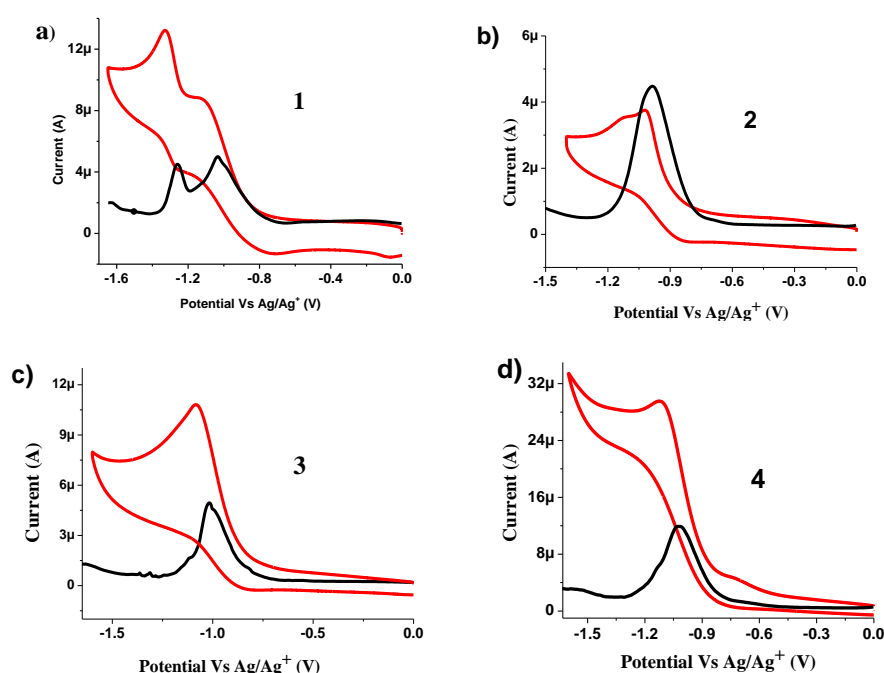


Figure 7.5. (red line) and DPV (black line) reduction plots of DPP based monomer (1), dimers (2 and 3) and trimer (4).

7.6. Density Functional Theory Calculation

The density functional theory (DFT) calculation was carried out to understand the geometry, and the electronic structure of the DPP based monomer (1), dimers (2 and 3) and trimer (4) using the Gaussian09W program.^[12] The geometry optimizations were carried out in the gas phase. The DFT calculations were performed at the B3LYP/6-31+G for C, H, N, S and O. The frontier molecular orbitals of DPP based monomer (1) and dimers (2 and 3) are shown in Figure 7.6 and Figure 7.7.

The HOMOs in DPP based monomer (1) and dimers (2 and 3) are spread over whole molecule while the LUMO in monomer and dimer is distributed on whole molecule but more electron density is concentrated on DPP lactam unit. The orbital distribution of electron density on trimer 4 shows that HOMO is spread over whole molecule (on triphenylamine as well as three DPP units) whereas in LUMO the electron density is concentrated on top two DPP units. The localization of HOMO on whole molecule and LUMO on DPP units in 4 shows acceptor nature of DPP and donor-acceptor interaction.

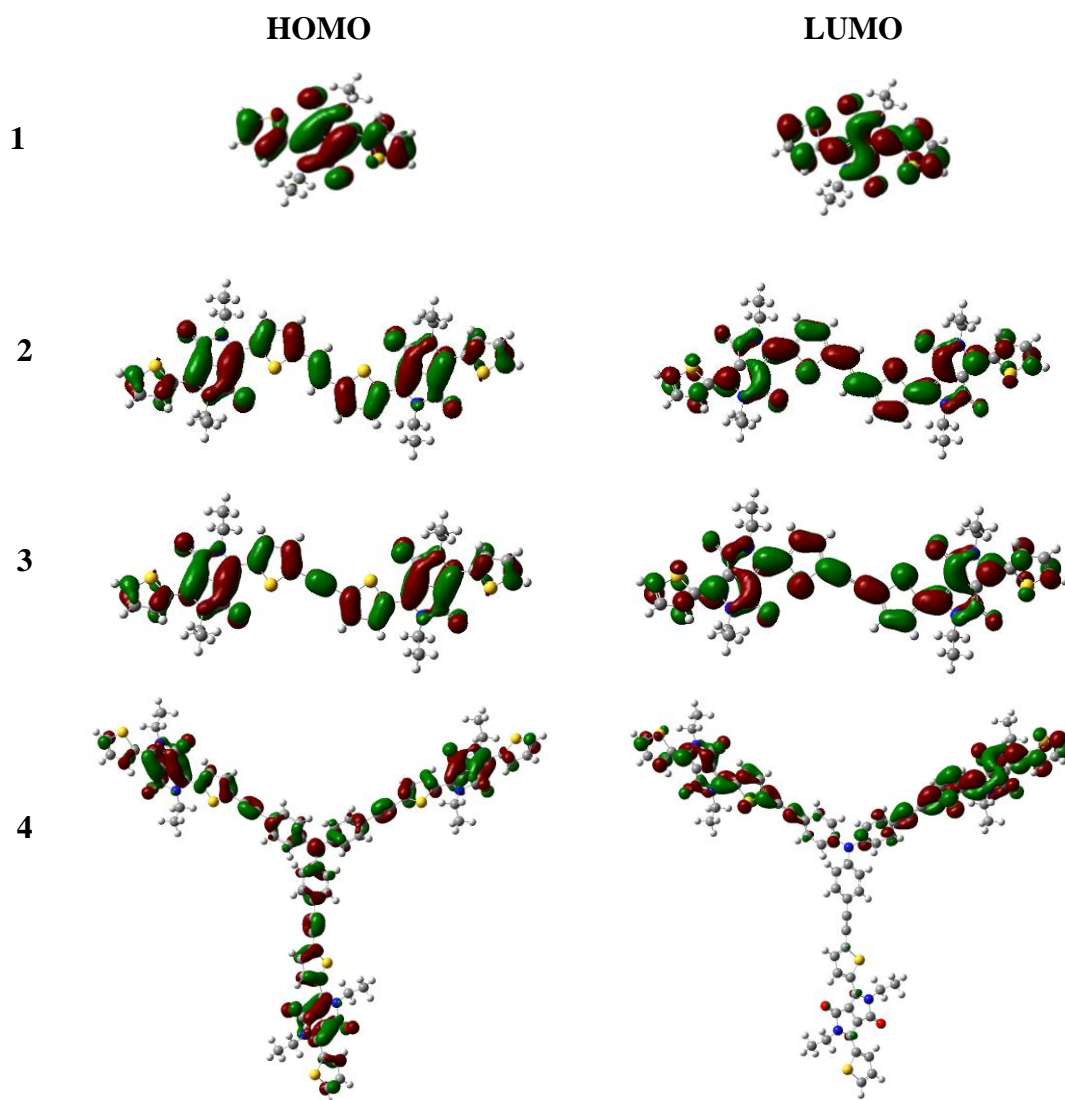
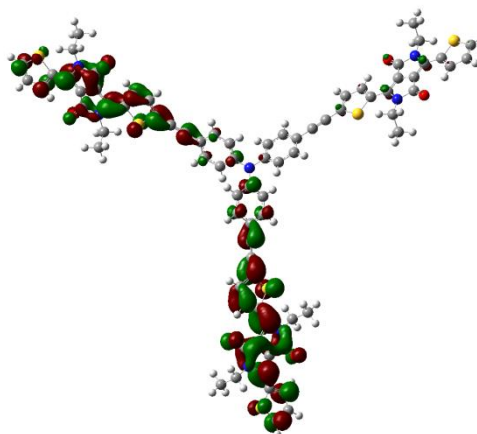


Figure 7.6. Frontier molecular orbitals of the DPP based monomer (**1**), dimers (**2** and **3**) and trimer (**4**) estimated by DFT calculation.

The time dependent density functional theory (TD-DFT) calculation was performed in order to get the idea of electronic transitions in DPP based monomer (**1**), dimers (**2** and **3**) and trimer (**4**). The major electronic transitions in DPP based monomer (**1**), dimers (**2** and **3**) and trimer (**4**) calculated from TD-DFT with composition and oscillator strengths are shown in Table 7.2.



LUMO+1

Figure 7.7. Frontier molecular orbital of the DPP based trimer (**4**) estimated by DFT calculation.

The DPP based monomer (**1**) and dimers (**2** and **3**) show the major transition from HOMO→LUMO which is related to $\pi\rightarrow\pi^*$ transitions of DPP unit whereas the trimer **4** exhibits two major transitions, one from HOMO→LUMO and second from HOMO→LUMO+1 due to intramolecular charge transfer (ICT) transitions.

Table 7.2. The major electronic transitions calculated from TD-DFT for DPP based monomer (**1**), dimers (**2** and **3**) and trimer (**4**) in the gas phase.

DPP	Wavelength (nm)	Composition	f^o	Transition
1	503	HOMO→LUMO (0.71)	0.43	$\pi\rightarrow\pi^*$ transition
2	526	HOMO→LUMO (0.70)	1.16	$\pi\rightarrow\pi^*$ transition
3	501	HOMO→LUMO (0.67)	0.91	$\pi\rightarrow\pi^*$ transition
4	652	HOMO→LUMO (0.70)	1.32	ICT transition
	651	HOMO→LUMO+1 (0.70)	1.38	ICT transition

f^o = Oscillation Strength

7.7. Application in Photovoltaics

We used ethene and ethyne bridged dimers **DPPs 2** and **3** as donor along with PC₇₁BM as the acceptor for the preparation of solution processed bulk heterojunction organic solar cells (BHJ-OSCs) an achieved power conversion efficiency upto 5.28% and 5.52% respectively.^[13]

7.8. Experimental Section

General Methods

The chemicals were used as received unless otherwise indicated. ^1H NMR (400 MHz) and ^{13}C NMR (100 MHz) spectra were recorded by using CDCl_3 as the solvent. The ^1H NMR chemical shifts are reported in parts per million (ppm) relative to the solvent residual peak (CDCl_3 , 7.26 ppm). The multiplicities are given as: s (singlet), d (doublet), m (multiplet), and the coupling constants, J , are given in Hz. The ^{13}C NMR chemical shifts are reported with relative to the solvent residual peak (CDCl_3 , 77.02 ppm). HRMS was recorded on a mass spectrometer (ESI-TOF). The UV-visible absorption spectra were recorded on UV-visible Spectrophotometer in dichloromethane. The TGA analyses were performed on the thermal analysis system at the heating rate of 10 °C per minute under a nitrogen atmosphere. Cyclic voltammograms (CVs) and differential voltammograms (DPVs) were recorded on an electrochemical analyzer using glassy carbon as working electrode, Pt wire as the counter electrode, and saturated Ag/Ag^+ as the reference electrode.

Synthesis of DPP Monomer 1

The reaction of 2-thiophenecarbonitrile with half equivalent of dimethyl succinate in presence of strong base sodium *tert*-butoxide in *tert*-butanol at 120 °C for 12 hours under argon atmosphere and worked up by methanol:hydrochloric acid (300ml methanol:15ml conc. HCl), filtered on Buchner funnel and finally washed with methanol yielded maroon solid. To make soluble it was further reacted with excess amount of 1-bromodecane in presence of base K_2CO_3 in *N,N*-dimethylformamide (DMF) at 145 °C for 12 hours under argon atmosphere. The reaction contents were cooled to room temperature and solvent was removed under vacuo. The crude compound was purified by silica column chromatography (eluted with 50% dichloromethane in hexane) yielded 23% shiny crystalline solid DPP monomer **1** after washing with hexane.

^1H NMR (400 MHz, CDCl_3): δ = 8.92 (m, 2 H), 7.62 (m, 2 H), 7.27 (d, 2 H), 4.06 (m, 4 H), 1.73 (m, 4 H), 1.30 (s, 24 H), 0.88 (m, 6 H) ppm; ^{13}C NMR (100 MHz, CDCl_3 , δ in ppm): 161.4, 140.1, 135.3, 130.7, 129.9, 128.7, 107.8, 53.5, 42.3, 31.9, 30.0, 29.6, 29.4, 29.3, 26.9, 22.7, 14.7; HRMS (ESI): calcd. for $\text{C}_{34}\text{H}_{48}\text{N}_2\text{O}_2\text{S}_2$ $[\text{M}]^+$ 581.3220; found 581.3343.

Synthesis of ethene bridged dimer 2

In 100 ml round bottom flask monobromodiketopyrrolopyrrole **DPP 1a** (0.100 g, 0.15 mmol) and bis(tributylstannyl)ethene (0.040 ml, 0.075 mmol) were dissolved in dry toluene (20 ml). The reaction mixture was degassed with argon for 10 minutes and Pd(PPh₃)₄ (0.035g, 0.030 mmol), was then added. The reaction mixture was stirred at 80 °C overnight. After completion of reaction, the reaction mixture was allowed to cool down to room temperature. The solvent was removed under vacuo and the product was purified by repeated silica-column chromatography with hexane:dichloromethane (1:1) as an eluent in 65% yield.

¹H NMR (400 MHz, CDCl₃, δ in ppm): 8.95 (2H, d, *J* = 4 Hz), 8.90 (2H, d, *J* = 4 Hz), 7.28 (4H, d, *J* = 4 Hz), 7.23 (2H, s), 4.09 (8H, m), 2.17 (16H, s), 1.76 (8H, m), 1.26 (40H, s), 0.86 (12H, m); ¹³C NMR (100 MHz, CDCl₃, δ in ppm): 161.4, 161.2, 147.0, 139.9, 139.1, 136.3, 135.4, 130.8, 129.8, 129.3, 128.7, 128.5, 122.8, 108.6, 108.1, 42.34, 42.26, 31.9, 30.1, 30.0, 29.6, 29.5, 29.30, 29.27, 26.93, 26.91, 22.7, 14.1; MALDI-TOF

Synthesis of ethyne bridged dimer 3

In 100 ml round bottom flask monobromo-diketopyrrolopyrrole **DPP 1a** (0.100 g, 0.15 mmol) and bis(tributylstannyl)acetylene (0.040 ml, 0.075 mmol) were dissolved in dry toluene (20 ml). The reaction mixture was degassed with argon for 10 minutes and Pd(PPh₃)₄ (0.035g, 0.030 mmol), was then added. The reaction mixture was stirred at 80 °C overnight. After completion of reaction, the reaction mixture was allowed to cool down to room temperature. The solvent was removed under vacuo and the product was purified by repeated silica-column chromatography with hexane : dichloromethane (1:1) as an eluent in 58% yield.

¹H NMR (400 MHz, CDCl₃, δ in ppm): 8.98 (2H, d, *J* = 4 Hz), 8.92 (2H, d, *J* = 4 Hz), 7.67 (2H, s), 7.45 (2H, s), 7.30 (2H, s), 4.08 (8H, m), 1.75 (8H, s), 1.44 (8H, m), 1.26 (46H, s), 0.87 (12H, m); ¹³C NMR (100 MHz, CDCl₃, δ in ppm): 161.3, 161.2, 140.6, 138.4, 135.8, 135.2, 135.1, 133.7, 132.2, 132.1, 131.6, 131.2, 13.4, 129.7, 128.7, 128.6, 128.4, 128.1, 127.9, 126.9, 109.0, 107.9, 90.5, 42.3, 31.9, 30.1, 29.9, 29.7, 29.5, 29.4, 29.3, 29.2, 26.2, 22.7, 14.1.

Synthesis of TPA based DPP trimer 4

In 100 ml round bottom flask monobromo-DPP **1a** (0.100 g, 0.32 mmol) and triethynyl triphenylamine (0.011 g, 1.10 mmol) were dissolved in toluene (30 ml) and triethylamine (8 ml). The reaction mixture was degassed with argon for 10 minutes

and Pd(PPh₃)₄ (0.018 g, 0.016 mmol) and CuI (0.003 g, 0.016 mmol) were then added. The reaction mixture was stirred overnight at 90 °C. After completion, the reaction mixture was allowed to cool down to room temperature. The solvents were removed under vacuo and product **4** was purified by silica-column chromatography with hexane: dichloromethane (1:3) as an eluent in 65% yield.

¹H NMR (400 MHz, CDCl₃, δ in ppm): 8.95 (3H, s), 8.91 (3H, s), 7.65 (2H, m), 7.46 (2H, m), 7.38 (3H, m), 7.29 (2H, s), 6.23 (6H, brs), 4.07 (12H, m), 1.76 (12H s), 1.42 (12H, m), 1.26 (71H, m), 0.87 (19H, brs); ¹³C NMR (100 MHz, CDCl₃, δ in ppm): 161.37, 161.35, 147.1, 140.3, 139.0, 135.6, 135.4, 133.94, 133.92, 132.92, 132.97, 131.0, 130.5, 129.8, 128.8, 124.27, 124.31, 117.4, 108.6, 108.0, 97.7, 82.7, 53.5, 42.4, 32.0, 30.8, 29.74, 29.72, 29.6, 29.47, 29.45, 29.39, 29.35, 29.3, 27.0, 22.8, 14.2.

7.9. Conclusions

In conclusion, we have designed and synthesized DPP based monomer (**1**), dimers (**2** and **3**) and trimer (**4**) and studied their photophysical, thermal and electrochemical properties, in order to investigate the effect of nature of bridging unit and number of DPP units. The absorption spectra show that the dimerization and trimerization of DPP red shifts the absorption with broadening of absorption in dimer analogues (**2** and **3**). The TGA analysis shows the dimerization and trimerization of DPP improves the thermal stability. The electrochemical study exhibited additional oxidation peak in trimer **3** related to the oxidation of triphenylamine unit. The effect of connecting bridge between DPP units in dimers and trimer of DPP has also been investigated which reveals the ethene bridged dimer exhibit good electronic communication between two DPP units.

7.9. References

- [1] (a) Zhu, Y., Rabindranath, A. R., Beyerlein, T., Tieke, B. (2007), Highly Luminescent 1, 4-Diketo-3,6-diphenylpyrrolo[3,4-c] pyrrole- (DPP-) Based Conjugated Polymers Prepared Upon Suzuki Coupling. *Macromolecules*, 40, 6981 (DOI: 10.1021/ma0710941). (b) Fischer, G. M., Ehlers, A. P., Zumbusch, A., Daltrozzo, E. (2007), Near-Infrared Dyes and Fluorophores Based on Diketopyrrolopyrroles. *Angew. Chem. Int. Ed.*, 46, 3750–3753 (DOI: 10.1002/anie200604763). (c) Yang, J., Tan, H., Li, D., Jiang, T., Gao, Y., Li, B., Qu, X., Hua, J. (2016), Synthesis, two-photon absorption and aggregation-induced emission properties of multi-branched triphenylamine derivatives based

- on diketopyrrolopyrrole for bioimaging. *RSC Adv.*, 6, 58434–58442 (DOI: 10.1039/C6RA11269B). (d) Tang, A., Zhan, C., Yao, J., Zhou, E. (2017), Design of Diketopyrrolopyrrole (DPP)-Based Small Molecules for Organic-Solar-Cell Applications. *Adv. Mater.*, 29, 1600013 (DOI: 10.1002/adma.201600013). (e) Patil, Y., Misra, R., Keshtov, M. L., Sharma, G. D. (2016), *1,1,4,4*-Tetracyanobuta-1,3-diene Substituted Diketopyrrolopyrroles: An Acceptor for Solution Processable Organic Bulk Heterojunction Solar Cells. *J. Phys. Chem. C*, 120, 6324–6335 (DOI: 10.1021/acs.jpcc.5b12307). (f) Patil, Y., Jadhav, T., Dhokale, B., Misra, R. (2016), Design and Synthesis of Low HOMO–LUMO Gap N-Phenylcarbazole-Substituted Diketopyrrolopyrroles. *Asian J. Org. Chem.* 5, 1008–1014 (DOI: 10.1002/ajoc.201600194). (g) Patil, Y., Misra, R., Keshtov, M. L., Sharma, G. D. (2017), Small molecule carbazole-based diketopyrrolopyrroles with tetracyanobutadiene acceptor unit as a non-fullerene acceptor for bulk heterojunction organic solar cells. *J. Mater. Chem. A*, 5, 3311–3319 (DOI: 10.1039/C6TA09607G).
- [2] (a) Li, S., Zhang, Z., Shi, M., Li, C.-Z., Chen, H. (2017), Molecular electron acceptors for efficient fullerene-free organic solar cells. *Phys. Chem. Chem. Phys.*, 19, 3440–3458 (DOI: 10.1039/C6CP07465K). (b) Liu, Q., Ho, C.-L., Lo, Y. H., Li, H., Wong, W.-Y. (2015), Narrow Bandgap Platinum(II)-Containing Polyynes with Diketopyrrolopyrrole and Isoindigo Spacers. *J Inorg Organomet Polym.*, 25, 159 (DOI: 10.1007/s10904-014-0120-2). (c) Lim, B., Sun, H., Lee, J., Noh, Y.-Y. (2017), High Performance Solution Processed Organic Field Effect Transistors with Novel Diketopyrrolopyrrole-Containing Small Molecules, *Scientific Reports*, 7, 164 (DOI:10.1038/s41598-017-00277-7). (d) (e) Favereau, L., Warnan, J., Pellegrin, Y., Blart, E., Boujtita, M., Jacquemin, D., Odobel, F. (2013), Diketopyrrolopyrrole derivatives for efficient NiO-based dye-sensitized solar cells. *Chem. Commun.*, 49, 8018–8020 (DOI: 10.1039/C3CC44232B). (e) Qiao Z, Xu Y, Lin S, Peng J, Cao D. (2010), Synthesis and characterization of red-emitting diketopyrrolopyrrole-alt-phenylenevinylene polymers, *Synth Met.*, 160, 1544–1550 (<https://doi.org/10.1016/j.synthmet.2010.05.019>). (f) Cao, D., Liu, Q., Zeng, W., Han, S., Peng, J., Liu, S. (2006), Synthesis and characterization of novel red-emitting alternating copolymers based on fluorene and diketopyrrolopyrrole derivatives, *J. Polym. Sci. A Polym. Chem.*, 44, 2395–2405

- (DOI:10.1002/pola.21354) (g) Rabindranath AR, Zhu Y, Heim I, Tieke B.(2006), Red Emitting N-Functionalized Poly(1,4-diketo-3,6-diphenylpyrrolo[3,4-c]pyrrole) (Poly-DPP): A Deeply Colored Polymer with Unusually Large Stokes Shift, *Macromolecules*, 39, 8250–8256; (h) Bürgi, L., Turbiez, M., Pfeiffer, R., Bienewald, F., Kirner, H.-J., Winnewisser, C. (2008), High-Mobility Ambipolar Near-Infrared Light-Emitting Polymer Field-Effect Transistors, *Adv. Mater.*, 20, 2217–2224 (DOI:10.1002/adma.200702775).
- [3] (a) Grzybowski, M., Gryko, D. T., Grzybowski, M., Gryko, D. T. (2015), Diketopyrrolopyrroles: Synthesis, Reactivity, and Optical Properties, *Advanced Optical Materials*, 3, 280–320 (DOI:10.1002/adom.201400559). (b) Ruff, A., Heyer, E., T. Roland, Haacke, S., Ziessel, R., Ludwigs, S. (2015), Electrochemical and optical properties of molecular triads based on triphenylamine, diketopyrrolopyrrole and boron-dipyrromethene, *Electrochimica Acta.*, 170, 847-859 (<https://doi.org/10.1016/j.electacta.2015.05.093>).
- [4] (a) Cai, Y., L. Pingping, Tang, Q., Yang, X., Si, W., Huang, W., Zhang, Q., Dong, X. (2017), Diketopyrrolopyrrole–Triphenylamine Organic Nanoparticles as Multifunctional Reagents for Photoacoustic Imaging-Guided Photodynamic/Photothermal Synergistic Tumor Therapy, *ACS Nano*, 2017, 11, 1054–1063 (DOI: 10.1021/acsnano.6b07927). (b) Liang P., Tang, Qianyun Cai, Y., Liu, G., Si, W., Shao, J., Huang, W., Zhang, Q., Dong, X., (2017), Self-quenched ferrocenyl diketopyrrolopyrrole organic nanoparticles with amplifying photothermal effect for cancer therapy, *Chem. Sci.*, 8, 7457-7463 (DOI: 10.1039/C7SC03351F).
- [5] (a) Dhar, J., Mukhopadhyay, T., Yaacobi-Gross, N., Anthopoulos, T. D., Salzner, U., Swaraj, S., Patil, S. (2015), Effect of Chalcogens on Electronic and Photophysical Properties of Vinylene-Based Diketopyrrolopyrrole Copolymers, *J. Phys. Chem. B*, 119, 11307–11316 (DOI: 10.1021/acs.jpcc.5b03145). (b) Yue, J., Liang, J., Sun, S., Zhong, W., Lan, L., Ying, L., Yang, W., Cao, Y., (2015), Effects of flanked units on optoelectronic properties of diketopyrrolopyrrole based π -conjugated polymers, *Dyes and Pigments*, 123, 64-71 (<https://doi.org/10.1016/j.dyepig.2015.07.021>).
- [6] Li, W., Hendriks K. H., Wienk, M. M., Janssen, R. A. J. (2016), Diketopyrrolopyrrole Polymers for Organic Solar Cells, *Acc. Chem. Res.*, 49, 78–85 (DOI: 10.1021/acs.accounts.5b00334).

- [7] (a) Patil, H., Gupta, A., Bilic, A., Bhosale, S. V., Bhosale, S. V. (2014), A solution-processable electron acceptor based on diketopyrrolopyrrole and naphthalenediimide motifs for organic solar cells, *Tetrahedron, Lett.*, 55, 4430–4432 (<https://doi.org/10.1016/j.tetlet.2014.06.017>). (b) Zhang, F., Brandt, R. G., Gu, Z., Wu, S., Andersen, T. R., Shi, M., Yu, D., Chen, H. (2015), The effect of molecular geometry on the photovoltaic property of diketopyrrolopyrrole based non-fullerene acceptors, *Synth. Met.*, 203, 249–254 (<https://doi.org/10.1016/j.synthmet.2015.02.038>). (c) Li, S., Yan, J., Li, C.-Z., Liu, F., Shi, M., Chen, H., Russell, T. P. (2016), A non-fullerene electron acceptor modified by thiophene-2-carbonitrile for solution-processed organic solar cells, *J. Mater. Chem. A*, 4, 3777–3783 (DOI: 10.1039/C6TA00056H). (d) Tang, A., Li, L., Lu, Z., Huang, J., Jia, H., Zhan, C., Tan, Z., Li, Y., Yao, J. (2012), Significant improvement of photovoltaic performance by embedding thiophene in solution-processed star-shaped TPA-DPP backbone, *J. Mater. Chem. A*, 1, 5747–5757 (DOI: 10.1039/C3TA10640C). (e) Lin, Y., Cheng, P., Li, Y., Zhan, X. (2012), A 3D star-shaped non-fullerene acceptor for solution-processed organic solar cells with a high open-circuit voltage of 1.18 V, *Chem. Commun.*, 48, 4773–4775 (DOI: 10.1039/C2CC31511D).
- [8] (a) Bijleveld, J. C., Karsten, B. P., Mathijssen, S. G., Wienk, M. M., de Leeuw, D. M., Janssen, R. A. Small band gap copolymers based on furan and diketopyrrolopyrrole for field-effect transistors and photovoltaic cells, (2011), *J. Mater. Chem.*, 21, 1600–1606 (DOI: 10.1039/C0JM03137B). (b) Woo, C. H., Beaujuge, P. M., Holcombe, T. W., Lee, O. P., Fréchet, J. M. (2010) Incorporation of Furan into Low Band-Gap Polymers for Efficient Solar Cells, *J. Am. Chem. Soc.*, 132, 15547 (DOI: 10.1021/ja108115y). (c) Li, Y., Sonar, P., Singh, S. P., Ooi, Z. E., Lek, E. S., Loh, M. Q. (2012), Poly(2,5-bis(2-octyldodecyl)-3,6-di(furan-2-yl)-2,5-dihydro-pyrrolo[3,4-c]pyrrole-1,4-dione-co-thieno[3,2-b]thiophene): a high performance polymer semiconductor for both organic thin film transistors and organic photovoltaics, *Phys. Chem. Chem. Phys.*, 14, 7162–7169 (DOI: 10.1039/C2CP40937B). (d) Tamayo, A. B., Tantiwivat, M., Walker, B., Nguyen, T.-Q. (2008), Design, Synthesis, and Self-assembly of Oligothiophene Derivatives with a Diketopyrrolopyrrole Core, *J. Phys. Chem. C*, 112, 15543 (DOI: 10.1021/jp804816c).

- [9] (a) Huo, L., Hou, J., Chen, H.-Y., Zhang, S., Jiang, Y., Chen, T. L., Yang, Y. (2009), Bandgap and Molecular Level Control of the Low-Bandgap Polymers Based on 3,6-Dithiophen-2-yl-2,5-dihydropyrrolo[3,4-c]pyrrole-1,4-dione toward Highly Efficient Polymer Solar Cells, *Macromolecules*, 42, 6564 (DOI: 10.1021/ma9012972). (b) Wood, S., Wade, J., Shahid, M., Collado-Fregoso, E., Bradley, D. D., Durrant, J. R., Heeney, M., Kim, J.-S. (2015), Natures of optical absorption transitions and excitation energy dependent photostability of diketopyrrolopyrrole (DPP)-based photovoltaic copolymers, *Energy Environ. Sci.*, 8, 3222 (DOI: 10.1039/C5EE01974E). (c) Bronstein, H., Chen, Z., Ashraf, R. S., Zhang, W., Du, J., Durrant, J. R., Tuladhar, P. S., Song, K., Watkins, S. E., Geerts, Y. (2011), Thieno[3,2-b]thiophene–Diketopyrrolopyrrole-Containing Polymers for High-Performance Organic Field-Effect Transistors and Organic Photovoltaic Devices, *J. Am. Chem. Soc.*, 133, 3272–3275 (DOI: 10.1021/ja110619k). (d) Ashraf, R. S., Meager, I., Nikolka, M., Kirkus, M., Planells, M., Schroeder, B. C., Holliday, S., Hurhangee, M., Nielsen, C. B., Siringhaus, H. (2015), Chalcogenophene Comonomer Comparison in Small Band Gap Diketopyrrolopyrrole-Based Conjugated Polymers for High-Performing Field-Effect Transistors and Organic Solar Cells, *J. Am. Chem. Soc.*, 137, 1314–1321 (DOI: 10.1021/ja511984q). (e) Sun, B., Hong, W., Yan, Z., Aziz, H., Li, Y. (2014), Record High Electron Mobility of $6.3 \text{ cm}^2\text{V}^{-1}\text{s}^{-1}$ Achieved for Polymer Semiconductors Using a New Building Block. *Adv. Mater.*, 26, 2636–2642 (DOI:10.1002/adma.201305981).
- [10] (a) Lee, J. W., Choi, Y. S., Jo, W. H., (2012), Diketopyrrolopyrrole-based small molecules with simple structure for high V_{OC} organic photovoltaics, *Organic Electronics*, 13, 3060–3066 (<https://doi.org/10.1016/j.orgel.2012.09.004>). (b) Choi, Y. S., Jo, W. H., (2013), A strategy to enhance both V_{oc} and J_{sc} of A–D–A type small molecules based on diketopyrrolopyrrole for high efficient organic solar cells, *Organic Electronics*, 14, 1621–1628 (<https://doi.org/10.1016/j.orgel.2013.03.031>).
- [11] (a) Stas, S., Balandier, J.-Y., Lemaire, V., Fenwick, O., Tregnago, G., Quist F., Cacialli, F., Cornil, J., Geerts, Y. H., (2013), Straightforward access to diketopyrrolopyrrole (DPP) dimers, *Dyes and Pigments*, 97, 198–208 (<https://doi.org/10.1016/j.dyepig.2012.12.005>). (b) Hong, T. R., Shin, J., Um, H. A., Lee, T. W., Cho, M. J., Kim, G. W., Kwon, J. H., Choi, D. H., (2014), New

π -extended diketopyrrolopyrrole-based conjugated molecules for solution-processed solar cells: Influence of effective conjugation length on power conversion efficiency, *Dyes and Pigments*, 108, 7-14 (<https://doi.org/10.1016/j.dyepig.2014.04.015>).

- [12] Frisch, M. J., Trucks, G. W., Schlegel, H. B., Scuseria, G. E., Robb, M. A., Cheeseman, J. R., Scalmani, G., Barone, V., Mennucci, B., Petersson, G. A., Nakatsuji, H., Caricato, M., Li, X., Hratchian, H. P., Izmaylov, A. F., Bloino, J., Zheng, G., Sonnenberg, J. L., Hada, M., Ehara, M., Toyota, K., Fukuda, R., Hasegawa, J., Ishida, M., Nakajima, T., Honda, Y., Kitao, O., Nakai, H., Vreven, T., Montgomery Jr, J. A., Peralta, J. E., Ogliaro, F., Bearpark, M., Heyd, J. J., Brothers, E., Kudin, K. N., Staroverov, V. N., Kobayashi, R., Normand, J., Raghavachari, K., Rendell, A., Burant, J. C., Iyengar, S. S., Tomasi, J., Cossi, M., Rega, N., Millam, J. M., Klene, M., Knox, J. E., Cross, J. B., Bakken, V., Adamo, C., Jaramillo, J., Gomperts, R., Stratmann, R. E., Yazyev, O., Austin, A. J., Cammi, R., Pomelli, C., Ochterski, J. W., Martin, R. L., Morokuma, K., Zakrzewski, V. G., Voth, G. A., Salvador, P., Dannenberg, J. J., Dapprich, S., Daniels, A. D., Farkas, Ö., Foresman, J. B., Ortiz, J. V., Cioslowski, J., Fox, D. J. (2009) Gaussian 09, revision D.01 Gaussian, Inc., Wallingford, CT, USA.
- [13] Patil, Y., Misra, R., Sharma, A., Sharma, G. D. (2016), D-A-D- π -D-A-D Type Diketopyrrolopyrrole Based Small Molecule Electron Donor for Bulk Heterojunction Organic Solar Cells. *Phys. Chem. Chem. Phys.*, 18, 16950-16957 (DOI: 10.1039/C6CP02700H).

Chapter 7

Conclusions and scope for future work

8.1. Conclusions

Diketopyrrolopyrrole (DPP) is an important building block possesses excellent properties such as strong electron affinity, light absorption in the visible region, highly conjugated coplanar molecular structure, and excellent photochemical stability.^[1] The derivatives of DPP show high solubility in common organic solvents, by appropriate substitution on amidic nitrogen of the bis-lactam core.^[2] DPP is one of the widely used acceptor unit for the synthesis of small molecules for various applications such as aggregation induced emission (AIE), dye sensitized solar cells (DSSCs) and bulk heterojunction (BHJ) organic solar cells (OSCs).^[3,4] Recently DPP derivatives have been used for OSC as efficient materials as donor as well as acceptor.

In this regard we have synthesized various donors and acceptor functionalized DPP based small molecules. We have investigated their photophysical, thermal and electrochemical properties which indicated their applicability for BHJ OSCs.

In chapter 3, we have designed and synthesized symmetrical and unsymmetrical ethyne bridged *N*-phenyl carbazole substituted **DPPs 5** and **6** by the Pd-catalyzed Sonogashira cross coupling reaction. Further [2+2] cycloaddition-retroelectrocyclization of **DPPs 5** and **6** with tetracyanoethylene (TCNE) resulted in tetracyanobutadiene (TCBD) derivatives **7** and **8**. The optical and electrochemical properties show that the incorporation of TCBD shifts the absorption from visible to near infra-red (NIR) region and additional reduction waves were observed at low voltage region. The excellent thermal stability, low HOMO – LUMO gap, absorption in visible to NIR region make these derivatives as a potential candidate for organic photovoltaics.

In Chapter 4, a set of symmetrical and unsymmetrical TPA substituted **DPPs 3** and **4** were designed and synthesized by Sonogashira cross-coupling reaction. The [2+2] cycloaddition-retroelectrocyclization of triphenylamine substituted **DPPs 3** and **4** with TCNE at room temperature resulted TCBD derivatives **DPPs 5 – 7**. The effect of triphenylamine as donor and TCBD acceptor on photophysical and electrochemical properties was evaluated. The TCBD substituted DPPs show

systematic red shift in absorption spectra with decrease in HOMO – LUMO gap. High thermal stability and low HOMO – LUMO gap of **DPPs 3 – 7** makes them potential candidate for organic photovoltaics. The results presented here will be useful in the design and synthesis of new molecular systems with low HOMO –LUMO gap for optoelectronic applications.

In chapter 5, we have synthesized symmetrical and unsymmetrical ferrocenyl DPPs **5** and **6** by Sonogashira cross-coupling and their TCBD derivatives (**7–9**) by [2+2] cycloaddition-retroelectrocyclization reaction respectively. The incorporation of TCBD in ferrocenyl DPPs improves the absorption with lowering of HOMO – LUMO gap values. The TCBD substituted DPPs show systematic red shift in absorption with enhanced thermal stability. High thermal stability and low HOMO – LUMO gap of DPPs (**5–9**) makes them potential candidate for organic photovoltaics.

In chapter 6, the synthesis, structural characterization, optical, thermal and electrochemical properties of symmetrical cobalt-dithiolene functionalized DPP **Co-DPP-Co** was investigated and compared with ferrocenyl based symmetrical **Fc-DPP-Fc**. The absorption spectra of **Co-DPP-Co** exhibited red shifted absorption in Vis-NIR region with shoulder band in longer wavelength region. The cobalt based **Co-DPP-Co** shows good thermal stability. The DFT investigation exhibited cis geometry of cobalt-dithiolene ring in **Co-DPP-Co** whereas the trans geometry of ferrocenyl unit has been observed in **Fc-DPP-Fc**. The broad absorption in NIR region, high thermal stability and low HOMO – LUMO gap values makes **Co-DPP-Co** as a potential candidate for photovoltaic applications.

In Chapter 7, we have designed and synthesized DPP based monomer (**1**), dimers (**2** and **3**) and trimer (**4**) and studied their photophysical, thermal and electrochemical properties, in order to investigate the effect of number of diketopyrrolopyrrole units. The absorption spectra show that the dimerization and trimerization of DPP red shifts the absorption with broadening of absorption in dimer analogues (**2** and **3**). The TGA analysis shows the dimerization and trimerization of DPP improves the thermal stability. The electrochemical study exhibited additional oxidation peak in trimer **4** related to the oxidation of triphenylamine unit. The effect of connecting bridge between DPP units in dimers and trimer of DPP has also been investigated which reveals the ethene bridged dimer **2** exhibit good electronic communication between two DPP units.

We have used some of donor functionalized ethyne bridged DPPs as donor for bulk heterojunction organic solar cells (BHJ OSCs) and achieved a PCE upto 6.44%. The incorporation of TCBD unit improves the accepting ability of resulting molecules. The use of TCBD derivatives as donors for BHJ OSCs is well known in literature but there were no reports where these molecules were used as an acceptor. For the first time we have explored TCBD bridged small molecule as a non-fullerene acceptor for BHJ OSCs and open up a new pathway to design highly efficient TCBD based small molecular acceptor. We have changed the end capping donor in order to see its effect on performance and achieved the PCE upto 7.19% which is highest efficiency for TCBD bridged non-fullerene acceptor till date.

8.2. Scope for future work

The thesis highlights smart methodology for design of DPP based donor-acceptor small molecules. The HOMO–LUMO gap of the DPP based donor-acceptor molecules can be tuned by changing terminal donor unit and incorporation of TCBD as strong acceptor. The variation of donor/acceptor strength resulted in the significant tuning of the HOMO–LUMO gap. The incorporation of strong cyano-based TCBD acceptor units in the ethyne bridged DPP resulted extension of absorption to near infrared region. The strong absorption in near infrared region with low HOMO-LUMO gap of small molecules make them promising candidates for optoelectronic applications.

8.3 References

- [1] (a) Tang, A., Zhan, C., Yao, J., Zhou, E. (2017), Design of Diketopyrrolopyrrole (DPP)-Based Small Molecules for Organic-Solar-Cell Applications, *Adv. Mater.*, 29, 1600013 (DOI: 10.1002/adma.201600013). (b) Roland, T., Heyer, E., Liu, L., Ruff, A., Ludwigs, S., Ziessel, R., Haacke, S. (2014), A Detailed Analysis of Multiple Photoreactions in a Light-Harvesting Molecular Triad with Overlapping Spectra by Ultrafast Spectroscopy, *J. Phys. Chem. C*, 118, 24290–24301 (DOI: 10.1021/jp507474r).
- [2] (a) Grzybowski, M., Gryko, D. T. (2015), Diketopyrrolopyrroles: Synthesis, Reactivity, and Optical Properties. *Adv. Opt. Mater.*, 3, 280–320. (DOI:10.1002/adom.201400559).
- [3] (a) Kaur, M., Choi, D. H. (2015), Diketopyrrolopyrrole: brilliant red pigment dye-based fluorescent probes and their applications, *Chem. Soc. Rev.*, 44, 58-77 (DOI: 10.1039/C4CS00248B). (b) Liang, N., Jiang, W., Hou, J., Wang, Z.

- (2017), New developments in non-fullerene small molecule acceptors for polymer solar cells, *Mater. Chem. Front.*, 1, 1291-1303 (DOI: 10.1039/C6QM00247A). (c) Josse, P., Dalinot, C., Jiang, Y., Dabos-Seignon, S., Roncali, J., Blanchard, P., Cabanetos, C. (2016), Phthalimide end-capped thienoisindigo and diketopyrrolopyrrole as non-fullerene molecular acceptors for organic solar cells, *J. Mater. Chem. A*, 4, 250-256 (DOI: 10.1039/C5TA09171C).
- [4] (a) Li, W., Hendriks, K. H., Wienk, M. M., Janssen, R. A. J. (2016), Diketopyrrolopyrrole Polymers for Organic Solar Cells, *Acc. Chem. Res.*, 49, 78–85 (DOI: 10.1021/acs.accounts.5b00334). (b) Yum, J.-H., Holcombe, T. W., Kim, Y., Rakstys, K., Moehl, T., Teuscher, J., Delcamp, J. H., Nazeeruddin, M. K., Grätzel, M. (2013), Blue-Coloured Highly Efficient Dye-Sensitized Solar Cells by Implementing the Diketopyrrolopyrrole Chromophore. *Scientific Reports*, 3, 2446 (DOI:10.1038/srep02446).